RMS Modeling of Grid-Forming Power Electronics for Renewable Energy Power Plant Integration and Classical Power System Stability Studies

Ibrahim Kucuk, Theyagarajan Thangamani

Energy Technology, WPS4-1050, 2020-05

Master's Thesis

STUDENT REPORT
AALBORG UNIVERSITY

The following programs have been used throughout the report: MATLAB®, DIgSILENT PowerFactory.

AALBORG UNIVERSITET
STUDENTERRAPPORT

Second year of Msc study at the Technical Science Faculty
Energy Technology
Pontoppidanstræde 111
9220 Aalborg Ø
http://www.tnb.aau.dk

Title

RMS Modeling of Grid-Forming Power Electronics for Renewable Energy Power Plant Integration and Classical Power System Stability Studies

Theme

Master Thesis on Renewable Energy Integration

Project Period:

04/02/20 - 29/05/20

Project Group:

WPS4-1050

Participants:

Ibrahim Kucuk
Theyagarajan Thangamani

Supervisor:

Filipe Miguel Faria da Silva

Pages: 74
Appendix: 4
Electronic Files: 8
Submission date: 29-05-2020

Abstract:

The share of the renewable energy sources (RESs) in electrical power system is continuously increasing. As a result, the conventional power plants, which mostly utilize large synchronous generators (SGs), are taken out from the operation and this leads to power system stability concerns. The conventional grid-following control strategies for RESs do not contribute to the stability. On the other hand, grid-forming (GF) controls acts as a voltage source in a system, and can perform an operation similar to SGs. In this study an RMS model of GF converter is built. The GF converter model is implemented to a simple power system and fed by a renewable energy source. The results showed that a GF converter can operate like a SG and it can perform load sharing based on its implemented droop curve. In addition, two adaptive droop control methods are introduced for frequency control in the power system. A battery storage system is proposed to support DC voltage during immediate power demands. The study is performed in DIgSILENT PowerFactory.

Preface

This master thesis is written during the 4th semester of the Wind Power Systems MSc. programme at Aalborg University Department of Energy Technology, Denmark. The project was proposed as a master thesis by Danish transmission system operator, Energinet. The authors would like to thank to Filipe Miguel Faria da Silva, who is the main supervisor, and Laurids Dall, who is the co-supervisor from Energinet, for their precious contribution and supervision throughout the report.

Reading Guide

Throughout this project the numeric system is used for citation, which means every source has been assigned a number. The details for each source can be found in the Bibliography.

The equations, figures, tables and appendices are arranged in order to its appearance in the text and a caption has been assigned to each element. The DIgSILENT PowerFactory™ models used in this project, are electronically attached.

Aalborg University, May 29, 2020

Ibrahim Kucuk
<ikucuk18@student.aau.dk>

Theyagarajan Thangamani
<tthang18@student.aau.dk>

Summary

The share of the renewable energy sources (RESs) in electrical power system is continuously rising. Comparing to classical synchronous generators (SGs), RESs mostly operate with a maximum power point tracker algorithm and they act as a power source. RESs are mostly connected to grid with a power electronic interface. For this operation, it is a conventional solution to follow the existing grid, by grid-following control strategies. However, power systems are becoming weaker as the share of RESs increases and synchronous generators (SGs) are decommissioned. In the future, operation of RESs should adapt to be more than a simple power source. One proposed control strategy is grid-forming control, which is utilized by power converters to form an AC voltage and frequency in an electrical system. It is a control strategy which has been mostly studied for microgrid operations. For this project, the main objective is to build a RMS model of grid-forming (GF) converter for classical power system stability studies.

Theories and trends regarding grid-forming converters and electrical power system are introduced through the report. In the introduction Chapter, recent trends in the electrical power system and the overview of the report and projects are provided. Recent regulations show that transmission system operators (TSOs) are imposing some control functions to renewable energy power plants (REPPs) for frequency and voltage support. Today's REPPs have grid-following control strategies, and they provide voltage and frequency support by a higher-level control which changes the operational active and reactive power set-points of the power plant. However, grid-forming control strategies can be used to support the voltage and frequency of the grid without any higher-level control.

In Chapter two, the importance of SGs from power system stability point of view is highlighted and grid-forming control strategy is introduced as a promising method for future power system applications. A SG is a rotating voltage source, and its rotation is heavily dependent on its implemented droop characteristic. Similarly, a GF control has its own voltage and frequency set-points, and its electrical frequency can be adjusted in relation with its loading with a proper droop control. Therefore, a GF converter can be operated like a SG in a power system, and it can perform load sharing with other generation units with droop control. This ability to control a GF converter with droop controls makes it a convenient control strategy for power system applications. The motivation in RMS modelling is also introduced in this Chapter. TSOs perform both short- and long-term studies for many purposes such as analyses, planning and operation of power systems. RMS models and simulations have provided reliable results and minimized the computational burden until now for classical power system stability analyses. RMS analysis are still likely to be used for the years to come because EMT models are more complex and detailed which increases the computational burden. It would take a significant development in the system to shift to EMT analysis. The reliability of RMS simulations should be re-evaluated for a power system where it is dominated by power electronic interfaced generation units.

In Chapter 3, the modelling of various elements used in the system are introduced. A simple power system is modelled with one external grid and one GF converter in PowerFactory. A REPP is used as a power source for the GF converter, and it is connected to the GF converter with a DC link. A shunt capacitor and a battery energy storage system (BESS) is implemented to DC bus of the GF converter. The GF converter is controlled by a cascaded voltage and current controller. The reference signals of voltage and frequency for the controller are provided by droop controls of the GF converter. The dedicated controls, block diagrams and important parameters of the previously mentioned elements in the system are introduced through the Chapter. Additionally, two adaptive droop control methods are introduced, which can provide frequency regulation for power systems. One method proposes shifting the frequency droop curve, and the other proposes changing the slope of the droop curve.

In Chapter 4, case studies are presented. The first study investigates the behaviour of the GF converter where the effect of the external grid on power flow is minimized by implementing a vertical droop curve. A large load relative to the total rating of the system is switched in to make a dynamic change in the system, and to observe the response of the GF converter. This case study shows that the DC bus voltage of the GF converter is strongly dependent to the power outputs of the GF converter and REPP. The GF converter acts a voltage source, and when there is a load change in the system, the GF converter responses to the demand and immediately delivers the power. However, the REPP cannot deliver the same power to the GF converter at the same time, and this leads to a discharge in the DC link capacitor, and a voltage drop consequently. This case study shows that the GF converter works as a voltage source and it tends to deliver or draw reactive power to form its reference voltage. In the second case, the previously mentioned two adaptive droop control methods are implemented to the first case, where GF converter is dominant. The results show that both methods can support the system frequency and it moves back to its nominal value in the simulated ideal scenario. In the third case, a BESS is applied to the DC bus of the GF converter to support the DC voltage stability. The first case is used as base study and it is observed that the power contribution of battery during the voltage drop supports the voltage recovery. The maximum voltage drop and recovery time becomes lower. In the last case, a realistic scenario is introduced. The effect of the external grid was minimized in the previous cases by implementing a vertical droop curve. The external grid is applied a proper droop curve for this case study. Also, in the second case study, the adaptive droop controls are simulated in an ideal scenario. For this case study, some control constrains are activated for adaptive droop control. As a result of the adjustments, the GF converter and external grid shares the load, when the same amount of load with previous studies is switched in. It is observed that the change in the loading in the GF converter is lower comparing to the previous cases thanks to the load sharing based on droop controls. As the loading is lower, voltage drop is also lower than the previous cases. After the load switching, adaptive droop control is also automatically activated based on the drop in the frequency. A frequency support is observed by the activation, however, it is not able to restore the system frequency back to its nominal due to the applied constrains.

From the simulation scenarios and the results of the designed RMS model of GF converter, it can be said that a GF converter can be operated like a SG in the future power system.

With droop control implementation, it can operate in parallel with other generation units and successfully share the load. Additionally, extra control function such as the introduced adaptive droop control can be implemented in the future to support system stability. However, there are also challenges in operation of a GF converter such as DC link voltage stability, reactive power flow and rate of change of frequency. A battery storage system can be used to support DC link voltage. Any potential overloading problem based on reactive power flow of GF converter may be solved by implementing an adaptive voltage droop curve, similar to the adaptive droop curve implemented in this study for frequency. And as last, the rate of change of frequency can be control by a virtual inertia implementation. These challenges should be investigated in detail by further studies.

A generic RMS model of GF converter is built in this study utilizing the PWM converter model in DIgSILENT PowerFactory. A cascaded voltage and current controller, which is the main control strategy for GF converters, is applied via DSL models to the converter. Voltage and frequency droop controls are also implemented to control the inputs of the converter. The GF converter controller can be exported and used for other RMS studies and it can be easily adapted to EMT analysis. The complete GF system, including the DC link capacitor, BESS and RES can be used for a power system level studies. These studies may include fluctuating or constant power source, different system events and different configuration of GF converter size, RES size and BESS size. Utilizing the introduced model and performing several studies by varying the configurations, needs of a GF converter operation can be analysed in terms of its power source, storage, parallel operation with other units or against different system event. The results from these studies can be evaluated by TSOs to determine the requirements of GF systems.

Nomenclature

Acronym	Abbreviation of:
AC	Alternating Current
BESS	Battery Energy Storage System
DC	Direct Current
DSL	DIgSILENT Simulation Language
EG	External Grid
EMT	Electro-magnetic Transient
GF	Grid-Forming
PI	Proportional Integrator
RES	Renewable Energy Source
REPP	Renewable Energy Power Plant
RMS	Root Mean Square
SG	Synchronous Generator
TSO	Transmission System Operator
VSG	Virtual Synchronous Generator
WTG	Wind Turbine Generator

Contents

Contents **xiii**

List of Figures **xv**

1 Introduction **1**
1.1 Problem Formulation . . . 2
1.2 Objectives . . . 3
1.3 Methodology . . . 3
1.4 Delimitation and Scope . . . 3
1.5 Content of the Report . . . 3

2 State of the Art **5**
2.1 Synchronous Generator - From Power System Stability Point of View . . . 5
2.2 Grid Forming . . . 7
2.3 RMS vs EMT . . . 10

3 System Modelling **13**
3.1 Power System . . . 13
3.2 High Level Control . . . 15
3.3 RES Control . . . 17
3.4 Renewable Energy Power Plant Inverter Control . . . 17
3.5 DC Bus Voltage Control . . . 19
3.6 GF Converter Control . . . 20
3.6.1 Cascaded Voltage and Current Controller . . . 20
3.7 Adaptive Droop Control . . . 22
3.7.1 Adaptive Droop Control - Shifting Method . . . 22
3.7.2 Adaptive Droop Control - Variable Slope Method . . . 27
3.8 Storage in DC Busbar . . . 30

4 Simulations and Results **33**
4.1 GF Converter Response - Base Case . . . 33
4.2 GF Converter Response with Ideal Adaptive Droop Control . . . 37
4.2.1 GF Converter Response with Shifting Method . . . 38
4.2.2 GF Converter Response with Variable Slope Method . . . 38
4.2.3 Comparison of the Methods . . . 41
4.3 GF Converter Response with BESS . . . 42
4.4 GF Converter Response with Realistic Constraints . . . 44

5 Discussion **51**

6 Conclusion **55**

Bibliography **57**

A Virtual Synchronous Generator Model and Simulation Results **59**

B Logical Controls **63**
- B.1 Functions 63
- B.2 Logical Controls 63
  - B.2.1 Logical Controls in Adaptive Droop Control Shifting Method 63
  - B.2.2 Logical Controls in Adaptive Droop Control Variable Slope Method 64

C Results **65**
- C.1 Extra Figures for Shifting Method Case Study 65
- C.2 Extra Figures for Variable Slope Method Case Study 66
- C.3 GF Converter Response with Realistic Constraints Case with Adaptive Droop Control Variable Slope Method 68

D Screenshots **71**

List of Figures

1.1 Total power generation capacity in the European Union 2008-2018 [1]. 1

2.1 Stages of frequency stability after a grid disturbance [2]. 6
2.2 Droop curve of external grid. 6
2.3 Droop curve of external grid. 7
2.4 Representation of grid following and grid forming converters. 8
2.5 Representation of droop based grid forming converter. 8
2.6 Layout of virtual synchronous generator based grid-forming control. 9
2.7 Time-frame Classification of Electrical Power Systems. 11

3.1 System layout. 14
3.2 Droop curve of external grid. 14
3.3 High level control diagram. 15
3.4 Droop curve of GF converter. 16
3.5 RES control diagram. 17
3.6 REPP inverter control diagram. 18
3.7 DC bus voltage control diagram. 19
3.8 GF converter. 20
3.9 Internal converter control diagram. 21
3.10 A droop curve and its variation based on slope or shifting. 22
3.11 The change in the electrical frequency as a result of changing power set-point. . 23
3.12 Droop curve with power set-point variation and important parameters. 25
3.13 Control diagram of adaptive droop control shifting method. 26
3.14 Droop curve of GF converter with the effect of high level control. 27
3.15 The change in the electrical frequency as a result of changing power set-point. . 27
3.16 Droop curve with slope variation and important parameters. 29
3.17 Control diagram of variable slope method. 30
3.18 BESS control. 31

4.1 Active power outputs of EG, GF converter and RES during GF converter response base case. 35
4.2 Grid frequency during GF converter response base case. 35
4.3 Reactive power outputs of EG and GF converter during GF converter response base case. 36
4.4 AC and DC bus voltages during GF converter response base case. 37
4.5 Deviation in power-set point during GF converter response with ideal shifting method case. 39
4.6 Grid frequency during GF converter response with ideal shifting method case. . 39
4.7 Deviation from 48 $[Hz]$ for maximum operation point and change in R during GF converter response with ideal variable slope method case. 40

4.8 Grid frequency during GF converter response with ideal variable slope method case. 40
4.9 Comparison of the grid frequencies under the GF converter response case, GF converter response with ideal shifting and variable slope methods case. 41
4.10 Comparison of the active power output of GF converter under the GF converter response case, GF converter response with ideal shifting and variable slope methods case. 42
4.11 DC Bus voltage with BESS 43
4.12 BESS Power Flow 43
4.13 State of Charge of BESS 43
4.14 Active power outputs of EG, GF converter and RES during GF Converter Response with Realistic Constraints case. 45
4.15 Grid frequency during GF Converter Response with Realistic Constraints case. 45
4.16 Deviation in power-set point during GF Converter Response with Realistic Constraints case. 46
4.17 AC and DC bus voltages during GF Converter Response with Realistic Constraints case. 47
4.18 Maximum operation point signal for GF converter, P_{max}, and power reference for capacitor charging, P_{dc_bus}, during GF Converter Response with Realistic Constraints case. 47
4.19 Reactive power outputs of EG, GF converter and RES during GF Converter Response with Realistic Constraints case. 48
4.20 Power output of BESS during GF Converter Response with Realistic Constraints case. 49

A.1 System layout of the initial model in the project with VSG. 59
A.2 Comparison of the system frequency with droop control based and VSG based GF converter. 60
A.3 Comparison of the active power output of GF converter with droop control and VSG. 61
A.4 Comparison of the AC bus voltage with droop control based and VSG based GF converter. 61
A.5 Comparison of the reactive power output of GF converter with droop control and VSG. 62

C.1 Active power outputs of EG, GF converter and RES during GF converter response with ideal shifting method case. 65
C.2 Reactive power outputs of EG, GF converter and RES during GF converter response with ideal shifting method case. 65
C.3 AC and DC bus voltages during GF converter response with ideal shifting method case. 66
C.4 Active power outputs of EG, GF converter and RES during GF converter response with ideal variable slope method case. 66
C.5 Reactive power outputs of EG, GF converter and RES during GF converter response with ideal variable slope method case. 67
C.6 AC and DC bus voltages during GF converter response with ideal variable slope method case. 67

C.7 Active power outputs of EG, GF converter and RES during Realistic Constraints case with variable slope method.Active power outputs of EG, GF converter and RES during GF Converter Response with Realistic Constraints case. 68
C.8 Grid frequency during GF Converter Response with Realistic Constraints case with variable slope method. 68
C.9 Deviation from 48 $[Hz]$ for maximum operation point during GF Converter Response with Realistic Constraints case with variable slope method. 69
C.10 Reactive power outputs of EG, GF converter and RES during GF Converter Response with Realistic Constraints case with variable slope method. 69
C.11 AC and DC bus voltages during GF Converter Response with Realistic Constraints case with variable slope method. 69
C.12 Maximum operation point signal for GF converter, P_{max}, and power reference for capacitor charging, P_{dc_bus}, during GF Converter Response with Realistic Constraints case with variable slope method. 70
C.13 Power output of BESS during GF Converter Response with Realistic Constraints case with variable slope method. 70

D.1 GF converter 71
D.2 Frequency droop control and calculation of phasor angle 72
D.3 Gf covnerter internal control 72
D.4 higher level control 73
D.5 RES control 73
D.6 Renewable energy power plant inverter control 74

Introduction 1

Electrical power system is experiencing a transition from conventional centralised power plants to distributed renewable energy sources (RESs) especially in Europe, in order to satisfy the Paris Agreement of being CO_2 neutral by 2050 [3]. Coal and natural gas power plants had the first and the second biggest installed power capacity for many years in Europe. However, wind and solar power plants have reached to the second and fifth biggest installed power capacity in 2018 while coal power plants decreased to from the first place to the third place [1].

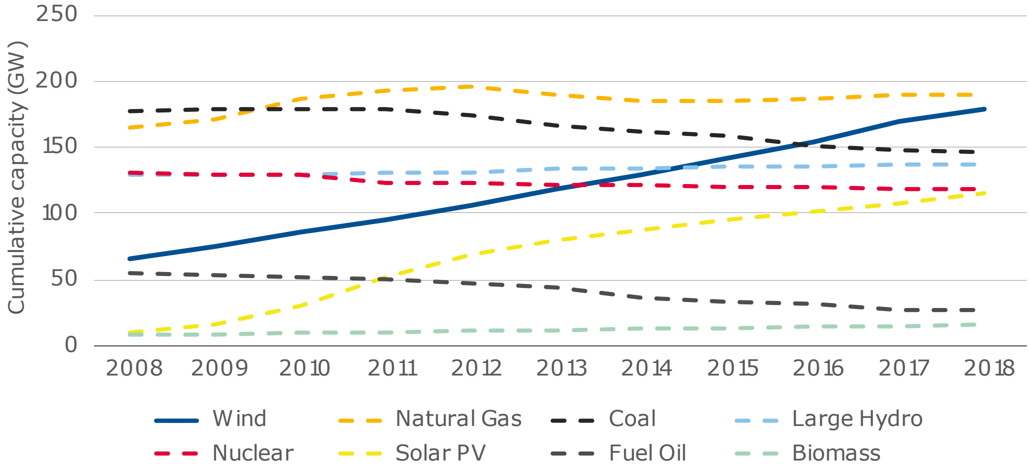

Figure 1.1: Total power generation capacity in the European Union 2008-2018 [1].

Conventional power plants mostly utilize synchronous generators (SGs) thanks to its contribution to system stability. However, the rise in the RESs has resulted in the decommissioning of some of these conventional power plants. Some of the RESs such as wind and solar have very different characteristics than classical SGs. Except the early generations of wind turbine generators (WTGs), the most recent WTGs, type 3 and type 4, utilize power electronic interface to connect to a grid [4]. And also a photovoltaic power plant has to use a power electronic interface to connect to a AC grid.

The increase in the power electronic interfaced generation causes the power system dynamics to be changed, especially from the stability point of view, because the number of the SGs decreases with penetration of RESs in the power system. On the contrary, SGs are one of the critical components of the power system in terms of stability criteria. A SG can prevent large frequency deviation in the power system by its inertial response and provide voltage control by its reactive power capability [5]. As a result of high penetration of RESs, it is expected that electrical power system stability will be a challenge for transmission systems operators (TSOs), and one of the prospected solution is to make RESs contributing to the power system stability.

TSOs have already been updating their requirements regarding grid connection of the RESs to maintain reliable system operation. In [6], some of these regulations are investigated for different countries. The paper demonstrates that, RESs are already required to be able to provide frequency and voltage support when it is necessary. For example, a wind power plant in Denmark with a installed power capacity between 11 $[kW]$ and 25 $[MW]$ should have a frequency response where the output power of the plant goes linearly to 0 during over-frequency based on a droop curve [7]. RESs such as wind and solar mostly utilize grid-following control strategies where a RES receives active and reactive power set-points and deliver these power to the existing grid by grid-following control [8]. Therefore, the mentioned regulations regrading frequency and voltage support require a high level control, which will dispatch the new set-points to the RESs to provide the required system support [8].

1.1 Problem Formulation

Although the share of RESs is continuously increasing, some conventional power plants, SGs, are still in operation. It is sometimes due to the generation deficit from RESs and sometimes to provide ancillary services to the grid while operating at base load even if there is enough generation from RESs. Also, SGs act as a voltage source and form the grid, which RESs follow to deliver active and reactive power. System support functions in the regulations for RESs are not enough to maintain the system stability when SGs are decommissioned from the grid. Because the existing RES controls requires an existing grid to follow. Therefore, a new approach on controlling RESs is needed to transition 100% inverter interfaced renewable generation. One of the proposed methods is grid-forming strategy which control the grid voltage and frequency like SGs. Grid-forming (GF) strategy has been mainly studied for microgrids. However, it is an emerging topic today for transmission system level as a result of high RES penetration. For example, UK's TSO, National Grid, is already working on a draft of for a grid-code for grid-forming control [9].

It is TSOs' responsibility to maintain electrical power system stability. To fulfil this responsibility, TSOs perform short term and long term analysis. Short term analyses are performed to simulate the expected operational scenarios and to observe if there is a risk of system failure [10]. These simulations are generally performed day-ahead and evaluated in terms of frequency stability, voltage stability, rotor angle stability, N-1 criteria etc. These analyses cause huge amount of computational burden due to the number of case that TSOs need to perform. In addition, the modelling of the components in the power system is another factor affects the simulation time. The majority of the analysis performed by TSOs are performed in RMS domain thanks to its advantages. The first advantage of RMS simulation is that it faster than EMT simulations, as the EMT models are highly complex vendor specif models compared to generic models. The second is that it traditionally and historically has provided reliable results for power system stability analysis [11].

1.2 Objectives

Grid forming control is a potential solution for forming a grid when conventional power plants are decommissioned from power system. Considering the need for grid-forming controls and the role of TSOs, the objective of this project is to build an RMS model of a grid-forming converter. With the RMS model, TSOs can perform system analysis where grid forming units are present in their power system, and they can determine the requirements in grid forming integration. The introduced model will serve as a screening model for TSOs. In addition, the methods to improve the performance and reliability of a power system with GF converter will be investigated. In this context, a battery energy storage system (BESS) and a method to regulate system frequency are introduced for GF converters through the report.

1.3 Methodology

A generic RMS model of GF converter is built in this study utilizing the PWM converter model in DIgSILENT PowerFactory. A cascaded voltage and current controller is applied via DSL models to the converter. The project will introduce a complete GF system, which includes a droop control based GF converter, a RES, a DC link capacitor and a BESS. The GF system will be implemented in a simple power system to analyse its behaviour. Then two additional method for frequency regulation will be introduced based on adaptive droop control. The BESSs aide to the DC bus voltage stability will be analysed. The introduced model will be analysed by several simulations and results will be evaluated from both power system and GF system point of view.

1.4 Delimitation and Scope

The project aims to built an RMS model of GF converter for classical power system stability studies. Modelling concerns regrading switching and transients are not considered. The control of the elements in the project are modelled by DIgSILENT simulation language (DSL) modelling in DIgSILENT PowerFactory but the equipment are chosen from the standard library. The measurement delays in the control systems are neglected in modelling.The simulations of the built models are performed in fundamental frequency and in a balanced network.

1.5 Content of the Report

In Chapter 2, the importance of a SG generator and GF converter strategy are introduced. Difference between the EMT and RMS analysis are highlighted. In Chapter 3,the system design and controls of the individual elements in the system are presented. In Chapter 4, the performance of the systems is evaluated. In Chapter 5, the choices and decisions made during the project are discussed. In Chapter 6 the main conclusions are summarised.

2 State of the Art

The advancements in the technology and the EU goals regarding decreasing carbon emissions led to an increase in the share of the RESs in electrical power system, and consequently to decommissioning of conventional power plants. Conventional power plants mostly consist of large SGs, and SGs are known to their capability of providing ancillary services to the power system. With the removal of conventional power plants, the operation of power system becomes more challenging.

In this Chapter, firstly the importance of SGs from power system stability point of view will be introduced together with the frequency and voltage stability. Then, grid-forming converter and virtual synchronous generator strategies will be introduced and discussed as a new control strategies for RESs.

2.1 Synchronous Generator - From Power System Stability Point of View

A SG can be shortly defined as an electrical machine which is a rotating mass and excited by a controlled circuit. These two features of a SG are important parameters for power system operation. Inertia is a resistance against a change in frequency in a electrical system, and mass of a SG provides inertia. On the other hand, excitation of a SG is a parameter to control the reactive power output of a SG, and reactive power is an important parameter on voltage stability.

The swing equation shown in Eq. 2.1 introduces the relation between the angular frequency deviation and torque difference between mechanical input and electrical output of a SG [5]. In the equation, T_m, T_e, D, H, w_s and w stand for mechanical torque, electrical torque, damping coefficient, inertia constant, angular frequency of the grid and angular frequency difference between SG and grid, respectively. Based on this equation, the variation in angular frequency, dw_s/dt, is inversely proportional to the inertia. Briefly, higher the inertia, lower the frequency deviation.

$$T_m - T_e - D \cdot w = \frac{2H}{w_s} \cdot \frac{dw_s}{dt} \tag{2.1}$$

The stages of frequency stability of a power system after a grid disturbance are displayed in Fig. 2.1. The first stage is inertial response where the dynamic changes can be explained by the previously explained swing equation. At this stage, the load demand in the system changes suddenly. As a result, electrical torque in the SGs change and it results in a deviation in the system frequency. This deviation on the frequency is strongly dependent to the system inertia. Then a primary control, which is a droop control, responses against the frequency deviation in the system. The deviation in the frequency stops after primary control acts. Then, secondary control acts to restore the system frequency back to its nominal. This stage operates slower than the primary control. After the system frequency is restored, tertiary control redistributes the operational commands for power plants. The main criteria of operational set point is based on economical aspects.

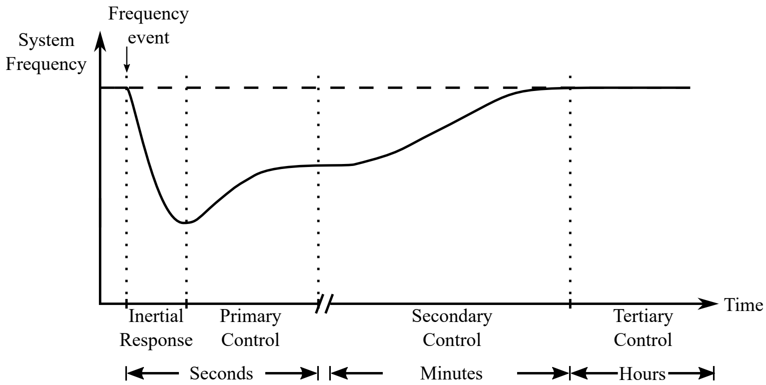

Figure 2.1: Stages of frequency stability after a grid disturbance [2].

A generic frequency droop curve is shown in Fig. 2.2 and can be expressed by Eq. 2.2 [5]. In the equation, P_{set}, P_{el}, R, w^* and w_{el} stand for active power set-point, electrical power output, slope, nominal frequency and electrical frequency, respectively. Based on the Eq. 2.2 the electrical output of a SG acts in an opposite direction of the electrical frequency. System frequency decreases when loading increases, and vice versa. With this method, several SGs operate in parallel and share the load based on droop characteristics without any communication requirement.

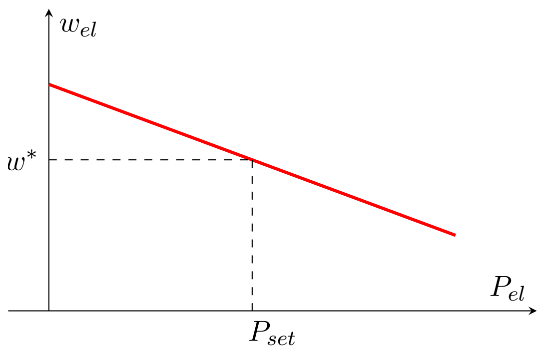

Figure 2.2: Droop curve of external grid.

$$P_{set} - P_{el} = -\frac{1}{R} \cdot (w^* - w_{el}) \tag{2.2}$$

Voltage stability is the other important concern in power system. One criteria for the voltage stability is that a bus voltage rises/reduces with an increase/decrease in the reactive power injection to the bus [5]. This effect also can be seen in power flow equation given in Eq. 2.3, when the cables have high reactance/resistance ratio. Here V_s and V_r are sending and receiving end RMS voltage magnitudes, Z is a line impedance and ϕ is an angle difference between two buses. From the equation, it can be said that injecting more reactive power to a bus results in an increase in V_s.

$$Q = \frac{V_s V_r \cos\phi - V_r^2}{Z} \cong \frac{V_s V_r - V_r^2}{Z} \tag{2.3}$$

Droop control is also commonly implemented strategy to control the bus voltages, as shown in the Fig. 2.3. Eq. 2.4 formulates the relationship between the reactive power output and bus voltage, where Q_{set} is reactive power set-point, Q is actual reactive power, V^* and V are nominal and actual voltages and n is the droop gain.

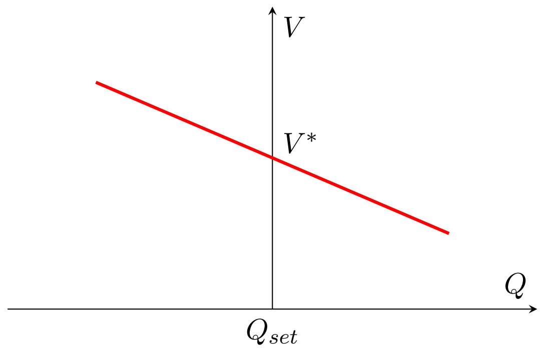

Figure 2.3: Droop curve of external grid.

$$(Q_{set} - Q) = \frac{1}{n} \cdot (V^* - V) \tag{2.4}$$

2.2 Grid Forming

Grid forming converter is an emerging control strategy for power electronic interfaced generation units. Conventional control strategies for RES connection are based on grid following control, where the control is designed to deliver the active and reactive power based on its set-points by following the grid via a phase locked loop [8]. In this strategy, dispatched active and reactive power set-points are converted into current references and the converter is controlled via a current control loop, consequently this type of converter acts as a current source, as displayed in Fig. 2.4 [8]. Although grid following control is a convenient application for RES integration, it is not the best control method from the power stability point of view as it focus on delivering the active and reactive power instead of supporting the system. However, it is possible to support the system by a higher level of control by setting the active and reactive set-points based on the power system requirements [8]. On the other hand, grid forming converter utilizes voltage and frequency set-points to form a grid. With voltage and frequency input, it is not possible to control the converter with commonly used current control loop as it requires active and reactive power set-point. Therefore, grid forming converters are implemented with a voltage control loops and this type of converters act as a voltage source, as shown in Fig. 2.4.

A grid forming converter can perform a standalone operation and this type of control is mainly for islanded operations. However, the situation alters for grid forming units in

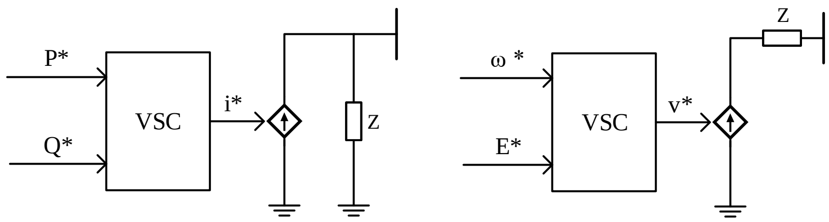

Figure 2.4: Representation of grid following and grid forming converters.

the transmission system level. The first difference is that the transmission system will be under operation with many other generation units, therefore grid forming converter cannot create a new reference voltage and frequency as it does in microgrid. The second difference is that there will be multiple generation units connected to grid, and these converters need to operate in parallel similar to operations of parallel connected SGs. The grid forming strategy shown in Fig. 2.5 receives additional active and reactive power reference together with voltage and frequency. In this strategy, output frequency and voltage of the converter are controlled together with active and reactive power and their respective control loops, which is most likely a droop control. The droop implementation enables multiple grid forming unit to operate in parallel similar to the operation of SGs. The ability of a converter on supporting system stability is significantly dependent on the applied control for active and reactive power. Same internal converter control strategy applied to a grid forming can be also applied to droop based grid forming converter, as they both have the same inputs, frequency and voltage.

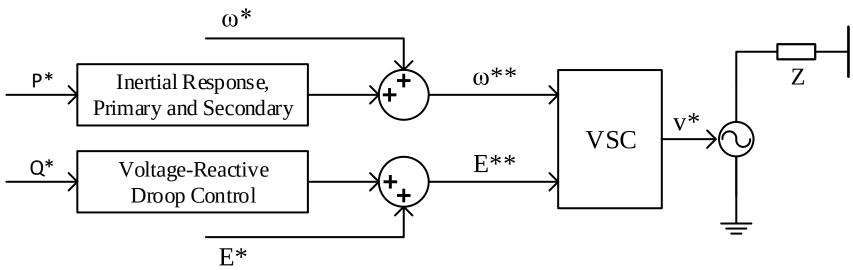

Figure 2.5: Representation of droop based grid forming converter.

Virtual Synchronous Generator

Virtual synchronous generator (VSG) is another control strategy which can be implemented as a grid forming. The main objective of the control strategy is emulating the behaviour of SGs by converter. A generic control scheme for a VSG is shown in Fig. 2.6.

Virtual inertial response block, which is the area highlighted by light green in the figure, contains of the equations regarding dynamic behaviour of a SG. The power and angular frequency relationship in the block is based on the swing equation of a SG, given in Eq. 2.1. The block receives power set-point, which is the equivalence of mechanical power input in real SG, and it compares the power set-point with the measured value. Based on the error, the virtual inertia block emulates acceleration or deceleration in the angular

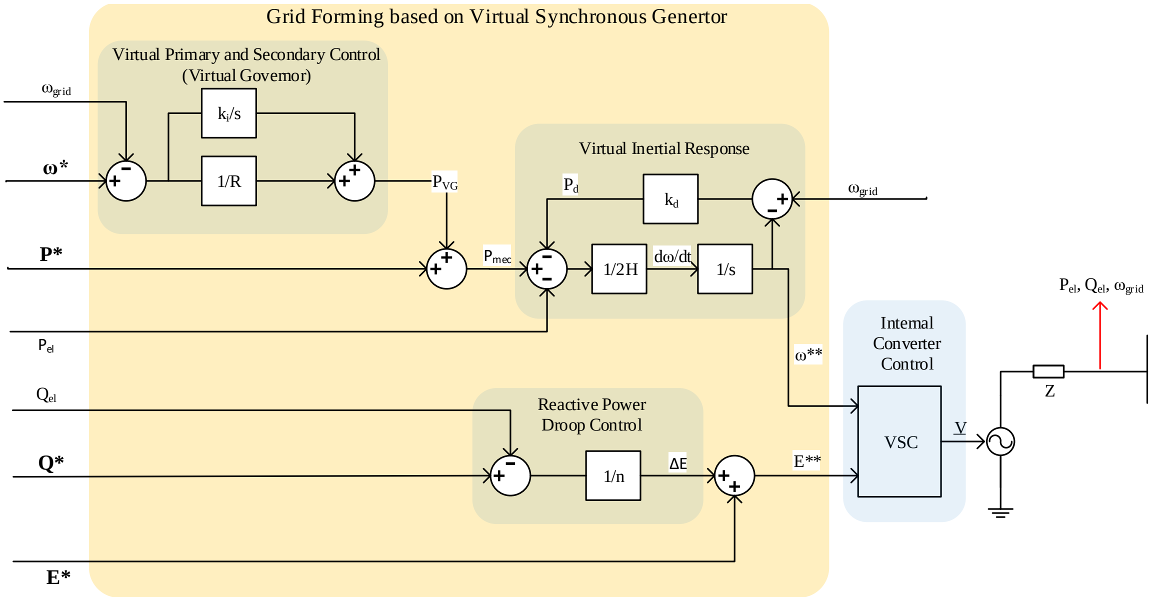

Figure 2.6: Layout of virtual synchronous generator based grid-forming control.

velocity in relation with the defined inertia constant. The acceleration or deceleration in the angular velocity remains temporally and the speed of the converter becomes equal to the grid again, when the error between power set-point and electrical output goes back to 0. The upper signal in the virtual inertia block is the damping signal, which tends to equalize the angular velocity of the converter with the existing grid. This signal, or the damping windings in a SG, prevents the angular speed of the converter to differ largely from the existing grid during the acceleration or deceleration as a consequence of system event, so that the generator does not lose its synchronization.

The electrical power output of a SG or a converter can be explained by active power flow equation shown in Eq. 2.5, where P, V_s, V_r, Z and ϕ are the active power output, sending end voltage, receiving end voltage, line impedance and load angle, respectively. This equation is valid only when line reactance is much higher than line resistance [8], and the cables in this project will be selected with high X/R ratio as it is the typical case in the transmission system. From the Eq. 2.5 it can be observed that the power flow is strongly dependent to the angle difference between to bus. During the moment of acceleration and deceleration in the angular speed of the converter becomes different than the grid and this results in change in the phasor angle of the bus. Electrical power output changes together with the change in the phasor angle, and it approaches to its set-point.

$$P = \frac{V_s V_r}{Z} \sin\phi \cong \frac{V_s V_r}{Z}\phi \tag{2.5}$$

VSG control can also be applied a primary response and secondary response control. A virtual governor is displayed in Fig 2.6. which has the primary and secondary response. The primary response is based on the droop control displayed in Fig. 2.2. The secondary control is an integral action which receives the error between the frequency set-point and frequency measurement. The outputs of the both primary and secondary controls are power and the virtual governor block outputs a power reference. This power reference adds up with the power set-point and the final power set-point is delivered to the virtual inertia block.

A VSG control with a primary response and a GF control with droop control have two different approaches in terms of the droop control. A GF converter does not provide a direct control on the active power. It acts as voltage source and based on the loading on the GF converter it adjusts its angular velocity of the AC voltage. On the other hand, A VSG has a direct control on the electrical output. The primary response receives the grid frequency and using the droop curve it changes the electrical power output set-point. Also, the second difference is appears in virtual inertia. A VSG control consists a virtual inertia block based on swing equation of a SG. For a GF converter, the response of the droop control is directly connected to the reference angular velocity inputs of the converter. Therefore, any change in the electrical power output is immediately delivered to converter control and there is no inertia. Although the GF control is mostly introduced together with classical droop control, it is possible to implemented virtual inertia. A method for implementation of virtual inertial which is equivalence of the virtual inertia in VSG control is introduced in [12].

This project was initiated by modelling the VSG control strategy. Firstly, it was implemented to an ideal controlled voltage source. Then the converter controller, which is a cascaded voltage and current controller, was built, and the VSG control is implemented to this converter controller. The model was analysed in both RMS analysis and EMT analysis. The initial results showed that the secondary control becomes dominant in the analysis and it is not convenient to analyse the operation of GF converter in parallel with other generation units, because secondary control continuously updates the electrical power output till the system frequency goes back to 50 $[Hz]$. In the following stages of the project, it is decided to implemented a droop controls, which are introduced in Section 2.2, instead of VSG. Both strategy are able to run a grid-forming converter control, therefore the built cascaded voltage and current controller kept same. The following Chapters will introduce the models and simulation regarding GF converter with droop control. However, the simulation results from the initial models with VSG control are presented in Appendix A.

2.3 RMS vs EMT

Transients, stability analyzes and dynamic control problems are important throughout modern power systems planning, design, and operation. TSOs develop various modelling strategies for operational and planning studies, which can be classified as follows [13],

- Long term Planning : The main objective of this study is to analyse the capability of grid for future scenarios and to evaluate various expansion plans. These studies focuses on power flow and fault analysis, although RMS analysis is done to analyse the long-term dynamic issues and robustness of future expansions.
- New Connection studies : This study is used to asses the impact of the new connection in the network and to verify the technical requirement compliance. During this process various models such as detailed vendor-specific EMT model, reduced vendor-specific EMT model, reduced vendor-specific RMS model and generic RMS

model could be used.

- Operational planning : This study is used to analyse network outage planning based on power flow, fault analysis with occasional dynamic simulation at critical transmission circuit outage. The stability analysis in this study is evolving into more complex dynamic study to adapt to the distributed generation units.
- Real-time studies : This study is used to analyse the situations and acts as a decision support tool for real time power system operation.

The transient in power systems are classified into three categories based on their time frame as [14],

- Short term or Electro-magnetic transients
- Mid term or Electro-mechanical transients
- Long term transients

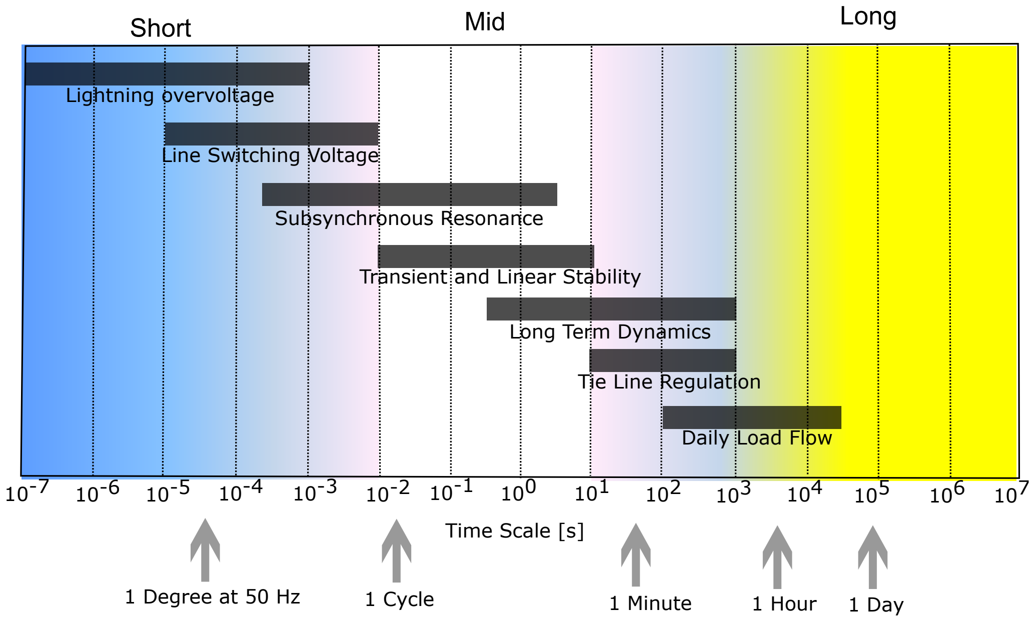

Figure 2.7: Time-frame Classification of Electrical Power Systems.

In EMT analysis, the instantaneous values of every phase is simulated and is used to perform various studies such as Dynamic Performance studies, Sub Synchronous Transient Interaction studies, Etc. While the vector magnitudes are simulated with the RMS analysis and is used in planning and classical stability studies. The RMS analysis is represented in the positive, negative and zero sequences in the unbalanced case, with the option of including only positive sequences in symmetric analysis. The benefit of using an RMS simulation is that the simulation time relative to an EMT simulation is significantly reduced. The improved simulation speed makes it possible to model longer events and far more complex systems [13]. In RMS analysis the transient oscillations within a cycle of operations are neglected.

RMS models are targeted to realize large scale power system analyses as they are simplified in terms of complexity and number of modelling components and hence computationally more efficient than electromagnetic transient (EMT) models, while capturing the sufficient representation of the related dynamics. RMS analysis are still likely to be used for the years to come because EMT models are more complex and detailed which increases the computational burden. It would take a significant development in the system to shift to EMT analysis. The reliability of RMS simulations should be re-evaluated for a power system where it is dominated by power electronic interfaced generation units.

System Modelling 3

GF control is a potential solution for the emerging power system stability issues of future power system. The aim of this Chapter is to introduce a simple power system with a GF converter. The introduced power system includes an external grid (EG), cables, loads and a GF converter. The introduced system will be used to analyse the behaviour of the GF converter during system disturbances.

The GF converter and the renewable energy power plant (REPP) is aimed to be a generic model. During the report, the important parameters for the operation of the GF converter will be highlighted.

The introduced models are designed to investigate the behaviour of the GF converter power system stability point of view. Therefore, potential harmonic emission from GF converter and its effects are not investigated. The models are design to perform with fundamental frequency positive sequence network.

3.1 Power System

GF converter are expected to operate in parallel with other units in a large power system. For simplicity, a simple power system with an external grid connection is introduced for this study. The other elements in the system are loads, a GF converter, a REPP, AC and DC cables, DC link capacitor and a BESS, as displayed in Fig. 3.1.

The EG is selected as slack bus in the system. It behaves as a voltage source behind its series connected impedance. It is implemented with a droop control, displayed in Fig. 3.2, with zero active power at nominal frequency. It would have given a power set-point when it crosses 50 $[Hz]$ but the DIgSILENT PowerFactory does not provide flexibility when an EG is selected as slack bus. Therefore, when power flows from external grid to the system,it operates below 50 $[Hz]$ and when power flows from the system to the EG, it operates above 50 $[Hz]$. Also for this study, operational frequency range of the system is considered from 48 $[Hz]$ to 52 $[Hz]$. Therefore the external grid reaches its nominal active power values at 48 $[Hz]$ and 52 $[Hz]$. The rate of change of the frequency is dependent on the inertia constant of the EG. EG will be the only element in the layout with inertial response. considering the increase number of RESs, system inertia gets lower. Considering this fact, a low inertia constant is selected for the external grid, which is 1 $[s]$. The parameters regarding EG and other elements in the layout are given in Table 3.1.

Two loads are used in the model. The first load is used to form the power flow in the system during the initialization of the system. The load is shared among the external grid and the GF unit based on the implemented droop characteristics. The second load is used

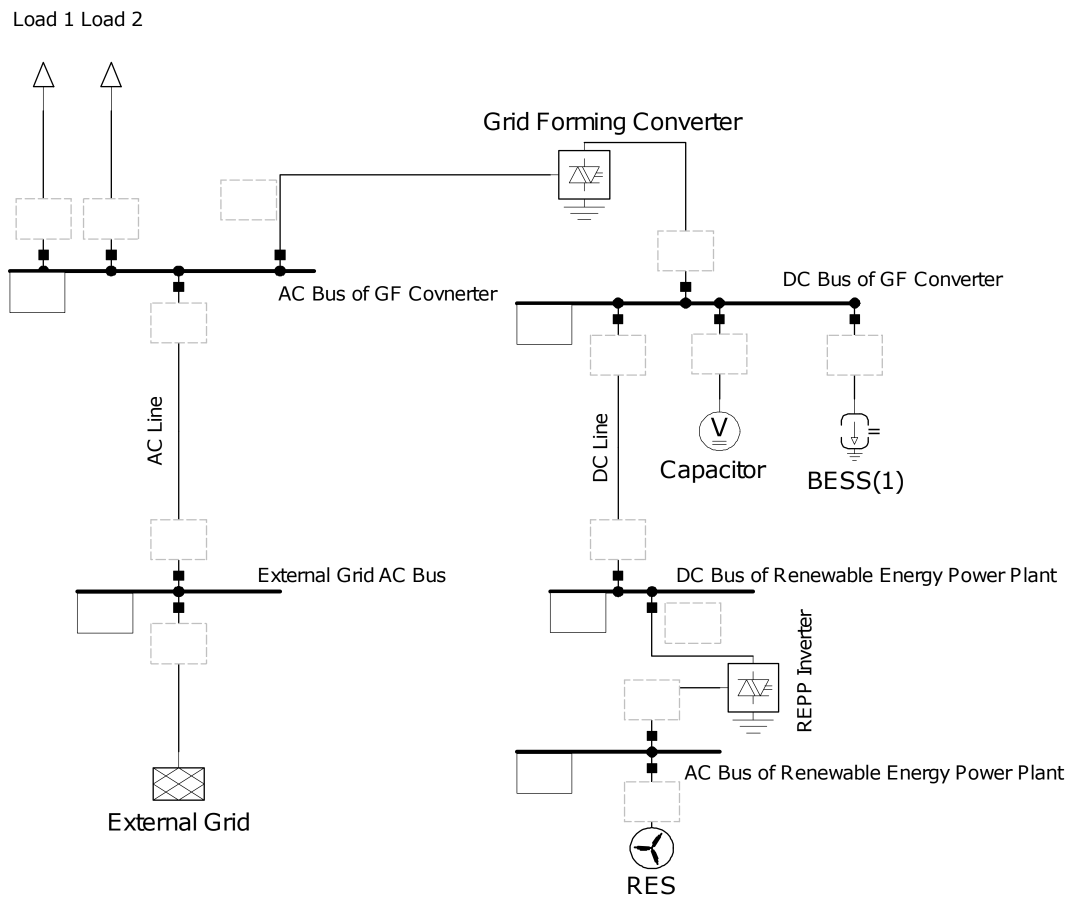

Figure 3.1: System layout.

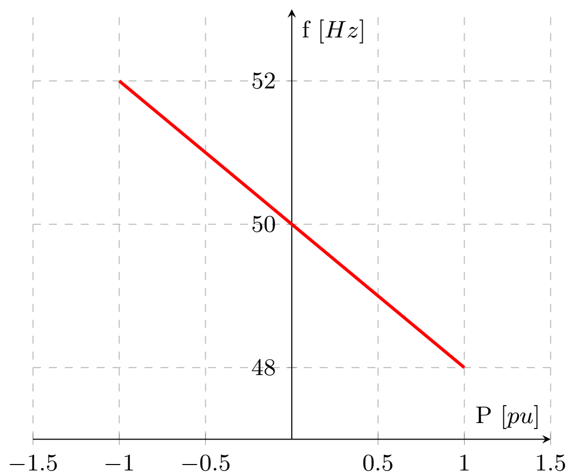

Figure 3.2: Droop curve of external grid.

to simulate dynamic changes in the system and to observe the behaviour of the GF unit and its contribution to the power system stability. The magnitudes of these loads are given in Chapter 4.

A GF converter is connected to the AC bus where the loads are placed. The GF converter works similar to a SG. It acts as a voltage source and it shares the load with external grid based on implemented droop control. From the DC side, it is connected to DC line which is the link between the GF converter and the REPP. A shunt capacitor is connected to the DC bus of the GF converter to maintain more stable voltage. The main task of the GF unit is to form the voltage at the AC bus where it is connected to.

A second inverter is placed between the DC link and the AC bus of the REPP. This inverter is responsible of forming the AC grid for power plant. Each RES is modelled as current source model and it follows the existing grid formed by REPP inverter to deliver the active and reactive power.

Grid Parameters	
External grid (EG) apparent power	2 [MVA]
GF inverter apparent power	1 [MVA]
AC cable resistance	0.026 [Ohm]
AC cable reactance	0.113 [Ohm]
DC link capacitance	10 [F]
WPP apparent power	1 [MVA]
WPP Inverter apparent power	1 [MVA]
DC cable resistance	0.039 [Ohm]
Inertia constant of EG	1 [s]

Table 3.1: Power system parameters.

3.2 High Level Control

Elements in the considered power system are introduced in Section 3.1. These components are controlled by their own dedicated control strategies and a high-level control. The main task of the high-level control is to manage the power flow among the GF unit, DC link capacitor and RES. The control diagram is displayed in Fig. 3.3

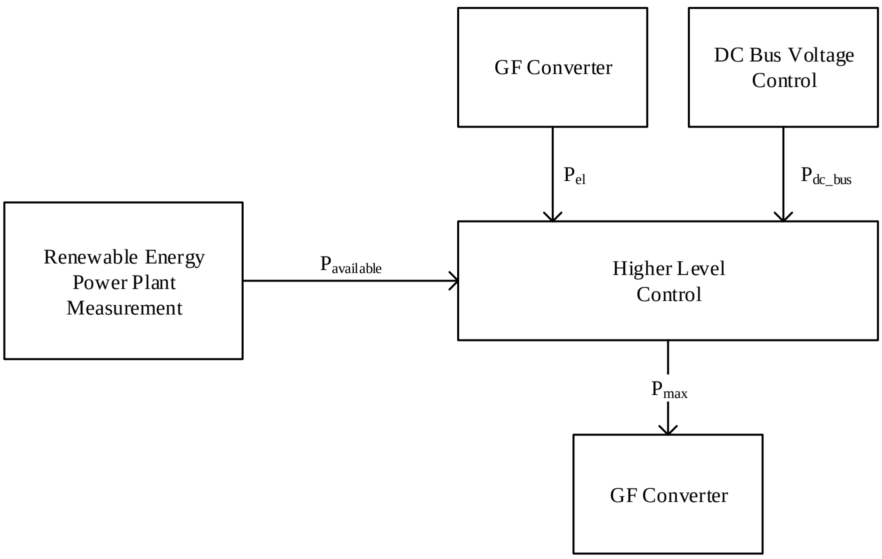

Figure 3.3: High level control diagram.

Some of the REPP have fluctuating power sources such as wind and solar irradiation profiles. The maximum available power at a renewable power plant should be high enough to respond the power demand from GF unit, otherwise the GF system may collapse and power plant trips. Therefore, one of the input in the high level control is the maximum available power at the RES. The power flow from RES can be summarized as combination of the power delivered to GF converter and DC link capacitor. The aim of the first power is to answer the power demand that the power system needs, and the second is to control the DC link voltages.

Based on the these power relations, the other two inputs for the higher control are the electrical power output of the GF converter and the power reference to control the DC bus voltage, labeled as P_{el} and P_{dc_bus}. The priority is given to controlling the DC bus voltage, because any voltage collapse at the DC bus would be seen by the AC side of the GF converter and it may cause disconnection of the GF converter. The control of DC bus voltage including how to obtain P_{dc_bus} is explained in Section 3.5. The power reference for DC bus voltage control is subtracted from the maximum power at the RES, Eq. 3.1, and the remaining power is set as the maximum power, P_{max}, at the droop curve of GF. In Fig. 3.4, the droop curve of the GF converter is displayed. Based on the Eq. 3.1, the power axis of the curve is scaled by P_{max}. The maximum power that a GF converter can deliver to power system at considered lowest operational frequency (48 $[Hz]$), can be controlled and overloading the RES can be avoided.

$$P_{max} = P_{available} - P_{dc\_bus} \tag{3.1}$$

In addition to parameters explained above, two important control constrains are also implemented. Firstly, a maximum and minimum power limits, $\pm P_{max\_dc\_bus}$, are applied to P_{dc_bus}. By this way, the maximum power point of GF converter's droop curve does not decrease significantly. With the limitations, the RES will be able to both restore the DC link voltage and deliver power to the grid. Secondly, ramp rate limiters for both GF converter and DC bus voltage control input, $P_{el\_ramp\_max}$ and $P_{dc\_bus\_ramp\_max}$, are implemented for power set-points of RES, P_{RES}.

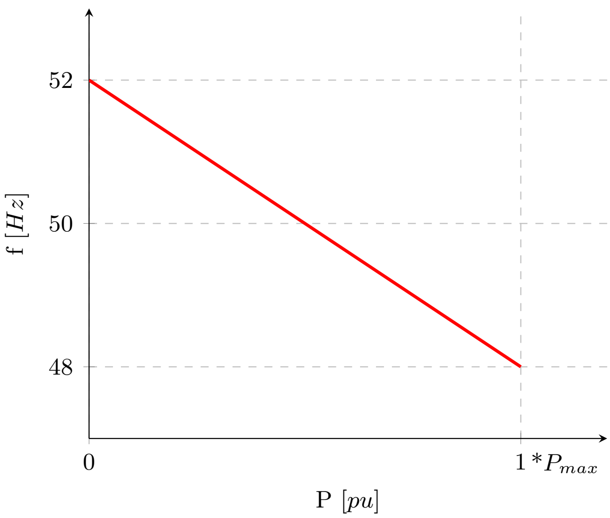

Figure 3.4: Droop curve of GF converter.

3.3 RES Control

The REPP in the project operates as a power source. Therefore, it is convenient to model RES as a aggregated current source model. The RES control receives active and reactive power setpoints, and AC bus voltage measurement data. Then the power set-points are converted to current setpoints by Eq. 3.2 and 3.3, where P_{set} and Q_{set} are the active and reactive power set-points, u_d, u_q, i_d, i_q are the d and q axis voltages and currents, and theta is the phasor angle. At the last step, the dq-axis currents are converted to positive sequence current by utilizing grid angle data, calculated by Eq. 3.4, where θ is the phasor angle. For simplicity, the synchronous reference frame of WTG control is aligned with grid voltage, which makes u_q 0, and reactive power is set to 0. Then i_d and i_q are calculated as Eq. 3.5 and 3.6. The control is performed by an open loop control as shown in Fig. 3.5.

$$P_{set} = u_d i_d + u_q i_q \tag{3.2}$$

$$Q_{set} = u_d i_q - u_q i_d \tag{3.3}$$

$$\theta = tan^{-1}\left(\frac{Im\{U_{ac}\}}{Re\{U_{ac}\}}\right) \tag{3.4}$$

$$i_d = \frac{P_{set}}{u_d} \tag{3.5}$$

$$i_q = 0 \tag{3.6}$$

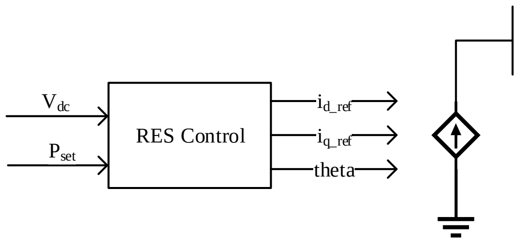

Figure 3.5: RES control diagram.

3.4 Renewable Energy Power Plant Inverter Control

The REPP consists of RES and the inverter, which connect the RES to DC bus of GF converter. The REPP inverter is responsible of forming the collection grid in the power plant. This collection grid is not connected to the main AC grid in the system and the inverter performs standalone operation. Therefore, it does not require any synchronization. For simplicity an open loop voltage control, displayed in Fig. 3.6. All the elements

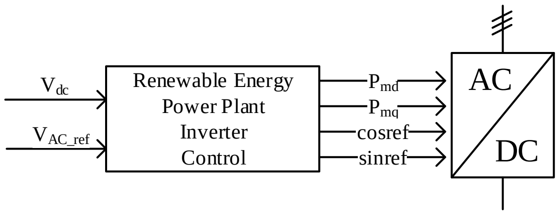

Figure 3.6: REPP inverter control diagram.

connected to this AC network work as current source and follow the grid created by power plant inverter.

The inverter is modelled by using the PWM converter model from the DIgSILENT PowerFactory library. The model utilizes the DC bus voltage to form the AC voltage. For operation, it requires inputs regarding modulation and angle to form the voltage magnitude and phase angle, respectively. The control loop receives the AC voltage set-point and DC bus voltage measurement data. Then it calculates the modulation index by using the relation between the AC and DC side voltage given by the Eq. 3.7, where U_{AC1}, U_{DC} and P_m are the positive sequence voltage, DC bus voltage and magnitude of modulation signal, respectively. The coefficient of 0.6124 is a modulation coefficient for sinusoidal modulation [15]. θ is the phase angle of the created voltage and it is calculated with a relation between given synchronous reference angle input, $sinref$ and $cosref$, and modulation signals, which are P_{md} and P_{mq}. Calculation of $cos\theta$, $sin\theta$, P_{md} and P_{mq} are given in Eq 3.8, 3.9, 3.10 and 3.11, respectively [15].

$$U_{AC1} = U_{DC} \cdot 0.6124 \cdot P_m \cdot (cos\theta + j \cdot sin\theta) \tag{3.7}$$

$$cos\theta = (P_{md} \cdot cosref - P_{mq} \cdot sinref)/Pm \tag{3.8}$$

$$sin\theta = (P_{md} \cdot sinref + P_{mq} \cdot cosref)/Pm \tag{3.9}$$

$$P_{md} = \frac{U_d}{U_{DC} \cdot 0.6124} \tag{3.10}$$

$$P_{mq} = \frac{U_q}{U_{DC} \cdot 0.6124} \tag{3.11}$$

The output voltage can be aligned with synchronous reference frame by setting U_q to 0. This can be achieved by setting P_{mq} as 0. Also, the synchronous reference frame can be aligned with 0 degree. Then $cosref$ and $sinref$ becomes 1 and 0, respectively. After these simplifications, the input signal of P_{md} can be expressas as;

$$P_{md} = \frac{U_{AC1}}{U_{DC} \cdot 0.6124} \tag{3.12}$$

PWM converter model receives P_{md}, P_{mq}, $sinref$ and $cosref$ signals and creates the U_{AC1} at the AC bus utilizing the Eq. 3.7.

3.5 DC Bus Voltage Control

The DC bus voltage is controlled at the DC side of the GF converter by controlling the capacitor voltage. The capacitor is modelled by a controlled voltage source. The reason is that the solver of the DIgSILENT PowerFactory requires reference nodes to initiate the analysis. The GF inverter (PWM Converter model from the DIgSILENT PowerFactory library) isolates the elements on the DC side of the GF inverter from the AC side where the external grid is a reference node. Therefore, a reference node (a voltage source) is needed for the DC side of the GF inverter to initiate the simulation as well as the DC cable, the REPP inverter and the RES.

The voltage source is controlled according to capacitor charge-voltage relation. The input of the control loop, displayed in Fig. 3.7, is the current through the capacitor. Then the current is integrated to calculate the stored charge in the capacitor. Then, the voltage is calculated by the Eq. 3.13 and given to the controlled voltage source as an input, where V is the calculated DC voltage, Q is the charge and C is the capacitance.

$$V = \frac{Q}{C} \tag{3.13}$$

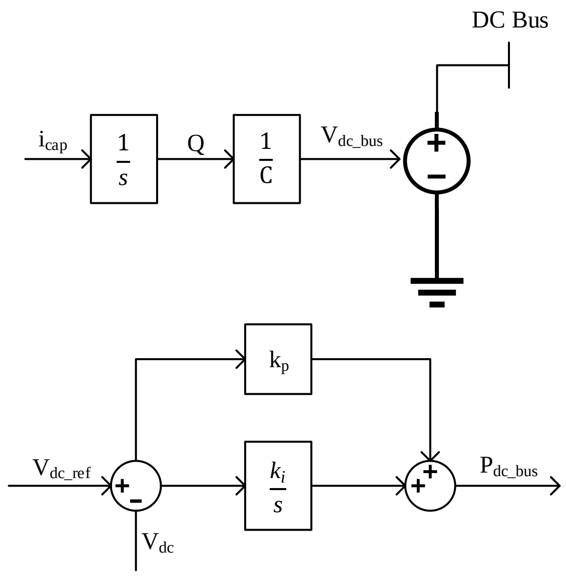

Figure 3.7: DC bus voltage control diagram.

The current following through the capacitor is a result of the DC bus voltage control, displayed in Fig. 3.7, placed in high-level control. The reference DC bus voltage is compared with the measured voltage and the error is calculated. The error is the inputs of the PI controller and the PI sets an additional power set-point to RES via higher level control. The control parameters are 10 and 1 for proportional, k_{p_dc}, and integrator, k_{i_dc}, respectively.

3.6 GF Converter Control

GF control is introduced in Section 2.2. Briefly, it is a control strategy to form an AC voltage and frequency. It can be implemented droop control and it can operate with other generation units in parallel like synchronous generators.

Fig. 3.8 displays the generic GF control scheme implemented in this project as an extended version of Fig. 2.5 including the PWM model and its corresponding signals. As it can be seen in the figure, the GF control includes two droop controls, which are frequency and voltage. The inputs of frequency droop is active power set-point, P_{set}, and electrical active power output, P_{el}. Based on these inputs, the frequency drop, Δw, is calculated using the Eq. 2.2. Then the electrical frequency, w^{**}, is calculated by subtracting the frequency drop from the nominal frequency, w^{*}. The inputs of voltage droop control are reactive power set-point, Q_{set}, and electrical reactive power output, Q_{el}. Based on these inputs, the voltage drop, ΔV, is calculated using the Eq. 2.4. Then the new voltage set-point, V^{**}, is calculated by subtracting the voltage drop from the nominal voltage, V^{*}. Following the droop controls, the internal GF converter control algorithm, which is a cascaded voltage and current controller, receives the new frequency and voltage set-points.

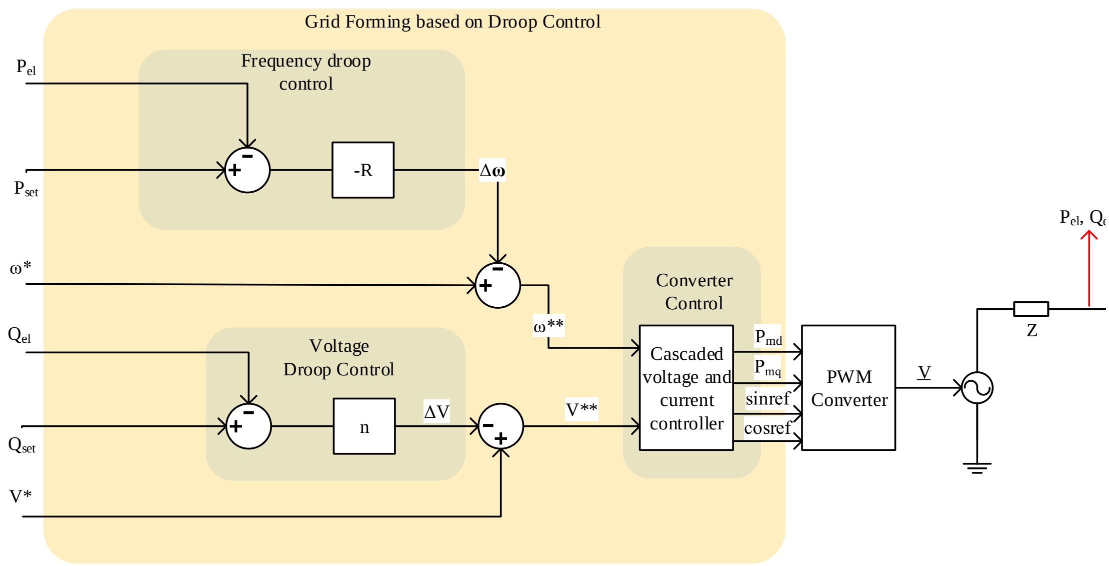

Figure 3.8: GF converter.

3.6.1 Cascaded Voltage and Current Controller

A cascaded voltage and current loop control is the main control strategy for a GF converter control [8]. Fig. 3.9 displays the implemented cascaded control in this project. The algorithm begins with voltage set-point received from external control. The voltage set-point is set as d-axis voltage reference and q-axis voltage reference is set to 0. Then the references are compared to measured voltage values. The error between the references and measured values are the inputs for voltage control loop. Voltage control loop creates the references for the inner current control loop. The inner current controller controls the current output and it creates a voltage deviation at the d- and q-axis voltage as outputs. At the end, the d- and q-axis voltage set-points, U_d and U_q, are obtained by summation of voltage measurements, deviation in voltage coming from the inner current controller and the cross element in current controller.

The GF converter is modelled using PWM converter in DIgSILENT PowerFactory. Equations regarding its operation are given in Section 3.4. Briefly, the input signals of the PWM converter model are P_{md}, P_{mq}, $sinref$ and $cosref$. Utilizing these control signals and DC input voltage it forms the AC voltage. The generic equations regarding operation of PWM converter are given in Eq. 3.7-3.11 in Section 3.4. Modulation parameters, P_{md} and P_{mq}, are calculated by Eq. 3.10 and Eq. 3.11 utilizing the obtained voltages, U_d and U_q.

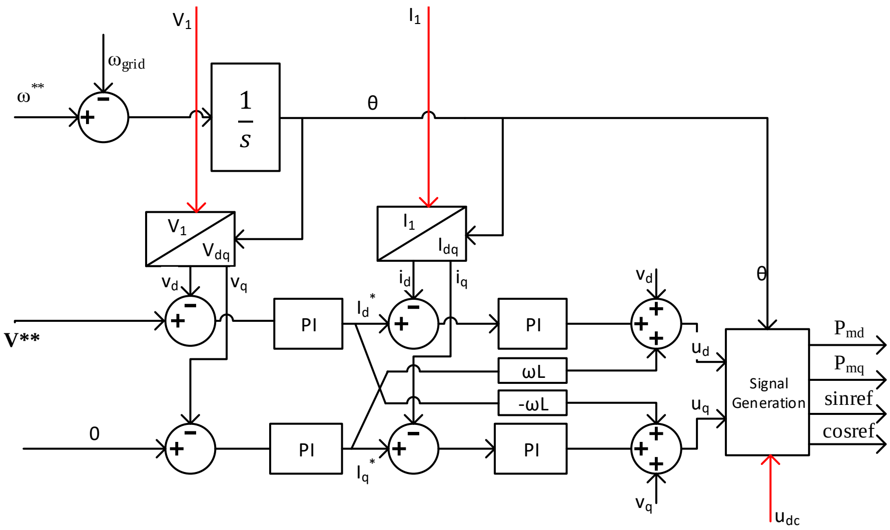

Figure 3.9: Internal converter control diagram.

The second input to the inverter controller is frequency. Normally, the angular frequency is integrated and angle data is obtained for the controller in EMT simulation, which goes from 0 to 360 degree. However, for a RMS simulation the method differs. In a RMS simulation, phasors are used, and these phasors do not rotate as angular velocity rotates. Therefore, a change in a phase angle can be calculated by integrating the difference between two frequency, instead of integrating the angular velocity of the phasor. If the calculated frequency for a considered phasor is higher or lower than the frequency where it is connected to, the phasor angle of the considered phasor increases or decreases by integrating the difference in the frequency. In Fig. 3.9, the angular velocity of the grid is subtracted from the angular velocity of the GF converter, and the difference is integrated to calculate the phase angle of voltage. Once the angle, θ, is obtained, it is used to calculate $sinref$ and $cosref$. Finally, P_{md}, P_{mq}, $sinref$ and $cosref$ are delivered to the PWM converter model and the model creates the AC bus voltage utilizing the DC connection and input signals. This controller can be easily modified to use in EMT simulations. w_{grid} can be removed from the model, or it can be multiplied by 0. Then the algorithm integrates the angular frequency of the converter and obtains the instantaneous phase angle.

3.7 Adaptive Droop Control

A droop control is a convenient control strategy for power system application which is capable of sharing loads among the generation units without communication requirement [16]. A droop control is implemented to a generation unit by a linear frequency-power curve, which can be formulated by Eq 3.14, where P_{set} is the power set-point for the droop curve, P_{el} is the electrical power output, R determines the slope, w^* is the nominal electrical frequency and w_{el} is the measured electrical frequency. Droop control provides frequency support to a system by contributing to the load sharing, however it can not provide further support for frequency control in the system as secondary control does in conventional systems.

$$P_{set} - P_{el} = -\frac{1}{R} \cdot (w^* - w_{el}) \tag{3.14}$$

One way to provide frequency support to a power system can be performed by implementing adaptive droop control. Adaptive droop control refers to a droop control strategy where a droop control curve is adjusted based on the state of a grid. In literature, different studies exist where an adaptive droop curve is utilized for different purposes, such as load sharing or improving the voltage stability of DC systems using the voltage-power droop curve [16]-[17][18][19][20]. The adjustments in the droop curve are called by several name in the papers such as adaptive droop curve, variable droop curve or variable droop coefficient. In this project, it is called as adaptive droop curve. In this project two different ways to adapt a frequency droop curve are considered. These are shifting a droop curve to right or left and changing the slope. The first one can be performed by adjusting the power set-point, P_{set}, and the second one can be performed by adjusting R in Eq. 3.14. Examples for these two adjusted curves and their reference curve are shown in Fig. 3.10.

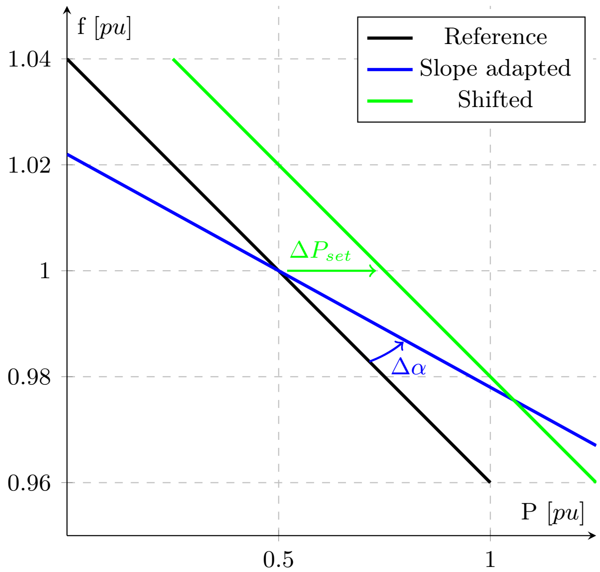

Figure 3.10: A droop curve and its variation based on slope or shifting.

3.7.1 Adaptive Droop Control - Shifting Method

A power set-point for a droop control refers to the power that it delivers to a grid at nominal frequency. By changing this power set-point, it is possible to move a droop curve to left or right side based on Eq. 3.14. An example is shown in Fig. 3.10 with green curve, and the change in the power set-point is displayed and named as ΔP_{set}. For this example, it is moved to right side.

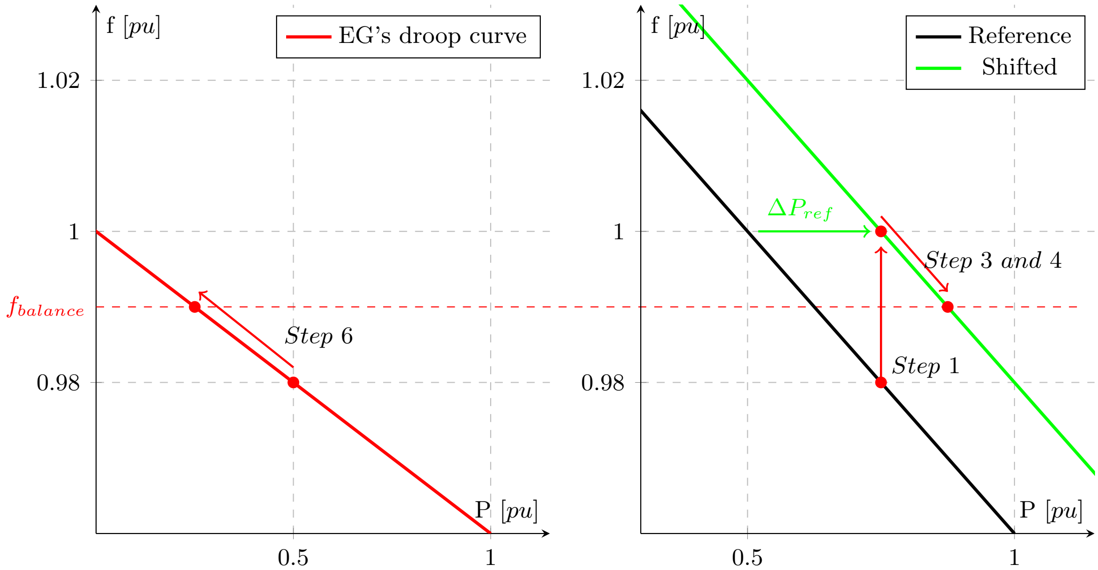

(a) A portion from external grid's droop curve in Fig. 3.2.

(b) A portion from adjusted droop curve in Fig. 3.10

Figure 3.11: The change in the electrical frequency as a result of changing power set-point.

As an example, the effect of moving a droop curve to right side at electrical frequency of 0.98 $[pu]$ (49 $[Hz]$) can be explained by following steps. For the explanation, the layout introduced in Section 3.1 is utilized, where there are two generation units; GF unit and external grid. A portion from these units' droop curves are given in Fig. 3.11 and the steps are displayed in the figure. It should be noted that R and w^* in Eq. 3.14 are constant for shifting method and are 0.08 and 1 $[pu]$, respectively. Also, w_{el} is lower than w^* ($w_{el}<w^*$) and P_{el} is higher than P_{set} ($P_{el}>P_{set}$) at this operation point for GF converter.

Step 1: P_{set} of GF converter is increased by user, and this results in an increase in electrical frequency, w_{el}, based on Eq. 3.14. Operation point moves to upward as shown in Fig. 3.11.

Step 2: The increase in electrical frequency makes the load angle of the GF converter larger.

Step 3: When the load angle increases, the electrical power output, P_{el}, increases based on the power flow equations, Eq. 2.5.

Step 4: While electrical power output increases, w_{el} start decreasing, based on Eq. 3.14.

Step 5: The system load is not changed. Therefore, when the electrical power output of the GF converter increases, and it decreases for the external grid.

Step 6: When electrical power output, P_{el}, decreases for the external grid, and electrical frequency increases, based on Eq. 3.14.

This relationship, where one generation unit increases its electrical power output and other decreases, continues till the new equilibrium point is found. Finally, the frequency of the system reaches a higher value than 49 $[Hz]$ after the droop curve is moved to right side.

For a droop curve moved to the left side of the reference curve, all the mentioned behaviour for a right-moved curve becomes opposite. Briefly, when the droop curve of the GF converter moves to left, it results in a decrease both in the electrical frequency and in the electrical output of the GF converter. The electrical output of the external grid increases. To sum up, the droop should move to left during over-frequency and to right side during under-frequency to support the system frequency, when an adaptive droop control is implemented by shifting method.

To obtain a proper operation with shifting method, some relevant parameters are defined to control the droop curve. Fig. 3.12 displays some of these parameter together with a reference and two shifted curve. These parameter are explained below.

- ΔP_{set}: ΔP_{set} is defined to express the variation in the P_{set} from its default setting.
- ΔF_{active} and ΔF_{reset}: ΔF_{active} and ΔF_{reset} are the two parameters which decide whether adaptive droop control should perform, or not. If electrical frequency is within the activation zone, which is above 1+ΔF_{active} and below 1-ΔF_{active} [pu], then the control activates and droop curve moves to left or right for over- and under-frequency, respectively. If electrical frequency is within the activation and resetting zone, the most recent droop curve is maintained. If electrical frequency is within the resetting zone, which is between 1+ΔF_{reset} and 1-ΔF_{reset} [pu], the droop curve moves towards to its reference curve, in other words ΔP_{set} goes to 0.
- ΔP_{set_max}: Another parameter regarding to shifting method is the maximum power range that variation in power set-point can reach, which is named as ΔP_{set_max}. In other words, it defines how far the droop curve can be moved from its reference curve. For this project, ΔP_{set_max} is defined same for positive and negative direction.
- $P_{min\_with\_\Delta P\_set}$ and $P_{max\_with\_\Delta P\_set}$: These two parameter defines the power range that adaptive droop control should operate without causing unwanted situations. For example, in Fig. 3.12, it can be seen that electrical power output can goes beyond 0 and become negative for left-moved curve when the frequency approaches to 52 [Hz]. For right-moved curve, it can go above 1 [pu] electrical power output and results in overloading when frequency approaches to 48 [Hz]. Briefly, while moving a droop curve supports system frequency, it can also cause overloading to generation unit or going into consumption mode at under and over frequency conditions, respectively. To avoid these two conditions, $P_{min\_with\_\Delta P\_set}$ and $P_{max\_with\_\Delta P\_set}$ are defined. The main objective of these two parameter are to define the operation range of adaptive droop control. With minimum generation point, $P_{min\_with\_\Delta P\_set}$, it can prevent the generation unit to goes into consumption mode. With maximum generation point, $P_{max\_with\_\Delta P\_set}$, it can prevent the generation unit to be overloaded. When the electrical power output across these two limits, the active droop control behaves like in resetting zone and ΔP_{set} goes towards to 0 and droop curve moves toward to its reference. However, it should be noted that these two parameters protects the GF converter against overloading and moving to consumption zone, only due to the effects of adaptive droop curve during over- and under-frequencies which was explained above. Regardless adaptive droop control in use or not, the standard protection functions should protect the GF unit against overloading and reverse power flow.

The control diagram regarding shifting method is shown in Fig. 3.13. The control is

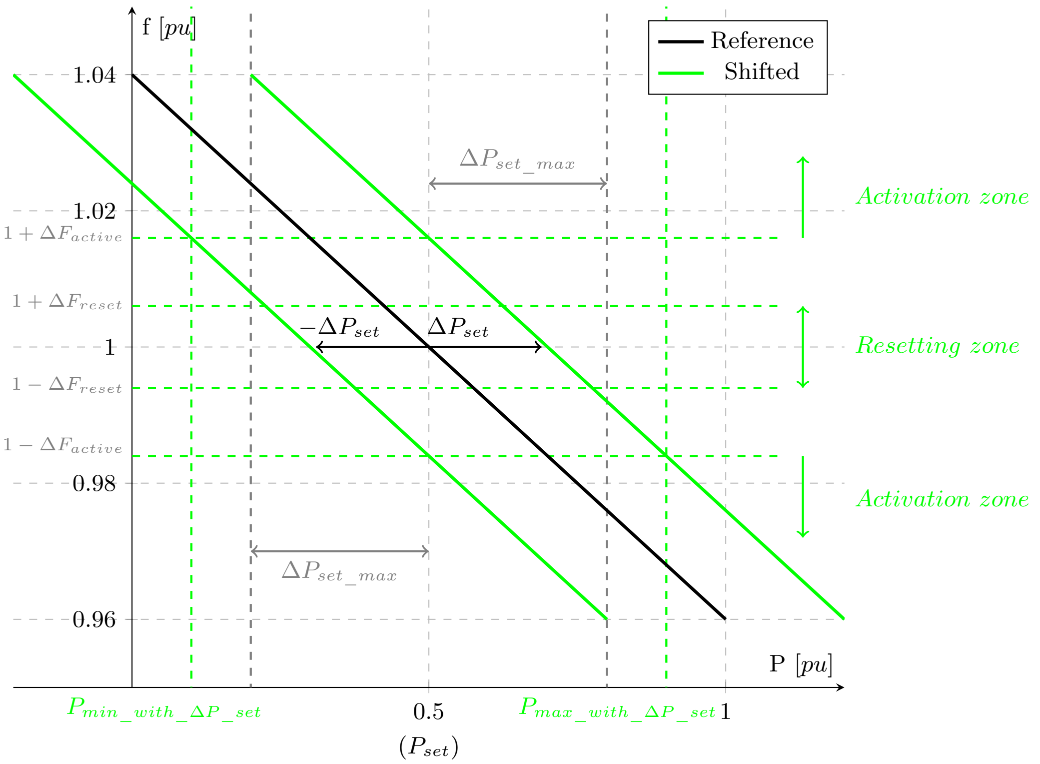

Figure 3.12: Droop curve with power set-point variation and important parameters.

designed as a combination of logical controls and an integral control. The logical controls are displayed as boxes in the figure. Based on the introduced method, three branches for three different movements are built. Logical controls are used to activate and deactivate the branches based on the status of the grid. The movements, in other words the branches in the control diagram, and their operations are explained below.

- Moving to Left: It defines the movement in the curve from its default to its left. It is activated when the frequency is above 50+ΔF_{active} $[Hz]$ and electrical power output higher than $P_{min\_with\_\Delta P\_set}$. When this branch is activated via the logical controls, it provides -1 to the system and ΔP_{set} goes negative values, which means movement in left direction.
- Moving to Right: It defines the movement in the curve from its default to its right. It is activated when the frequency is below 50-ΔF_{active} $[Hz]$ and electrical power output lower than $P_{max\_with\_\Delta P\_set}$. When this branch is activated via the logical controls, it provides +1 to the system and ΔP_{set} goes positive values, which means movement in right direction.
- Moving to Default: It defines the movement in the curve where it goes back to its nominal. There are three conditions for this. These are where electrical power output is lower than $P_{min\_with\_\Delta P\_set}$, where electrical power output is higher than $P_{max\_with\_\Delta P\_set}$, or where the frequency of the system is within the resetting zone. When this branch is activated via the logical controls, a close loop control with reference signal of 0 is activated, and it takes ΔP_{set} to 0.

The logical controls illustrated in Fig. 3.13 is explained in detail in Appendix B.

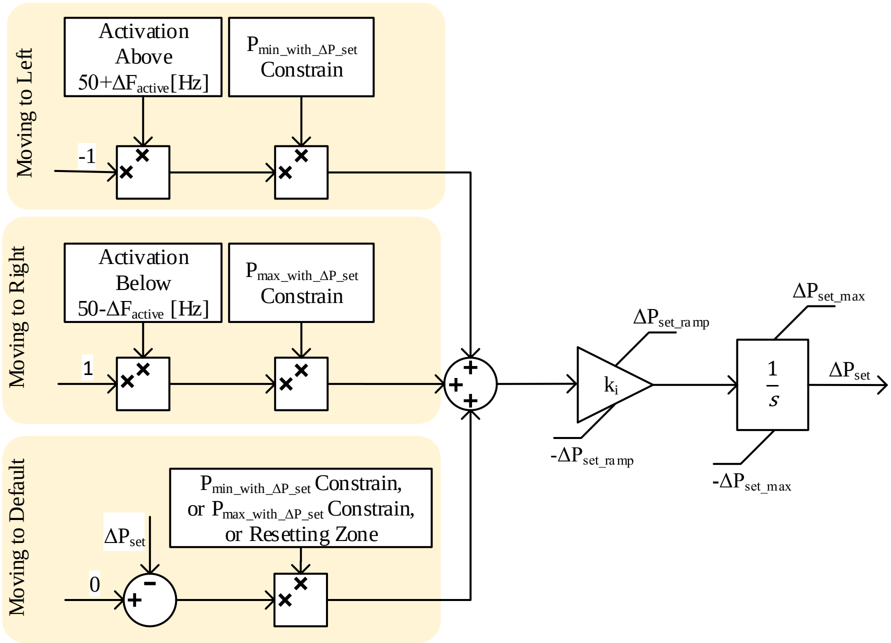

Figure 3.13: Control diagram of adaptive droop control shifting method.

A Second Look for High Level Control

The high level control is introduced in the earlier stages of this project. The main objective is to limit the maximum power that GF converter demand, so that GF converter would not demand more than RES can provide. The detailed explanation of this control is given in Section 3.2. After the adaptive droop control with shifting method was built in the project, similarities were observed between these two control. The effect of the high level control on the droop curve can be shown by Fig. 3.14. As it can be seen, the maximum power point moves left while the maximum power power is being limited by higher level control. This movement is not identical to the movement in the adaptive droop control shifting method where the droop curve moves left or right as parallel to its default. However, the movement in the curve in Fig. 3.14 is still similar to the movement in the adaptive droop curve shifting method because the curve still moves left or right in overall. As a result, high level control can cause similar dynamic changes in the system frequency as adaptive droop control shifting method does.

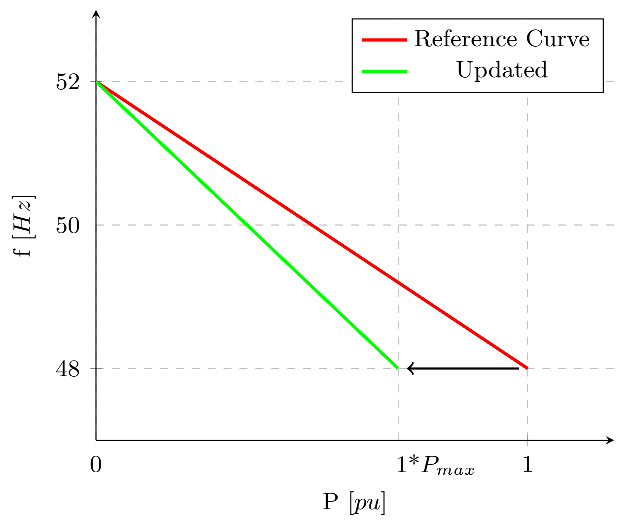

Figure 3.14: Droop curve of GF converter with the effect of high level control.

3.7.2 Adaptive Droop Control - Variable Slope Method

An adaptive droop control with variable slope method refers to a droop control where the power set-point is kept constant but the slope is variable. An example is shown in Fig. 3.10 with blue, and the change in the angle is shown by $\Delta\alpha$. As the power set-point is kept constant, the adapted blue curve intersects with the reference curve at power set-point. As a result of this, the curve moves to the right of the reference curve below 50 $[Hz]$, and to the left above 50 $[Hz]$.

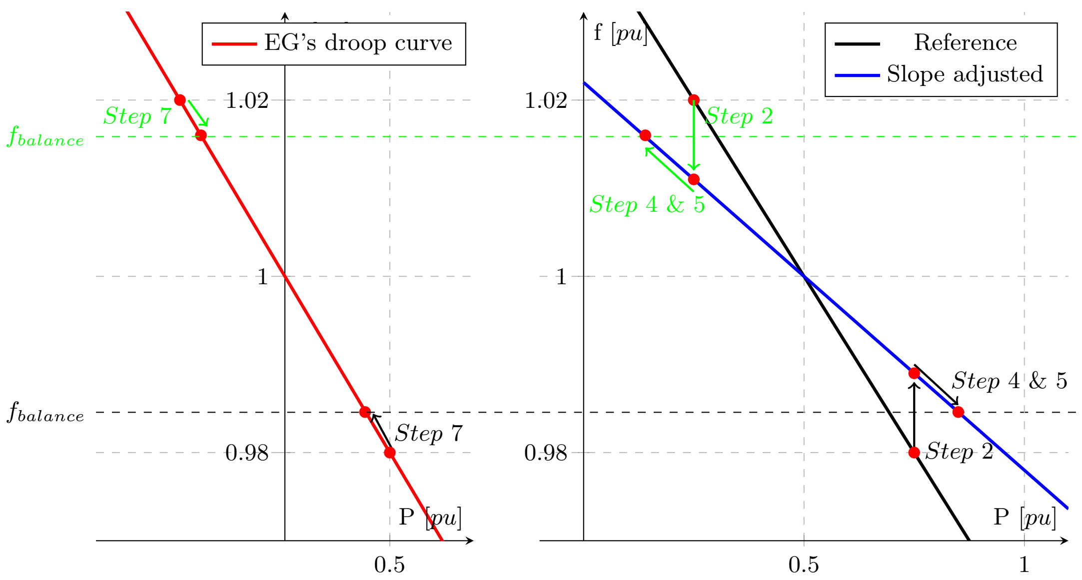

(a) A portion from external grid's droop curve in Fig. 3.2.

(b) A portion from adjusted droop curve in Fig. 3.10

Figure 3.15: The change in the electrical frequency as a result of changing power set-point.

As an example, the effect of changing the slope of a droop curve at electrical frequency of 49 $[Hz]$ can be explained by following steps. It should be noted that P_{set} and w^* in Eq. 3.14 are constants for variable slope method and are 0.5 $[pu]$ and 1 $[pu]$, respectively. Also,

w_{el} is lower than w^* (w_{el}<w^*) and P_{el} is higher than P_{set} (P_{el}>P_{set}) at this operation point for GF converter. The steps connected to the following explanations are marked with black in Fig. 3.15.
Step 1: If the slope of a droop curve is to be decreased by a user, as shown in Fig. 3.15, this is performed by decreasing R in Eq. 3.14.
Step 2: P_{set} and P_{el} are not changed in the system. Therefore, when R decreases, w_{el} increases based on Eq. 3.14.
Step 3: The increase in electrical frequency causes the load angle of the generation unit to get larger.
Step 4: When the load angle increases, the electrical power output, P_{el}, increases based on the power flow equations, Eq. 2.5.
Step 5: While electrical power output increases, w_{el} starts decreasing, based on Eq. 3.14.
Step 6: The system load is not changed. Therefore, when the electrical power output from one of the generation unit increases, other decreases.
Step 7: When electrical power output, P_{el}, decreases for the external grid, electrical frequency increases, based on Eq. 3.14.

This relationship, where one generation unit increases its electrical power output and other decreases, continues till the new frequency balance point is found. Finally, the frequency of the system reaches a higher value than 49 $[Hz]$ after the slope is reduced.

For an operation point above 50 $[Hz]$, the effect of changing the slope differs than the ones below 50 $[Hz]$. An example for 51 $[Hz]$ and the steps regarding system behaviour after changing the slopes are introduced below. It should be noted that, w_{el} is bigger than w^* (w_{el}>w^*) and P_{el} is lower than P_{set} (P_{el}<P_{set}) at this operation point for GF converter. The steps connected to the following explanations are marked with green in Fig. 3.15.
Step 1: If the slope of a droop curve is to be decreased by a user, as shown in Fig. 3.15, this is performed by decreasing R in Eq. 3.14.
Step 2: P_{set} and P_{el} are not changed in the system. Therefore, when R decreases, w_{el} decreases based on Eq. 3.14.
Step 3: The decrease in electrical frequency causes the load angle of the generation unit to get lower.
Step 4: When the load angle decreases, the electrical power output, P_{el}, decreases based on the power flow equations, Eq. 2.5.
Step 5: While electrical power output decreases, w_{el} starts increasing, based on Eq. 3.14.
Step 6: The system load is not changed. Therefore, when the electrical power output from one of the generation unit decreases, other increases.
Step 7: When electrical power output, P_{el}, increases for the external grid, electrical frequency decreases based on Eq. 3.14.

This relationship, where one generation unit decreases its electrical power output and other increases, continues till the new frequency balance point is found. Finally, the frequency of the system reaches a lower value than 51 $[Hz]$ after the slope is reduced. Briefly, reducing the slope of a droop curve helps electrical frequency to get closer to its nominal during both under- and over-frequency.

Some relevant parameter regarding operation with a variable slope method are illustrated in Fig. 3.16. These parameter are explained below.

- ΔF: Even though the main strategy is to adapt the slope of a droop curve, in this project it is performed by defining a variation in frequency, ΔF, from 0.96 $[pu]$ (48 $[Hz]$) where the generation unit delivers 1 $[pu]$ power in its reference curve, as shown in Fig. 3.16.
- ΔF_{active} and ΔF_{reset}: These two parameter operates as same they do in shifting method. If electrical frequency is within the activation zone, which is above 1+ΔF_{active} and below 1-ΔF_{active} $[Hz]$, then the control activates and the slope of a droop curve decreases, in other words ΔF increases. If electrical frequency within the activation and resetting zone, the most recent droop curve is maintained. If electrical frequency is within the resetting zone, which is between 1+ΔF_{reset} and 1-ΔF_{reset}, the slope of a droop curve moves towards to its reference curve, in other words ΔF goes to 0.
- ΔF_{max}: ΔF_{max} limits the maximum value that ΔF can reach.
- $P_{max\_with\_\Delta F}$ and $P_{min\_with\_\Delta F}$: As it is explained in the shifting method, changing droop curve can cause overloading during under-frequency, and moving into consumption mode during over-frequency conditions. To avoid the overloading and moving into consumption mode due to change in the droop curve, these two parameter, $P_{max\_with\_\Delta F}$ and $P_{min\_with\_\Delta F}$, are used to define the power range that adaptive droop control can perform. Therefore, when electrical power output across these two limits, the active drop control behaves like in resetting zone and the droop curve moves toward its reference, in other words ΔF goes to 0.

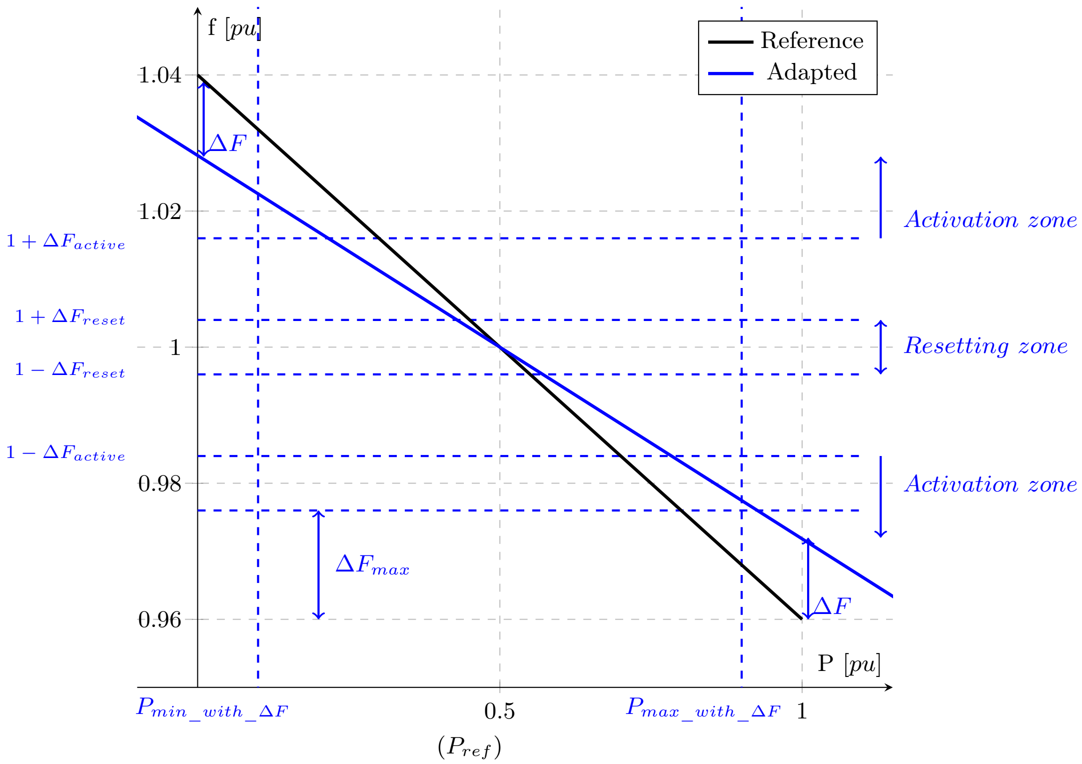

Figure 3.16: Droop curve with slope variation and important parameters.

The diagram regarding variable slope method is shown in Fig. 3.17. The control is designed as a combination of logical controls and a integral control. The logical controls are displayed as boxes in the figure. Based on the introduced method, two branches for two different movements in the curve are built. Logical controls are used to activate and deactivate the branches based on the status of the grid and GF converter. The movements, in other words the branches in the control diagram, and their operations are explained below.

- Decreasing the Slope: It defines the movement where ΔF increases. It is activated under two conditions, which the frequency should be either larger than $50+\Delta F_{active}$ or smaller than $50\text{-}\Delta F_{active}$, and for both condition the electrical output should be within $P_{max\_with\_\Delta F}$ and $P_{min\_with\_\Delta F}$. When this branch is activated via the logical controls, it prodived 1 to the control's input and ΔF increases, in other words slope decreases.
- Moving to Default: It defines the movement in the curve where it goes back to its nominal. There are three conditions for this. These are when electrical power output is lower than $P_{min\_with\_\Delta P\_set}$, or electrical power output is higher than $P_{max\_with\_\Delta P\_set}$, or the frequency of the system is within the resetting zone. When this branch is activated via the logical controls, a close loop control with reference signal of 0 is activated. It takes ΔF to 0.

The logical controls illustrated in Fig. 3.17 is explained in detail in Appendix B.

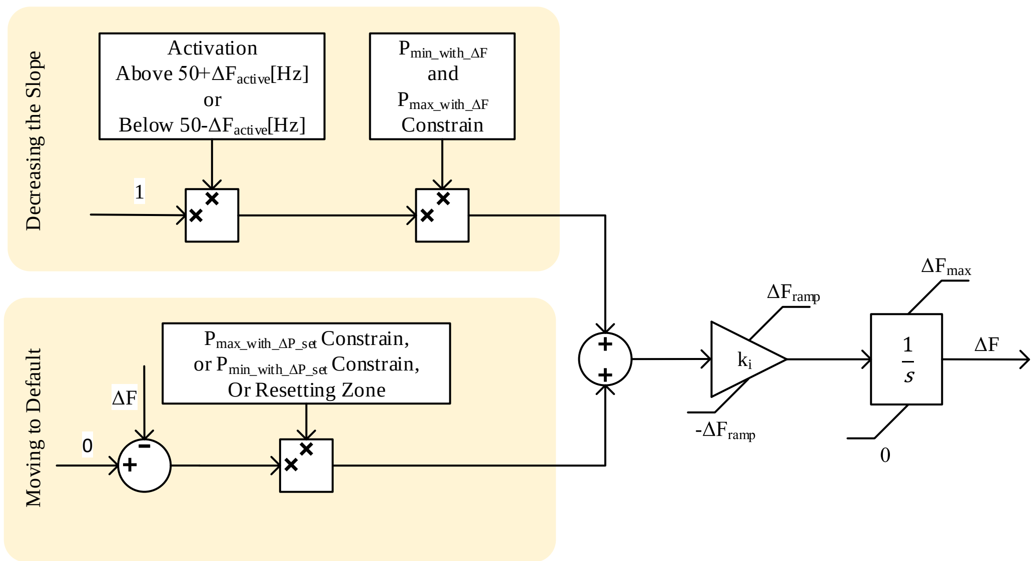

Figure 3.17: Control diagram of variable slope method.

3.8 Storage in DC Busbar

Typical battery energy storage system (BESS) consists of two parts. The first part is a storage element which stores/restores energy in an electro-chemical process. The second part is a power electronic interface controls power flow from or to a battery. The storage is connected to the DC bus of the GF converter. The position of the storage system to DC busbar is to provide a voltage support to the DC bus voltage maintenance and this not only reduces the response time delay in the system but also has an economical benefit considering that the DC-Dc converters are cheaper than the DC-AC converters. As discussed in Section 3.5, the DC side of the GF inverter is isolated from the AC grid. The response of DC bus voltage to dynamic change in system changes in stability analysis is an interesting case to be analysed. The analysis on the impact of stable DC voltage to dynamic disturbance in the system requires an approach where the storage is connected in parallel to the DC link capacitor. This study is mainly focused on the variation in dynamic system response to the different DC bus voltage regulating mechanism.

The BESS is modelled as a DC current source with simplified model considering the power output, Bus voltage and initial state of charge of the battery. The control schematic of the BESS is designed to maintain the DC bus voltage at its nominal value. The simplified model that could satisfy the requirements of the proposed design would act on the two input variables of DC bus voltage and the amount of power transferred from BESS. These two inputs contribute to the required calculation of state of charge of the battery and the corresponding current input to the DC current source.

The steps connected to the control scheme, displayed in Fig. 3.18, is as follows.
Step 1: Measure the voltage at the DC bus terminal and check if the state of charge of the battery is above the minimum level.
Step 2: The error signal of the measured bus voltage and nominal is passed through a PI control which generates a corresponding control signal to the DC current source.
Step 3: The power required from the BESS is provided to the system to make the DC bus voltage close to its nominal value without the state of charge reaching its minimum level.
Step 4: An integration of the power delivered is processed to determine the current state of charge, based on its initial value as displayed in Eq 3.15, where SOC_t and SOC_{t0} are the state of charge of the battery at t $[s]$ and initial moment, respectively.

$$SOC_t = SOC_{t0} + \frac{100}{RatedCapacity[kWh]} \int_{to}^{t} P(t)dt \tag{3.15}$$

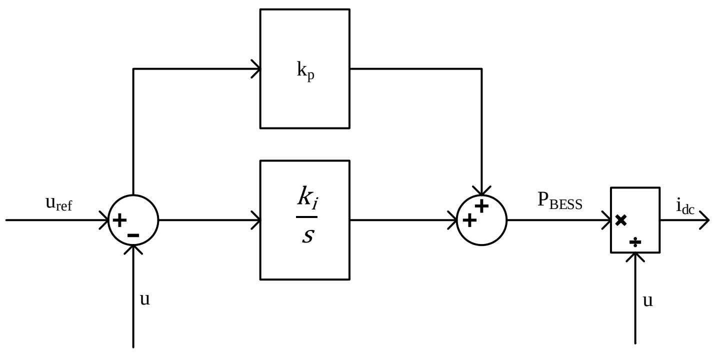

Figure 3.18: BESS control.

The BESS is modelled neglecting the charging schematic of the storage unit as it depends on many other factors of economical availability of power generation at renewable source. Two basic constraints are implemented. These are that the BESS could only consume active power if the battery is not fully charged, and the second is that the BESS could only supply active power if the battery is not fully discharged and the battery should be recharged if the SOC is below a certain level. One of the important issues in modeling GF converter is providing a simple and applicable model although it is comprehensive.

Therefore these models are very much useful in analysing the impact of maintaining the DC bus voltage.

Simulations and Results 4

This Chapter introduces the simulation cases and results. Four different simulation cases are briefly explained below. The power system which is displayed in Fig. 3.1 and introduced in Chapter 3, is utilized in the cases.

GF Converter Response - Base Case : This simulation case is designed to observe the response of a GF converter after a load switching while the effect of external grid is minimized. The objective is to observe the dynamic response of GF converter where it dominates the system.

GF Converter Response with Ideal Adaptive Droop Control : In this case, the base case is taken one step further and adaptive droop control is activated after the induced dynamic change in the system. It is aimed restore the electrical frequency back to its nominal value.

GF Converter Response with BESS : This case utilises the base case to introduce a method of supporting DC voltage stability. BESS is implemented to DC bus of GF converter to analyse its impact during dynamic change in the system.

GF Converter Response with Realistic Constraints : This case is designed to observe the system behaviour where both GF converter and EG are implemented with its realistic droop controls. The adaptive droop control and BESS are implemented with operational constraints.

GF converter is considered as connected to the power system prior to the initialization of the simulations. Simulations are performed in DIgSILENT PowerFactory as RMS simulation. Simulation cases are explained in detail in the following sections.

4.1 GF Converter Response - Base Case

This case is designed to analyse the response of the designed GF converter RMS model. The GF converter is expected to respond to a load change in the system, while the external grid does not contribute feeding the load. External grid is not contributing to minimize its effect on GF converters operation. Therefore, the external grid is applied a vertical droop characteristic. This is performed by changing the secondary frequency bias setting of the external grid in DIgSILENT PowerFactory to 0.0001 $[MW/Hz]$. So that the droop curve shown in Fig 3.2 approaches to be a vertical line as much as possible, with a power set-point of 0 $[MW]$.

Through Chapter 3, each element and their respective control strategies in the system are introduced. To observe the behaviour of GF converter, some control functions are deactivated. For this case, maximum power limitation at higher level control, which aims to avoid overloading renewable energy source, is deactivated. The limitations regarding ramp rate limiters kept active.

The simulation is initiated with no load. Then, a 1 $[MW]$ load, which is equal to the rated power of the GF converter, is switched in.

Important parameters regarding the simulations are given in Table 4.1. Some of the parameters in the table belongs to the following case studies and will be explain in their corresponding sections.

Important Parameters	
Switched Load	1 $[MW]$
$P_{RES\_ramp\_max}$	0.15 $[MW/s]$
$P_{el\_ramp\_max}$	0.1 $[MW/s]$
$P_{dc\_bus\_ramp\_max}$	0.05 $[MW/s]$
ΔF_{active}	0 $[Hz]$
ΔP_{set_max}	5 $[MW]$
$P_{min\_with\_\Delta P\_set}$	-5 $[MW]$
$P_{max\_with\_\Delta P\_set}$	5 $[MW]$
ΔF_{max}	1.95 $[Hz]$
$P_{max\_with\_\Delta F}$	5 $[MW]$
$P_{min\_with\_\Delta F}$	-5 $[MW]$

Table 4.1: Operational parameters.

Fig. 4.1 displays that the simulation is initiated with no-load, the power outputs of the EG, GF and RES are almost zero. In actual numbers EG and GF have electrical power output of -0.0008, +0.0008 [MW], respectively. The reason why EG has minus power output is its droop curve. As it is mentioned earlier, it is implemented a very steep curve to keep its output at 0 $[MW]$ active power all the time. However, because the system frequency is almost 52 $[Hz]$ during the initial condition, the operation point still goes into a minus region for EG's droop curve and results in a negative generation point. However, it is still negligible.

In Fig. 4.2 the electrical frequency is shown. When there is no load in the system, the system frequency is 51.995 $[Hz]$. As the EG is implemented a vertical droop curve, it tends to give 0 $[MW]$ active power at every frequency level. Therefore GF, converter is dominant determining on the system frequency. Fig. 3.4 displays the droop characteristics of the GF converter and it has 0 $[MW]$ active power at 52 $[Hz]$, which is almost system frequency during the initial condition.

At 10 $[s]$ the switching of the load is performed. The load causes an electrical power output spikes at both GF and EG, reaching up to 0.31 and 0.84 $[MW]$, respectively (not simultaneously). After the transient region, power outputs of GF and EG reaches to 0.84 and 0 $[MW]$ at 10.4 $[s]$, respectively. The frequency of the system decreases to 48.7 $[Hz]$ at this moment. After the switching and fast decrease in the electrical frequency, frequency continues to decrease slightly till it reaches a stable operating point. The reason behind the continuously but slight decrease is that the loading slightly increase and operation point moves slightly to a lower frequency in the droop curve. The logic behind this relation is

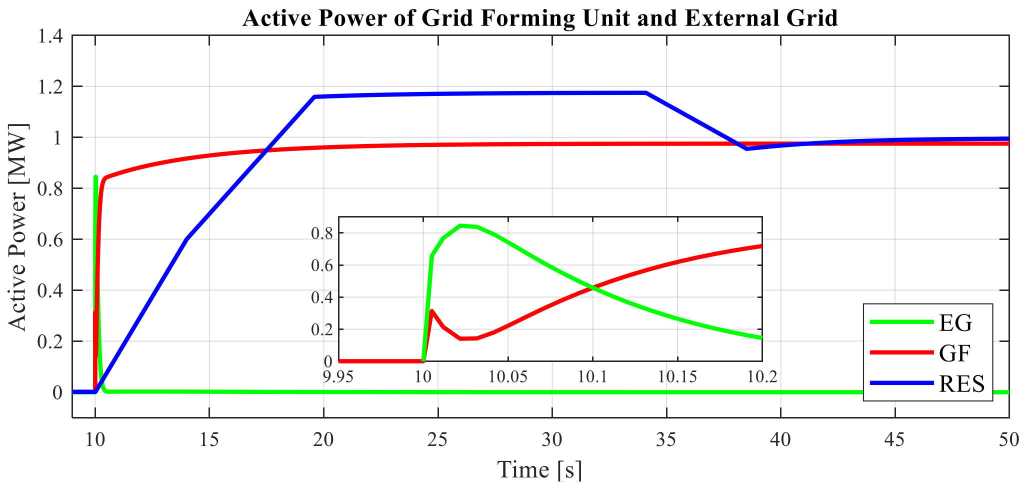

Figure 4.1: Active power outputs of EG, GF converter and RES during GF converter response base case.

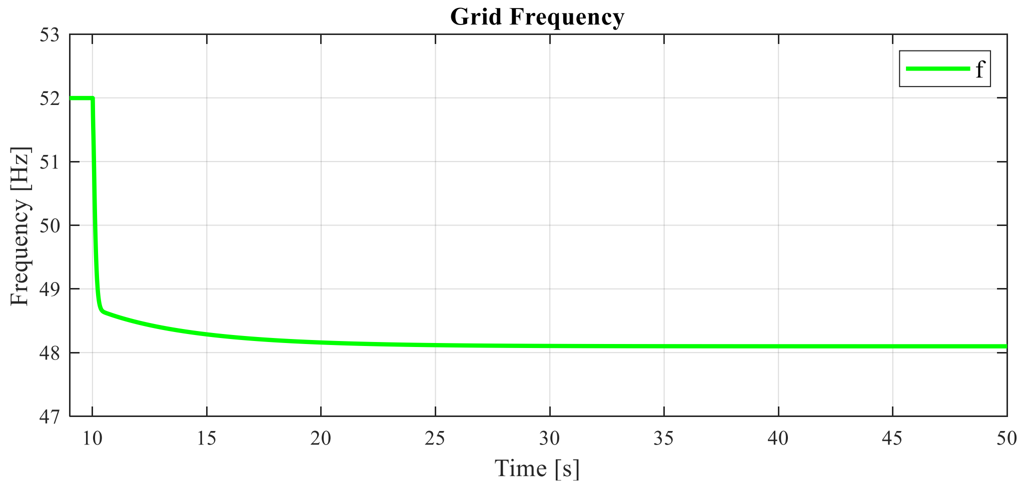

Figure 4.2: Grid frequency during GF converter response base case.

that the loads are modelled as constant impedance and due to the voltage drop after the connection it demands less than its rated power (this is also the reason why electrical output power reaches to 0.84 instead of 1 $[MW]$). Then, towards to the end of the simulation, the loading continues to increase slightly, as the voltage is continuously being restored at the load bus.

After the load switching, the electrical power output of the RES increases too, but it has a very different characteristic comparing to the GF converter's electrical power output. The biggest difference between the RES and GF converter is that RES acts as active and reactive power source in the power system, while GF converter act as a voltage source. This means that when the load is connected to the system, the GF converter immediately feeds the load, however the RES needs to receive the relevant power reference data to deliver the power the system needs. As it is explained in Section 3.2, the RES receives its power set point, P_{el}, as soon as GF converter gets loaded. This power set-point is implemented ramp rate limiter and it results that the electrical power output of RES increases slowly and linearly as displayed in Fig. 4.1. Meanwhile, the capacitor discharges and compensates the power deficit between the GF and RES. As a result, the RES receives the second power set-point, P_{dc_bus}, from higher level controller to recharge the capacitor. The ramp rate limits for P_{el} and P_{dc_bus} are set individually and 0.1 and 0.05 $[MW/s]$ respectively. When these two power reference is delivered to the RES, they results in a maximum ramp rate of 0.15 $[MW/s]$ at the RES, $P_{RES\_ramp\_max}$. This ramp rate is visible in Fig. 4.1 following the switching moment. After the 4 $[s]$ from the switching, P_{dc_bus} reaches its maximum, which is 0.2 $[MW]$, and only P_{el} continues to increase the output of RES with 0.1 $[MW/s]$. When it reaches to the top at 19.6 $[s]$, it delivers power of 1.16 $[MW]$. At 34 $[s]$, the electrical output of RES starts decreasing again because the power reference of P_{dc_bus} decreases while the dc bus voltage gets close to its nominal. However, because of the ramp rate limiter, P_{dc_bus} can not go to 0 $[MW]$ immediately once the dc bus voltage hit to 1 $[pu]$ and RES continue to deliver power for dc bus voltage for a short time period which causes a slight voltage rise in the dc bus. Then the voltage rise in the dc bus creates a negative reference in the higher level control, which takes the output of the RES below the GF at 38.3 $[s]$. Then capacitor slowly discharges itself and DC bus voltage goes back to its nominal. Finally the negative P_{dc_bus} reference goes towards 0 and power output of RES goes above of GF. At the end of the simulation, the electrical output of the GF and RES reaches to 0.97 and 0.99 $[MW]$, respectively. The deficit between them is due to the power losses in the system.

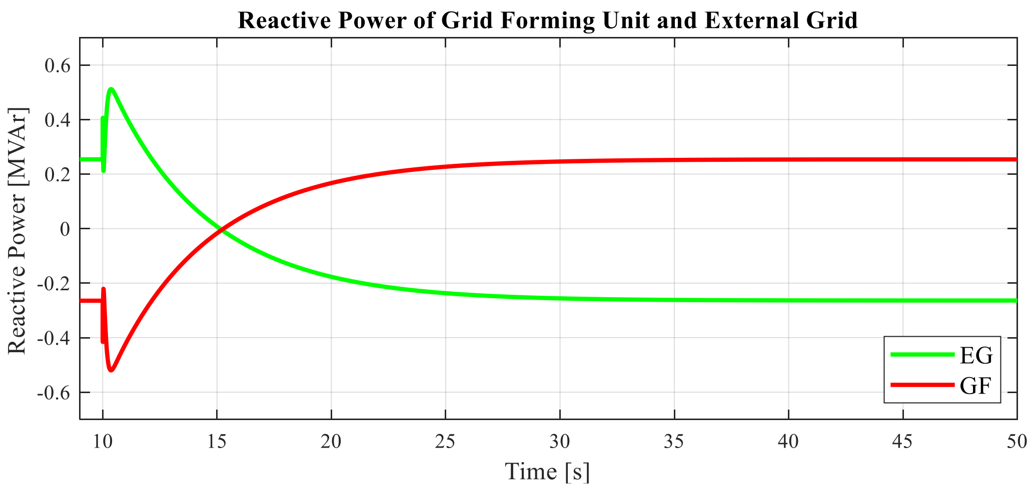

Figure 4.3: Reactive power outputs of EG and GF converter during GF converter response base case.

Reactive power flow in the system is heavily dependent on the internal converter control of the GF. The GF converter receives a voltage set point and form the voltage magnitude at the bus. To form it, it can draw or deliver reactive power. However, the reactive power flow has also an effect on the voltage set point based on the voltage droop control, which is shown in Fig. 2.3. As can be seen in Fig. 4.4, initially there is an over-voltage at the GF bus. The voltage set point of the converter control is 1 $[pu]$, therefore the converter control orders to draw reactive power from grid to GF converter to decrease the bus voltage and this results a negative reactive power output. Meanwhile, operation point in the voltage droop control moves to left, where reactive power in negative region, and it results in an increase in the reference voltage. Finally, the system finds its equilibrium point with the help of droop control. For this case, the equilibrium point is at 1.013 $[pu]$ voltage and -0.26

$[MVAr]$ reactive power output during the initial phase.

After the connection of the load, a voltage drop appears at the GF bus. Once the converter internal controller receives the voltage drop data, it starts injecting reactive power to the grid. And as a result of reactive power injection, the reactive power droop control results in a voltage drop at the reference, and the equilibrium point is found below at 1 $[pu]$ voltage, at 0.987 $[pu]$ receiving 0.253 $[MVAr]$ from the grid.

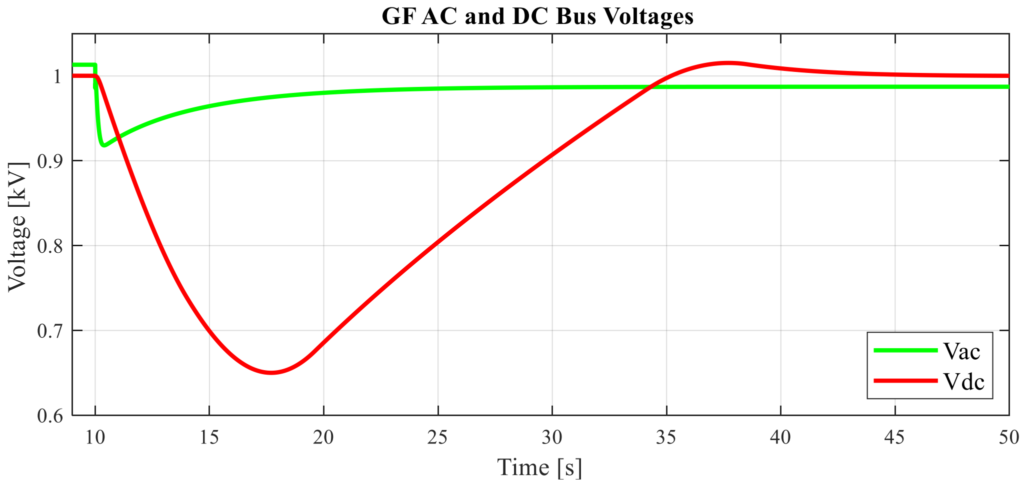

Figure 4.4: AC and DC bus voltages during GF converter response base case.

One conclusion regarding this case is that a GF converter needs a room for its reactive power response to the grid. As it acts as a voltage source, it tends to deliver or receive reactive power based on its voltage reference. For a case where a GF converter is heavily loaded, like this case scenario where the GF converter delivers 0.99 $[pu]$ active power which is almost its rated, the reactive power injection or consumption can cause over loading a GF converter, which is the case for this scenario. The second conclusion is that the DC bus voltage experience voltage drops while the GF converter delivers more power than RES provides. Based on the difference between these two power and the duration DC bus voltage drop can be significantly large. The third conclusion can be drawn from the frequency curve. As there is no any physical or virtual inertia implemented to GF converter and the external grid has a low inertia constant, the frequency curve has a very sharp decrease. In Appendix A, the contribution of the virtual inertia as a part of virtual synchronous generator control strategy is introduced and it effect on frequency is demonstrated.

4.2 GF Converter Response with Ideal Adaptive Droop Control

Adaptive droop control is introduced in Section 3.7 as a method for frequency support. The strategy relies on adapting the droop curves, either shifting to left or right, or changing the slope. This case is designed to observe the ideal contribution of adaptive droop curve methods on system frequency, which is restoring the system frequency back to its nominal.

The first case study in Section 4.1 is utilized as base for this case. Then, the two adaptive droop control methods, which are shifting and variable slope, are applied as two different sub-cases at 20 [s]. The simulations and results till 20 [s] will be identical to the first case. Therefore, the content of this section will mainly focus on the results after 20 [s] to avoid the repetition with the first case. The frequency and relevant parameters in operation of adaptive droop curve will be shown in this Chapter. Figures regarding power and voltage will be given in Appendix C. Comparison of the two introduced adaptive control methods will be made at the end of this section.

4.2.1 GF Converter Response with Shifting Method

Shifting method proposes to move the droop curve of a GF converter to left or right based on the frequency of the system to support the system frequency. In Section 3.7.1, it is explained that moving a droop curve to right results in an increase in the electrical frequency, while moving it to left results in a decrease.

To obtain the ideal contribution in this sub-case, some of the control functions and parameters regarding adaptive droop control are disabled for this study. One change is performed in the activation of the strategy. As it is introduced in Section 3.7.1, the method activates and resets itself based on the electrical frequency. However, in this case it is activated at the 20 [s] and kept active constantly. This is performed by setting the parameter of ΔF_{active} to 0. The second change is performed in the maximum variation in the power set-point, ΔP_{set_max}, and the limit is disabled by setting a large value, which is 5 [MW]. The third change is performed in the electrical power output range of GF converter that adaptive droop control performs, which are defined within $P_{min\_with\_\Delta P\_set}$ and $P_{max\_with\_\Delta P\_set}$. These two limitations are disabled by setting large values, which are -5 and 5 [MW], respectively.

Fig. 4.5 displays that ΔP_{set} starts rising with the activation of the adaptive droop control at 20 [s]. The increase in ΔP_{set} is in positive polarity, which means that the droop curve is moving to right side. It is expected that it should result in frequency increase, and Fig. 4.6 displays that the electrical frequency of the system increases as well, reaching to 50 [Hz] at 30 [s] from 48.16 [Hz] at 20 [s]. The rise in ΔP_{set} and frequency continues till the frequency reaches its nominal value at ΔP_{set} of 0.5 [MW]. After this point, the active droop control causes some ripples in the system. The reason is that the control always tends to move the curve to left or right. And once it across the 50 [Hz], it wants to decrease the frequency. Then once it goes below to 50 [Hz], it wants to increase it. Therefore, once the frequency reaches to 50 [Hz], the control causes ripples. These ripples could be avoided by modifying the control displayed in Section 3.7.1. If the nominal frequency was used as reference for a PI controller to control ΔP_{set}, the system would reach to nominal frequency smoothly. As a second method, a deadband could have been applied to avoid the ripples. However for practical reasons and time limitations, this ideal scenarios are simulated by adjusting the previously mentioned parameters.

4.2.2 GF Converter Response with Variable Slope Method

Variable slope method proposes to change the slope of the droop curve based on the frequency of the system to support the system frequency. In Section 3.7.2, it is explained that decreasing the slope results in an increase in frequency for under-frequency and a decrease in frequency for over-frequency.

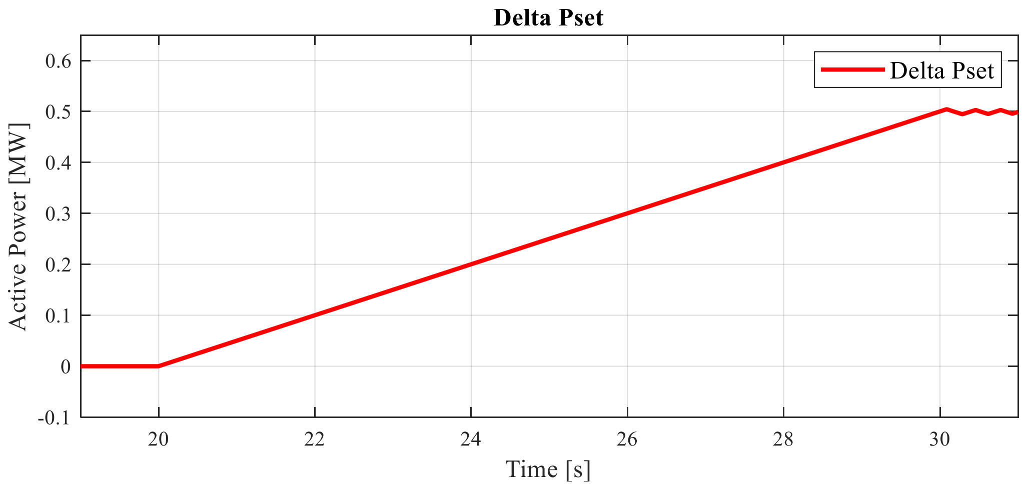

Figure 4.5: Deviation in power-set point during GF converter response with ideal shifting method case.

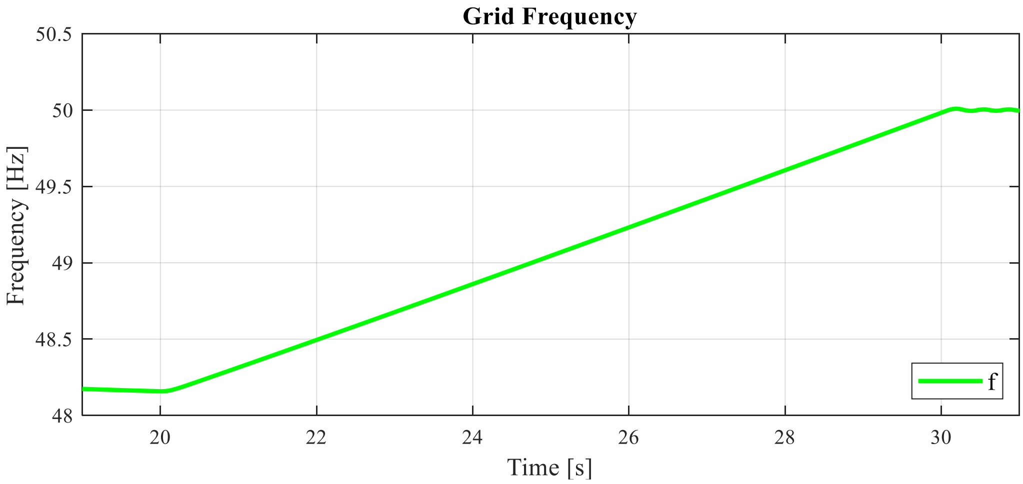

Figure 4.6: Grid frequency during GF converter response with ideal shifting method case.

To obtain the ideal contribution in this sub-case, some of the control functions and parameters regarding adaptive droop control are disabled similar to the adjustments in the previous sub-case. The first change is as same as the one in the previous sub-case, which is to activate the active droop control strategy at 20 $[s]$ and to keep it activated constantly regardless the frequency. This is performed by setting the parameter of ΔF_{active} to 0. The second change is performed in the maximum variation in the frequency, ΔF. As explained in Section 3.7.2, ΔF is used to control the slope of the curve. It is defined as the variation from 48 $[Hz]$ in the operation point where GF converter delivers 1 $[pu]$, and for this sub-case the maximum variation, ΔF_{max}, is limited to 1.95 $[Hz]$. So that the frequency point of the droop curve where it delivers 1 $[pu]$ power can go up to 49.95 $[Hz]$. Once it reaches to 49.95 $[Hz]$, the droop curve becomes almost horizontal around 50 $[Hz]$, and GF converter delivers every power level at close to 50 $[Hz]$. ΔF_{max} limitation could not be removed completely, because if the ΔF parameter goes beyond 2 $[Hz]$, the slope of the droop curve goes from $-$ to $+$ and it leads unstable operation for GF converter. The third change is also identical to the third change in the previous sub-case which is to disable the electrical power output range of GF converter that adaptive droop control performs, which are defined by $P_{max\_with\_\Delta F}$ and $P_{min\_with\_\Delta F}$. These control parameter are given 5 and -5 $[pu]$ to act like disabled, as given in Table 4.1.

Fig. 4.7 displays that ΔF starts rising, and the slope starts decreasing with the activation of the adaptive droop control at 20 $[s]$. This means that the droop curve is approaching to be a horizontal line at 50 $[Hz]$. It is expected that it should deliver every power level at close to 50 $[Hz]$ when the droop curve approaches to be a horizontal curve. Fig. 4.8 displays that the electrical frequency of the system starts rising from 48.16 $[Hz]$ and reaches to 49.95 $[Hz]$ at 23.90 $[s]$. The rise in ΔF and frequency continues till the frequency reaches to 49.95 $[Hz]$, instead of 50 $[Hz]$ due to ΔF_{max} constrain considering the previously mentioned instability concern. After this point, the control successfully maintains the system frequency at this level with acceptable level of ripples. As it is mentioned in the previous sub-case, utilizing a PI control with frequency reference inputs to output ΔF could increase the quality of the results.

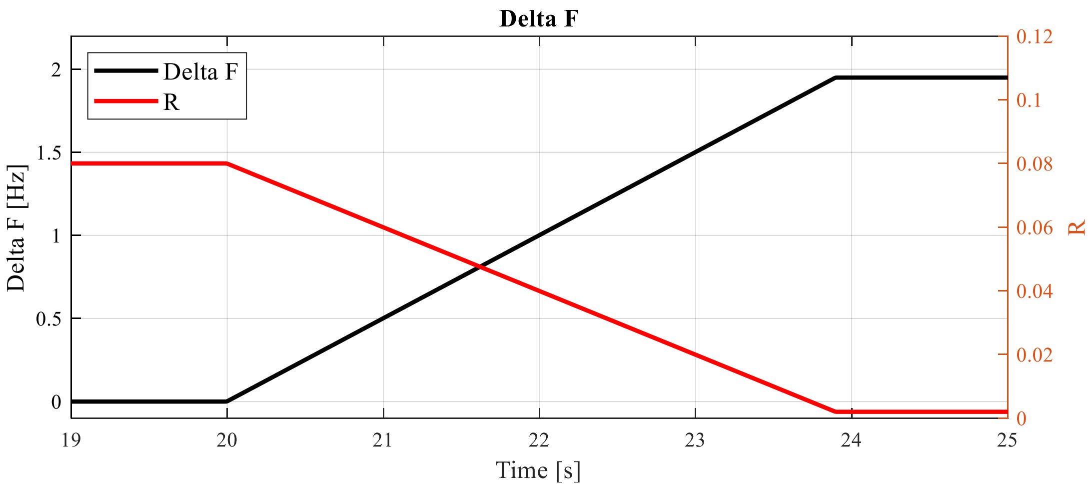

Figure 4.7: Deviation from 48 $[Hz]$ for maximum operation point and change in R during GF converter response with ideal variable slope method case.

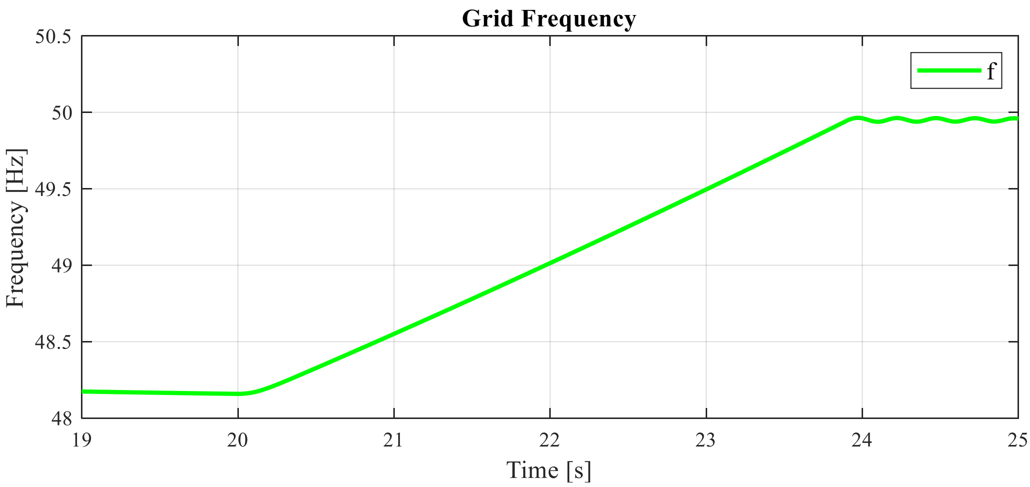

Figure 4.8: Grid frequency during GF converter response with ideal variable slope method case.

4.2.3 Comparison of the Methods

Two different approaches for adaptive droop control are investigated in previous two subsections. Despite the difference between adaptive droop control shifting method and variable slope method, it was shown that both methods are capable of regulating the system frequency with minor differences. The comparisons of active power output and electrical system frequency under the previously introduced three simulation cases are displayed in Fig. 4.9 and 4.10. Fig. 4.9 displays that, both shifting method and variable slope method recovers the frequency with very minor differences. One difference in the figure appears where frequency increases. For the given parameters, variable slope method has a steeper curve. However, the slope in the curves are dependent to the implemented ramp rate limiters and there was no any objective to make them equal during the design process. Therefore, one cannot conclude any certain results from the steepness of the curves. However, both curve shares one thing in common during the increase and it is the linearity in the curves. Control parameter, ΔP_{set} and ΔF, are displayed in Fig. 4.5 and 4.7, and it can be concluded that the increase in the frequency follows the linearity in the control parameters. The second difference is the frequencies that the two methods restore the system. Frequency reaches to its nominal under the shifting method, whereas it reaches a set point below the nominal frequency with variable slope method. The reason is that the droop curve is not an ideal horizontal line and will always have a frequency drop for certain electrical power output. And the last differences is the ripples where system frequency reaches it nominal (or almost nominal for variable slope method). For variable slope method, temporary ripples are exist. These ripples are seen when the change in the slope suddenly stops, then they fade away. For shifting method, the ripples are permanent. The reason is that the control strategy continuously increase and decrease the frequency once it crosses the 50 $[Hz]$. These ripples for two method can be minimized by a proper PI controller which utilizes frequency inputs to control ΔP_{set} and ΔF.

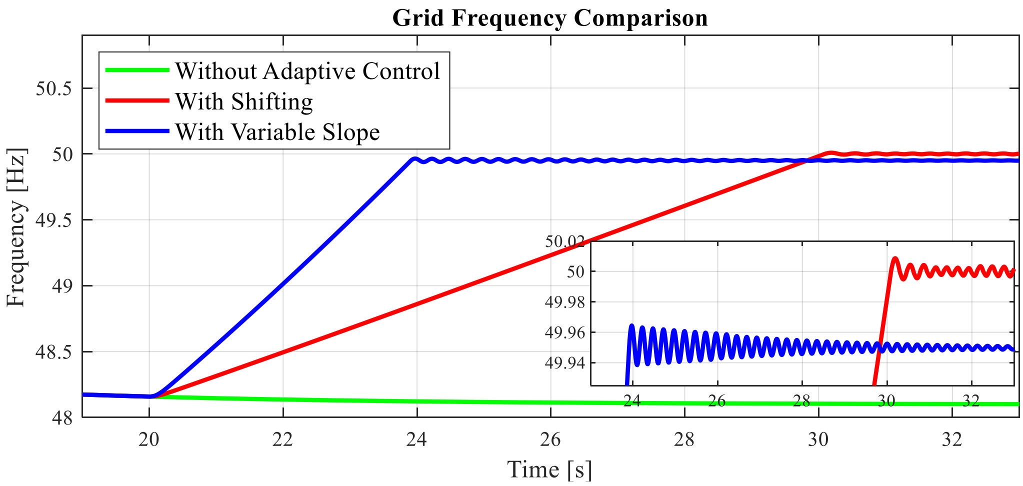

Figure 4.9: Comparison of the grid frequencies under the GF converter response case, GF converter response with ideal shifting and variable slope methods case.

The electrical power output curves show the same ripple pattern that the frequency curves have. This is reasonable, because the electrical power output is strongly dependent to the phasor angles and any change in frequency affects the phasor angles in the system. Briefly, the power curve contains temporary ripples with variable slope, whereas it has permanent

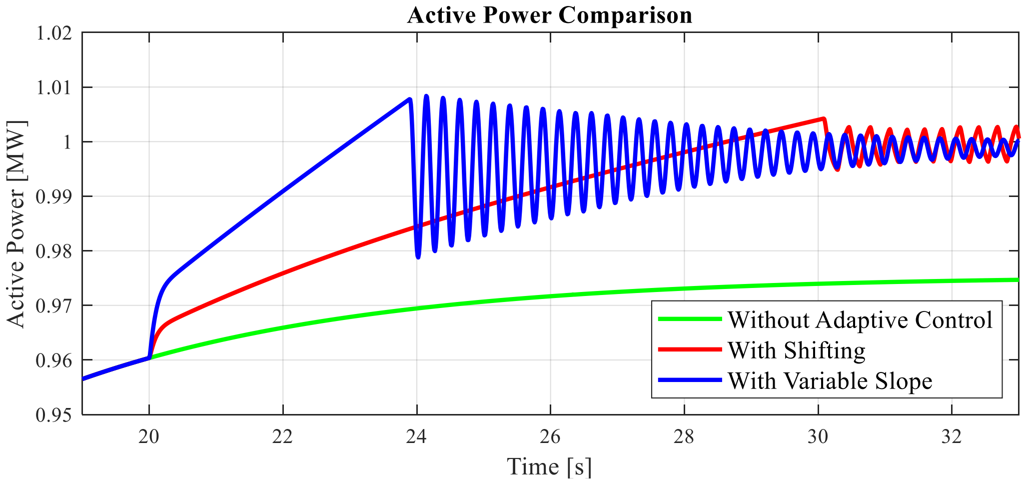

Figure 4.10: Comparison of the active power output of GF converter under the GF converter response case, GF converter response with ideal shifting and variable slope methods case.

ripples with shifting method. Also, an increase in the power outputs comparing to the base case can be seen in the figure. This is an indirect results of the adaptive droop control strategy. The bus voltage in the AC bus increases after the activation of the adaptive droop controls, and the total load demand increases as a result. Graphs regarding active power, reactive power and voltages are provided in Appendix C.

4.3 GF Converter Response with BESS

This case is designed to analyse the impact of a battery storage system in a DC busbar of a GF converter and the response of the system, when the DC bus voltage is restored using external system. In this case the ideal GF converter system is used as a base case and BESS is added to its DC bus.

The observational point of the simulation with the 11 $[MWh]$ BESS is to initiate the system with no load and a 1 $[MW]$ load is switched in. The transients during the operation is analysed. The initial state of charge of the battery is considered to be 100 [%] and the rate of discharge of the BESS is limited 0.13 $[MW/s]$. As there is no voltage drop in the bus, the power output of the BESS is zero. At 10 $[s]$ the load is switched and the DC bus voltage of the system is displayed in Figure 4.11. It can be observed that the recovery of the DC bus voltage happens 33.33 [%] faster than in the base case.

The swift change in the DC bus voltage is achieved by the injected power flow by BESS as displayed in Figure 4.12. It can be observed that the rate of increase in power flow is at a rate of 0.1286 $[MW/s]$ and is directly proportional to the deviation of DC bus voltage, when there is a voltage drop. The net amount of energy transferred to the system from BESS during this dynamic change is 277.21 $[kWh]$. Even though the maximum power transferred at a instant is 0.3714 $[kW]$, it supports in bringing back the system to its nominal values at a faster rate. The initial state of charge of the battery is considered to be at 100 [%] and the response of the BESS provides a SOC profile as displayed in Figure 4.13.

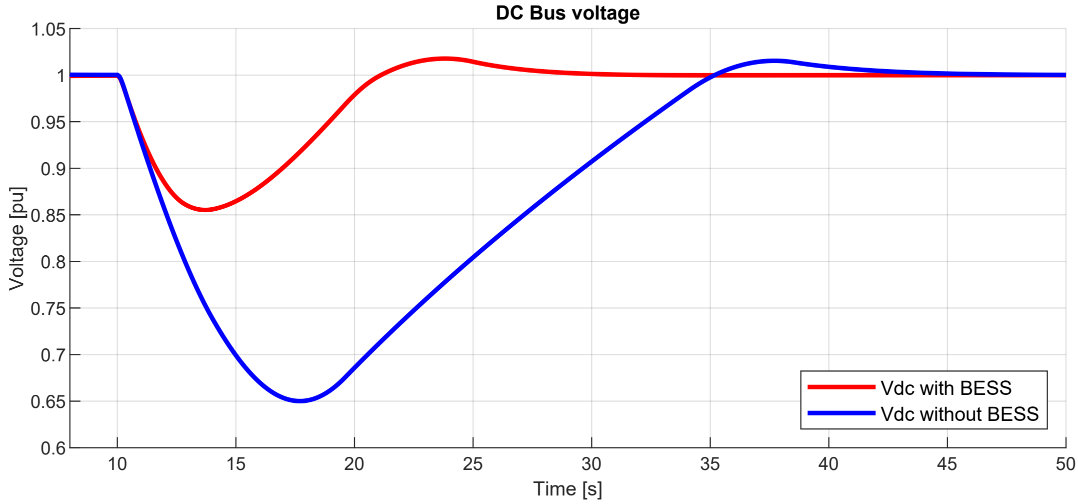

Figure 4.11: DC Bus voltage with BESS

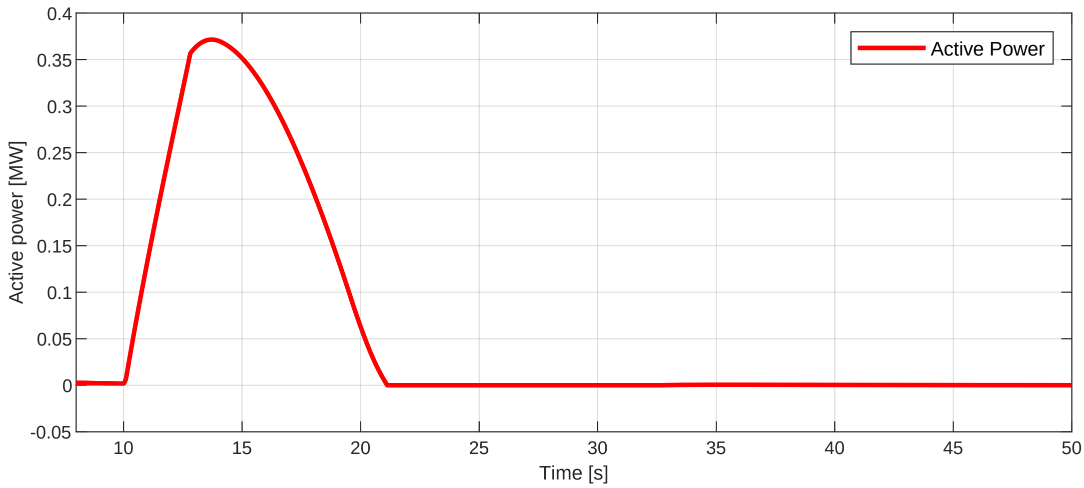

Figure 4.12: BESS Power Flow

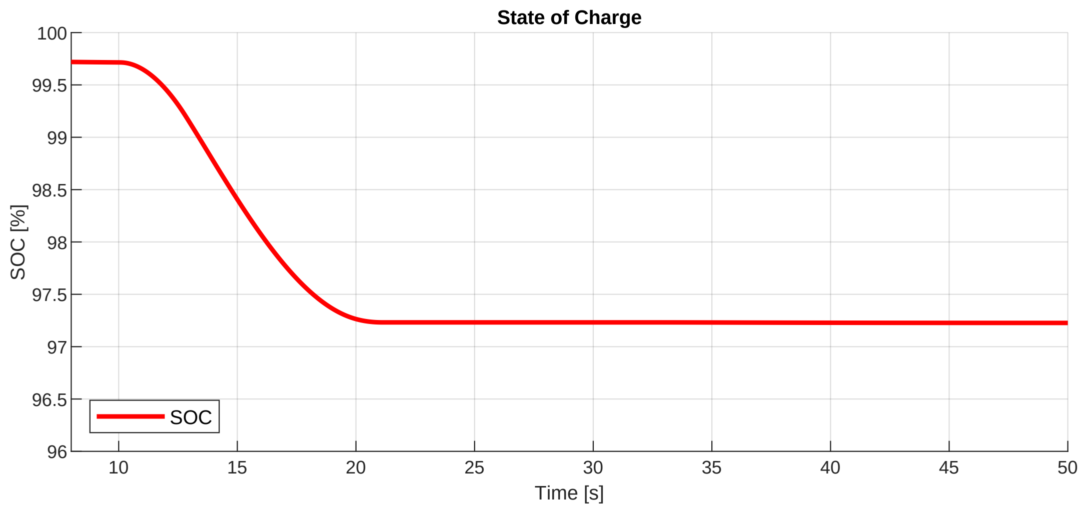

Figure 4.13: State of Charge of BESS

4.4 GF Converter Response with Realistic Constraints

This case is designed to observe the behaviour of both the grid and GF converter under a realistic scenario. As different from the previous scenarios, this case utilizes all the control functions introduced through the report. For example, external grid has the droop control which is introduced in Section 3.1, whereas it was applied as vertical line in the previous case scenarios. Therefore, both the GF converter and external grid will have an impact on the power flow in the system, and they will share the load.

Higher level control, which is introduced in Section 3.2, is the another control which is not utilized in previous case studies. The main objective of this control is to avoid demanding more power than the maximum available power at RES when the RES is delivering power for both GF converter and DC bus voltage control. This is performed by setting the maximum power point of the GF converter's droop curve. This control is activated for this case study.

The previous studies aimed to observe the response of a GF converter while the response of an external grid was minimized. By setting a vertical droop curve to external grid, its effect on system frequency was minimized and the GF converter became dominant. The simulations were initialized with no-load and as a result of GF converter's droop curve, grid frequency was 52 $[Hz]$ prior to load connection. For this case, the initial load of the system is 0.5 $[MW]$ which results in 50 $[Hz]$ equilibrium point in the droop curves of external grid and GF converter. Then the same amount of load with previous cases, 1 $[MW]$, is switched in to observe the dynamic response of the equipment in the system.

Important Parameters	
Initial Load	0.5 $[MW]$
Switched Load	1 $[MW]$
$P_{RES\_ramp\_max}$	0.15 $[MW/s]$
$P_{el\_ramp\_max}$	0.1 $[MW/s]$
$P_{dc\_bus\_ramp\_max}$	0.05 $[MW/s]$
ΔF_{active}	0.5 $[Hz]$
ΔF_{reset}	0.1 $[Hz]$
ΔP_{set_max}	0.3 $[pu]$
$P_{min\_with\_\Delta P\_set}$	0.1 $[pu]$
$P_{max\_with\_\Delta P\_set}$	0.9 $[pu]$

Table 4.2: Operational parameter of realistic scenario.

Adaptive droop control with shifting method is applied to this case study. The study is also repeated with adaptive droop control with variable slope method. The results are provided in Appendix C.3 to avoid the repetition. In the previous case studies, adaptive droop control was activated at 20 $[s]$. For this study, the operation of active droop control is automated by its activation and reset frequency settings. The frequencies that adaptive droop control will active are set to below 49.5 and above 50.5 $[Hz]$ by setting ΔF_{active} to 0.5 $[Hz]$. The frequency range where active droop control resets and goes back to its default is set between 49.9 and 50.1 $[Hz]$, by setting ΔF_{reset} to 0.1 $[Hz]$. The operation range of the adaptive droop control is defined within 0.1 and 0.9 $[pu]$ active power, by $P_{min\_with\_\Delta P\_set}$ and $P_{max\_with\_\Delta P\_set}$. The maximum variation in power set-point is limited to 0.3 $[pu]$ by ΔP_{set_max}. These parameter are introduced in detail in Section 3.7.1. The storage system is applied as same as the case scenario in Section 4.3.

Fig. 4.14 displays the active power output of the elements in the system. During the initial phase, only 0.5 $[MW]$ load is connected to the system. The power outputs of the GF unit and external grid are 0.5 and 0 $[MW]$, respectively. These loading were expected because the initial load of the system is adjusted to have 50 $[Hz]$ in the system frequency and external grid has 0 $[pu]$ active power reference where it cross the 50 $[Hz]$. The reason is that the external is the slack bus and it has 0 $[pu]$ active power set-point at nominal frequency, as mentioned in Section 3.1. After the switching, the loading in the GF converter and external grid rises up to 0.79 and 0.82, respectively. Following to the switching transients, the system frequency drops 49.25 $[Hz]$ at 10.2 $[s]$. At this point, the loading of the GF converter and external grid becomes 0.69 and 0.74 $[MW]$, respectively.

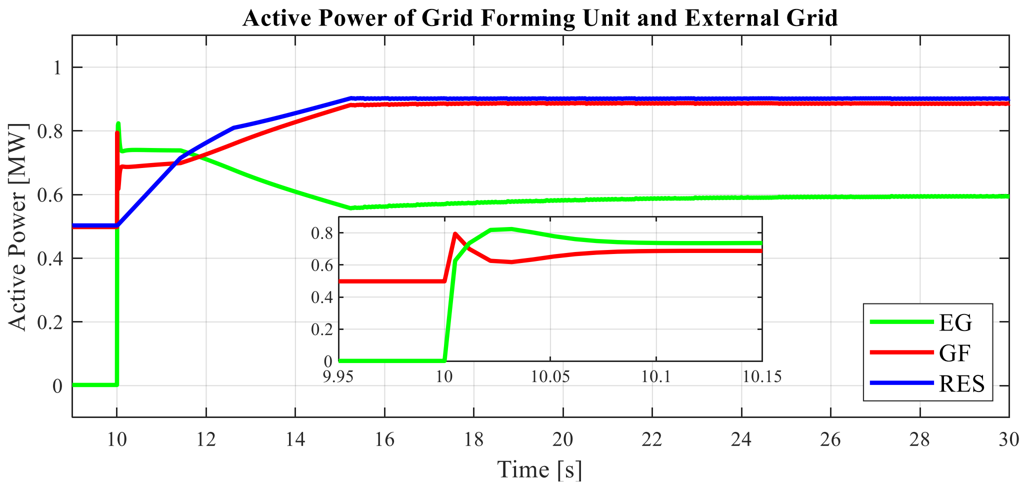

Figure 4.14: Active power outputs of EG, GF converter and RES during GF Converter Response with Realistic Constraints case.

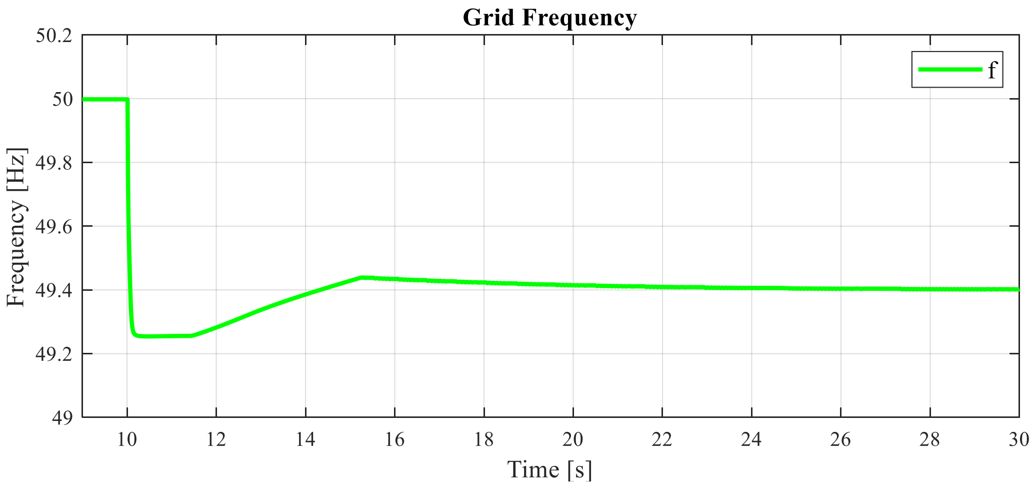

Figure 4.15: Grid frequency during GF Converter Response with Realistic Constraints case.

The change in system parameter result in activation of the previously introduced control strategies. The system frequency dropped below 49.5 $[Hz]$ after the switching and it activates the adaptive droop control for given settings, which is listed in Table 4.2. As a results, the droop curve of the GF converter moves right side to support the system frequency and it is expected to increase the electrical output of the GF converter. The deviation in the power set-point of the GF converter's droop control is displayed in Fig. 4.16 and the rise in ΔP_{set} can be seen. However, this is not the only control activates at this point. The Fig. 4.17 displays the AC and DC bus voltages. DC bus voltage starts decreasing after the load switching. The reasons is that GF converter draws power from capacitor and the discharge in the capacitor leads to voltage drop. Once the voltage drop is detected, the higher level control receives an additional power set-point from DC bus voltage controller introduced in Section 3.5 to charge the capacitor. Once the power reference is created for capacitor, the higher level control calculates the maximum power point for GF converter's droop control as explained in Section 3.2. Briefly, the higher level control re-scales power axis of the droop curve. Re-scaling the power axis of a droop curve results in a similar action to adaptive droop control shifting method, which explained in Section 3.7.1. As a result, when the power reference for charging capacitor rises, the maximum power point of the droop curve decreases and this results a similar action to moving a droop curve to left side.

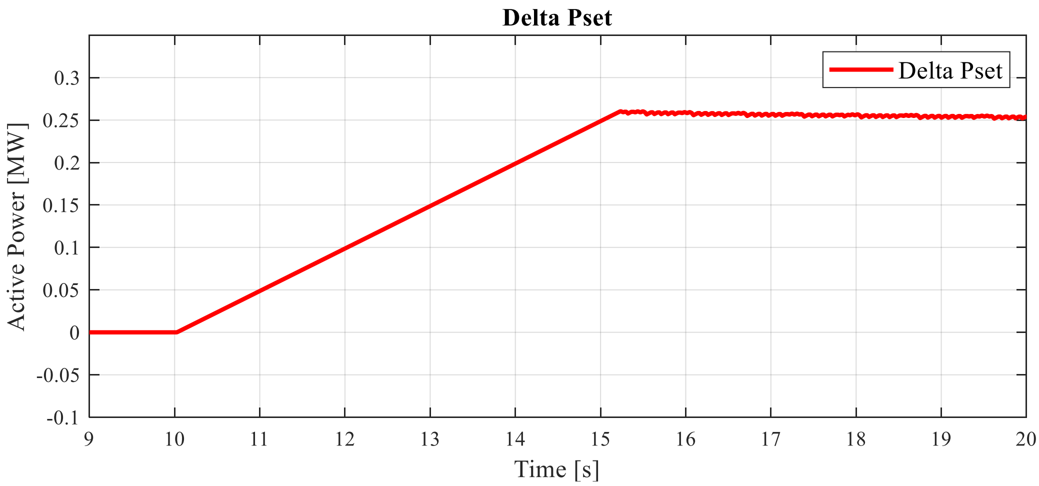

Figure 4.16: Deviation in power-set point during GF Converter Response with Realistic Constraints case.

Considering the operation of these two control functions, they are working against each other in terms of electrical power output of the GF converter when DC bus voltage decreases and frequency is below 49.5 $[Hz]$ at the same time. Because, higher level control tends to decrease the output power of GF converter to create a room for dc bus voltage restoration, however adaptive droop control tends to increase the output power of GF converter to support the system frequency. From Fig. 4.18, it can be seen that the power reference of RES for capacitor charging increases from 10 to 11.41 $[s]$. From the power flow figure, the output power of the GF converter has a slight increase from 0.69 to 0.70 $[MW]$ from 10.2 to 11.41 $[s]$. Frequency almost remains same at 49.25 $[Hz]$. The key comment which should be given about these region, from 10.2 $[s]$ to 11.41 $[s]$, is that a frequency rise would be exist if there was no higher level control, and the voltage drop in the DC bus would be lower if there was no adaptive droop control. In other words, higher level control steals some power flow from GF converter to charge the capacitor, but active droop control steals it back to GF converter.

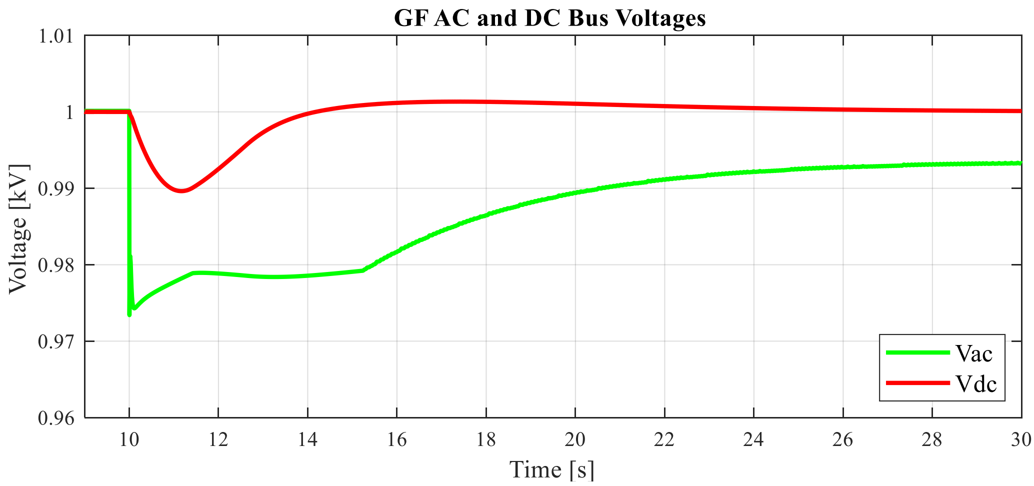

Figure 4.17: AC and DC bus voltages during GF Converter Response with Realistic Constraints case.

One can discuss if one of these controls, adaptive droop and higher level control, should have a priority or not. From the TSO point of view, the adaptive droop control might be given a priority as it helps to control the system frequency. DC bus will be behind the GF converter and will not be seen directly by any transmission system. However, the higher level control might also be given priority if DC bus is weak and voltage is not stable. Otherwise, it may lead to disconnection of GF converter. For the introduced case study, it can be concluded that the adaptive droop control would be given priority and higher level control would be deactivated. The reason is that the voltage drop is already very low thanks to the BESS and load sharing among generation units. Also, the simulation case is performed where RES has 1 $[pu]$ available power source, therefore RES can easily deliver the power that GF converter need.

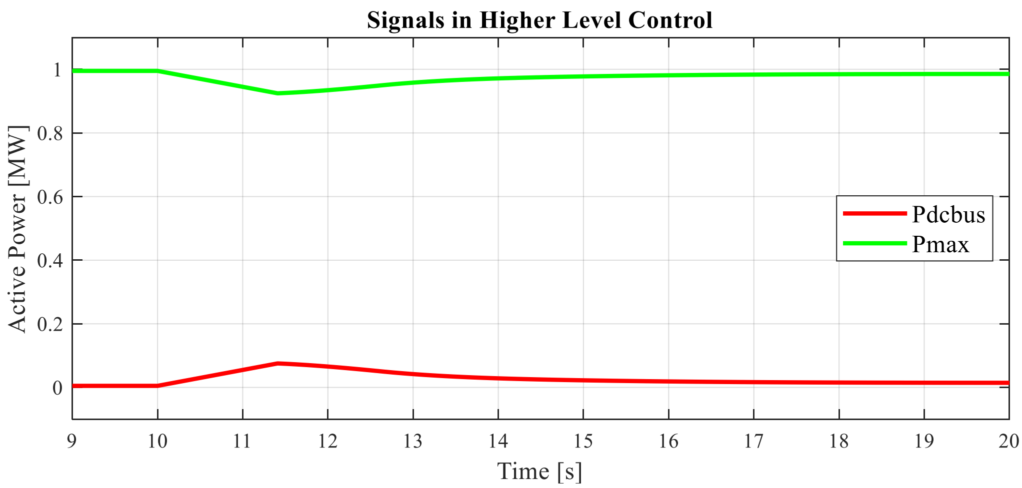

Figure 4.18: Maximum operation point signal for GF converter, P_{max}, and power reference for capacitor charging, P_{dc_bus}, during GF Converter Response with Realistic Constraints case.

After 11.41 $[s]$, P_{dc_bus} starts decreasing as can be seen in Fig 4.18. The parameter created by higher level control, P_{max}, starts increasing back to 1 $[pu]$. It is the parameter which re-scales the power axis of droop control and when it goes back to 1, the effects of higher level control fades away. As a result, adaptive droop control becomes dominant in the system. From 11.41 [s] to 15.22 [s], the power output of GF converter, the system frequency, and ΔP_{set} increase. The increase stops at 15.22 [s], because the electrical output of GF converter reaches to 0.9 [pu], which is the maximum power for operation range of adaptive droop control. After 15.22 [s], adaptive droop control cannot continue to perform and the increase in ΔP_{set}, in other words shifting in droop curve, stops. As a result, electrical frequency of the system rises till 15.22 [s] and goes up from 49.25 to 49.40 [Hz]. Active power output of external grid drops from 0.74 to 0.59 [MW].

From 11.41 [s] to 15.22 [s], AC bus voltage, Fig. 4.17, displays a relatively steady region. The active droop control does not control the AC voltage but it has an indirect effect on the bus voltage. When active droop control activates, it changes the power flow and this results in a change in the phasor angle of the voltage. When this angle changes, the measured d- and q-axis voltage changes. Consequently, the operation of the converter controller, which is a cascaded voltage and current controller, is affected. This effect also can be seen in reactive power flow, displayed in Fig. 4.19.

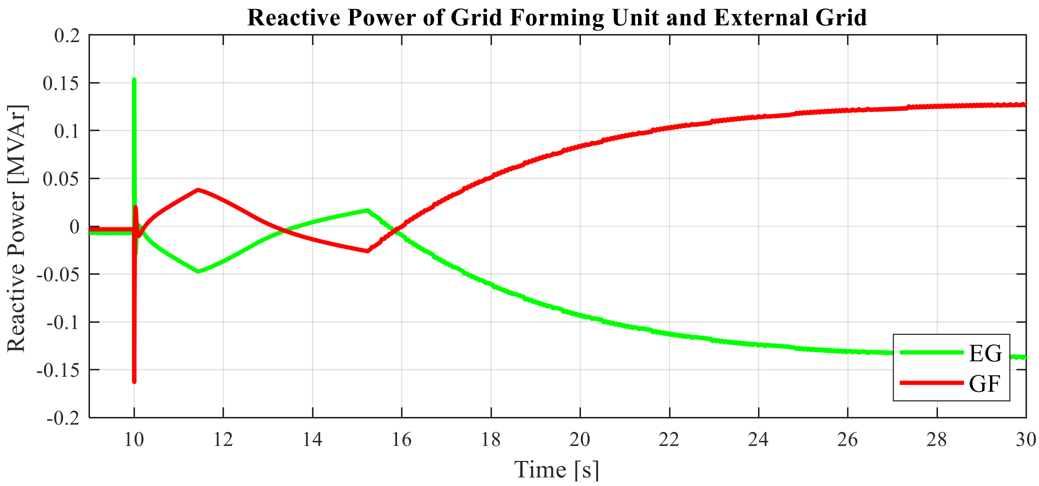

Figure 4.19: Reactive power outputs of EG, GF converter and RES during GF Converter Response with Realistic Constraints case.

The power support of the BESS is shown in Fig. 4.20 against the under voltage at the DC bus. The output of the BESS is significantly lower than the previous case. The reason is that the voltage drop in the DC bus is also significantly lower for this case compering to the previous cases, where the voltages drop to 0.86 and 0.99 [pu] for the previous and this case, respectively. In the previous cases, GF converter was heavily loaded with the connection of the load, and the discharge in the capacitor were very large. For this case, the increase in the loading of the converter is significantly lower comparing to the previous cases and this leads to lower voltage drop at the DC bus. However, if there was no higher level control, there would be bigger voltage drop, and the output power of the BESS would be bigger.

One certain conclusion can not be drawn for a higher level control and adaptive droop control. However, from the simulation results some suggestion can be made. For a GF converter system where a BESS is implemented for DC bus voltage support, it is analysed that the voltage drop is significantly lower. Therefore, the voltage control can be performed

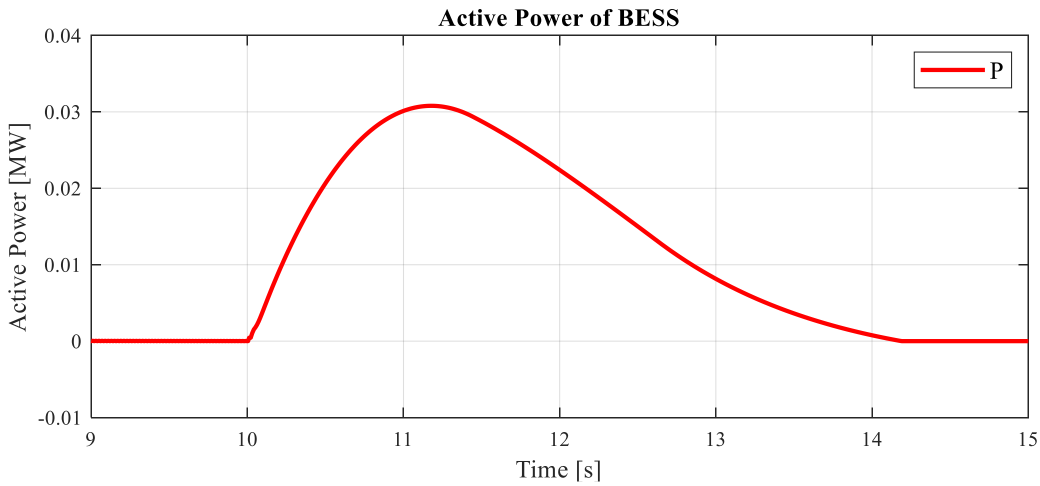

Figure 4.20: Power output of BESS during GF Converter Response with Realistic Constraints case.

by BESS and RES can be responsible only supplying power to GF converter. This will be performed by preventing the higher level control to update maximum power point in the droop curve. Then, the maximum power point will be defined only based on the available power at RES and will be kept fixed. As a result, adaptive droop control can immediately support system frequency when it is needed, while BESS can provide stable DC bus voltage.

Discussion 5

In this section, the choices and decisions made during the project will be reflected upon. This project was initiated by modelling the VSG control strategy. Firstly, it was implemented to an ideal controlled voltage source. Then the converter controller, which is a cascaded voltage and current controller, was built, and the VSG control is implemented to this converter controller. The model was analysed in both RMS analysis and EMT analysis. The initial results showed that the secondary control becomes dominant in the analysis and it is not convenient to analyse the operation of GF converter in parallel with other generation units, because secondary control continuously updates the electrical power output till the system frequency goes back to 50 $[Hz]$. In the following stages of the project, it is decided to implemented droop controls, which are introduced in Section 2.2, instead of VSG. Both strategy are able to run a grid-forming converter control, therefore the built cascaded voltage and current controller kept same. GF converter is implemented frequency and voltage droop controls. These droop controls allow a GF converter to operate in parallel with other generation units in an electrical power system. The final voltage and frequency set-points are processed by a cascaded voltage and current controller which is a common grid forming converter control strategy.

Several case studies are introduced in Chapter 4 to observe the behaviour of both the GF converter and the power system. The first case study is designed to observe the behaviour of the GF converter system, including the RES behind it. To highlight the behaviour of the GF converter system, the effect of the external grid is minimized in this study. GF converter became the dominant generation unit in the system. Then a large load relative to the total rating of the system is switched in and GF converter is heavily loaded, as the effect of the external grid is minimized. After a load switch, it is observed that the GF converter can handle the loading and maintain the power system operation. However, as the power system is designed with low inertia, the rate of change of frequency was very high. GF converter can be implemented with a virtual inertia strategy to prevent fast frequency change in the system. As displayed in Appendix A, implementation of VSG can contribute to the system inertia. The second challenge is a voltage drop in the AC bus following the switching moment. The GF converter was also successful to restore the AC voltage thanks to the grid-forming cascaded voltage and current controller. The internal converter controller increases or decrease the reactive power injection or consumption to form the reference voltage. However, this voltage controller leads to a concern in the GF converter. As the active power and reactive power are not controlled directly in GF converter, the converter should not be loaded fully by active power. Otherwise, the converter can be overloaded when voltage controller also demands reactive power. During the design process, the sizing of the GF converter should give some free room for the reactive power. The third challenge regarding the GF system is the DC bus voltage. A GF converter acts as a voltage source and when there is a load demand in the system, the GF converter feeds the load immediately. For this case, GF converter was dominant, and the effect of the external grid was minimized. Therefore, GF converter was heavily loaded after the load connection. The power source behind GF converter should follow the power that GF converter delivers to the grid. However, a RES may not increase or decrease its output power as GF converter can response very quickly. In the case study, it can be seen that RES increased its power output in relation with its ramp rate limiters, and during the time where GF converter delivers more power than RES delivers, the capacitor connected to DC link discharged. As a result, DC bus voltage dropped significantly, after heavily loading of the GF converter. For this project, only loading a GF converter is analysed, but it would be the opposite if there was a load loss in the system. It would immediately decrease the loading of the GF converter and RES would be delivering power more than the demand for a short while. And this would result in a over voltage in the DC bus.

Droop control provides load sharing to the generation units in a power system and support the system frequency. The drawback is that it can not provide further control for frequency. If the electrical power output of one of the generation can be increased, the other will automatically decrease, and based on the less loading, the frequency can increase. Electrical output of a generation unit can be controlled by controlling its droop curve. Two different adaptive droop control methods are proposed in the project for frequency regulation. One strategy offers to shift the droop curve, whereas the other offers changing the slope. These two adaptive droop control is applied to the GF converter model and tested under ideal scenario in the second case study. It was seen that electrical frequency of a power system can be controlled by adapting droop curves. For the ideal scenario, it was successful to restore the system frequency back to its nominal.

A BESS is proposed a as solution to the DC bus voltage concern experienced in the first case. In the third case study, a BESS is connected in parallel to the DC link capacitor. The system is controlled to response against any voltage drop in the bus. Other parameters and events kept identical to the first case. Then it was seen that the voltage recovery is faster, and voltage drop in the bus is lower comparing to the first case. A BESS can also be used during over voltage. It can draw active power from the DC bus and helps DC link capacitor to discharge. For this analysis, the main purpose of the BESS is to support the DC voltage regulation during the over and low voltages for a short time, however such a system placed behind the GF converter can also be used for long term energy storage. A GF converter can take the advantage of long-term storage system and increase the power system reliability in operation.

In the last case study, realistic constraints were applied, where both GF converter and external grid have an active role in the system. Therefore, the adjustments in the external grid, which minimizes its effect in the system, are removed in this case. Also, the introduced BESS and adaptive droop control with shifting method are applied in this case study. The control constrains of the adaptive droop control are utilized in this study, whereas this method was simulated as ideal scenario in the second case study. The same switching event, which is to connect a large load relative to the total rating of the system, is also applied in the last case study. It was observed that the change in the loading in the GF converter was lower comparing to the previous cases. The reason is that the external grid and GF converter shared the load among themselves based on the droop controls. It is explained that the voltage drop in the DC bus is strongly depend to the change in the loading of GF converter. The voltage drop was also very low in this case comparing to the other case studies. Following the switching event, adaptive droop control was also got activated based on its activation frequency settings. A rise in the system frequency was observed, however it was not as ideal as in the second case study. The reasons is that the loading in the GF converter increased while the adaptive droop control performs. Once the loading of the GF converter reached to maximum power range of adaptive droop control, the operation of the adaptive droop curve stopped.

6 Conclusion

A generic RMS model of GF converter is built in this study utilizing the PWM converter model in DIgSILENT PowerFactory. A cascaded voltage and current controller, which is the main control strategy for GF converters, is applied via DSL models to the converter. Voltage and frequency droop controls are also implemented to control the inputs of the converter. The complete GF system, including the DC link capacitor, BESS and RES is used for the power system level studies. Four different simulation cases are analysed to observe the behaviour of both the GF converter and the power system. The base case which is designed to observe the response of a GF converter after a load switching, while the effect of external grid is minimized. The second case is the implementation of adaptive droop control in the system. Two different adaptive droop control methods are proposed in the project for frequency regulation. One strategy offers to shift the droop curve, whereas the other offers changing the slope. These two adaptive droop control is applied to the GF converter model and it was successful to restore the system frequency back to its nominal. In the third case, a BESS is proposed a as solution to the DC bus voltage concern experienced in the base case. It was observed that the voltage recovery is faster, and voltage drop in the bus is lower comparing to the base case. In the last case study, realistic constraints were applied, where both GF converter and external grid have an active role in the system. Therefore, the adjustments in the external grid, which minimizes its effect in the system, are removed in this case. Also, the introduced BESS and adaptive droop control with shifting method are applied in this case study.It was observed that the change in the loading in the GF converter was lower comparing to the previous cases. As the external grid and GF converter shared the load among themselves based on the droop controls.

Through the report and case studies, it is observed that the designed RMS model of GF converter is successful of forming the voltage and frequency at the AC bus where it is connected to. It is able to perform load sharing with the other generation unit. It can be concluded that a GF converter can be used in a power system similar to a SG in the future. However, it will bring another challenges to power systems. A GF converter will mostly likely be fed by a RES. Some of the RESs have a fluctuating nature, which means that the available power varies in time. A GF converter does not provide direct control on the active power flow as grid-following control does. A GF converter provides active power to the power system based on its droop control. Considering this nature of GF converter, there should always be a reliable power source behind it. Because at any moment, where a GF converter needs to deliver a certain amount of power to the power system, but RES can not provide it, will results in tripping GF converter off. A BESS can be a solution for this challenge, and it can compensate the power deficit between the GF converter and

RES during the fluctuations in the source (such as wind an solar). A GF converter brings also other challenges and some of them are mentioned through the report and case studies, which are DC bus voltage stability, reactive power flow and rate of change of frequency.

The introduced GF converter controller can be exported and used for other RMS studies and it can be easily adapted to EMT analysis. The complete GF system, including the DC link capacitor, BESS and RES can be used for a power system level studies. These studies may include fluctuating or constant power source, different system events and different configuration of GF converter size, RES size and BESS size. Some of the subjects that can be analysed by the introduced model are;

- analysing the effects of fluctuating power source (such as wind and solar) on GF converter operation.
- analysing the potential contribution of a BESS as power source during the fluctuating power input.
- determining the size of the BESS for a given power level and time duration.
- analysing the operation of a GF converter with different droop control settings.
- analysing the response of a GF converter against different system event.

GF converter is a promising control strategies for future power system. The introduced model can be used to perform system studies such as mentioned above, and the results from these studies can be evaluated by TSOs to determine the requirements of GF systems.

Bibliography

[1] Pineda Ivan Colin Walsh. Wind energy in Europe in 2018. page 8, 2018.

[2] A. Ulbig, M. D. Galus, S. Chatzivasileiadis, and G. Andersson. General frequency control with aggregated control reserve capacity from time-varying sources: The case of phevs. *2010 IREP Symposium Bulk Power System Dynamics and Control - VIII (IREP)*, pages 1–14, 2010.

[3] Energy Danish Ministry of Climate and Utilities. *Energiaftalen*. `https://en.kefm.dk/media/12222/energiaftale2018.pdf`, 2018. Visited 25-09-2019.

[4] Standard models for variable generation. Technical report, NORTH AMERICAN ELECTRIC RELIABILITY CORPORATION, NERC, 2010.

[5] Prabha Kundur. *Power System Stability And Control*. 1993.

[6] E. M.G. Rodrigues, G. J. Osório, R. Godina, A. W. Bizuayehu, J. M. Lujano-Rojas, and J. P.S. Catalão. Grid code reinforcements for deeper renewable generation in insular energy systems. *Renewable and Sustainable Energy Reviews*, 53:163–177, 2016.

[7] Energinet.dk. Technical regulation 3.2.5 for wind power plants above 11 kW. pages 1–108, 2016.

[8] Joan Rocabert, Alvaro Luna, Frede Blaabjerg, and Pedro Rodríguez. Control of power converters in AC microgrids. *IEEE Transactions on Power Electronics*, 27(11):4734–4749, 2012.

[9] Grid Forming Capability, Generating Unit, Power Park Module, Synchronous Power, Generating Module, Power Park Module, Non-synchronous Electricity Storage, Inertia Power, Non-cusc Party, Dynamic Reactive, and Synchronising Torque. Draft Grid Code – Grid Forming Converter Specification 10 th February 2020. (February):3–7, 2020.

[10] P. Kundur, J. Paserba, V. Ajjarapu, G. Andersson, A. Bose, C. Canizares, N. Hatziargyriou, D. Hill, A. Stankovic, C. Taylor, T. Van Cutsem, and V. Vittal. Definition and classification of power system stability ieee/cigre joint task force on stability terms and definitions. *IEEE Transactions on Power Systems*, 2004.

[11] Andrew J Roscoe, Mengran Yu, Adam Dyśko, Richard Ierna, and Jiebei Zhu. A VSM (Virtual Synchronous Machine) Convertor Control Model Suitable for RMS Studies for Resolving System Operator / Owner Challenges. *15th Wind Integration Workshop*, 2016.

[12] Salvatore D'Arco and Jon Are Suul. Equivalence of virtual synchronous machines and frequency-droops for converter-based Microgrids. *IEEE Transactions on Smart Grid*, 5(1):394–395, 2014.

[13] Babak Badrzadeh, Zia Emin, Emil Hillberg, David Jacobson, L Kocewiak, G Lietz, F da Silva, and Marta Val Escudero. The need or enhanced power system modelling techniques and simulation tools. *CIGRE SCIENCE & ENGINEERING*, 17(Febr):30–46, 2020.

[14] User Manual. DIgSILENT PowerFactory. 2019.

[15] PowerFactory. PowerFactory 2019,Technical Reference Documentation - PWM Converter. page 7;34, 2019.

[16] J. M. Guerrero, J. C. Vasquez, J. Matas, M. Castilla, and L. Garcia de Vicuna. Control strategy for flexible microgrid based on parallel line-interactive ups systems. *IEEE Transactions on Industrial Electronics*, 56(3):726–736, 2009.

[17] A. Bubshait and M. G. Simões. Design of fuzzy logic-based dynamic droop controller of wind turbine system for primary frequency support. In *2018 IEEE Industry Applications Society Annual Meeting (IAS)*, pages 1–7, 2018.

[18] C. Wang, J. Meng, Y. Wang, and H. Wang. Adaptive virtual inertia control for dc microgrid with variable droop coefficient. In *2017 20th International Conference on Electrical Machines and Systems (ICEMS)*, pages 1–5, 2017.

[19] G. Li, Z. Du, C. Shen, Z. Yuan, and G. Wu. Coordinated design of droop control in mtdc grid based on model predictive control. *IEEE Transactions on Power Systems*, 33(3):2816–2828, 2018.

[20] N. R. Chaudhuri and B. Chaudhuri. Adaptive droop control for effective power sharing in multi-terminal dc (mtdc) grids. *IEEE Transactions on Power Systems*, 28(1):21–29, 2013.

Virtual Synchronous Generator Model and Simulation Results A

The Fig. A.1 displays the initial model created in this project. Comparing with the final model in the project, the initial model has an ideal DC voltage source on the DC bus of the converter. Therefore, it is not possible to analyse any dynamic on the DC side in this model whereas it is possible to analyse the DC bus voltage, BESS, and the behaviour of RES in the latest model. However, the AC side of the converter in both this model and final model in the report are almost identical. The only difference is that there is one more line in this mode between the load terminal and AC bus of the GF converter. It should not have much impact on the power flow. Therefore this model and the final model in the report can be compared in terms of the behaviour in the power system.

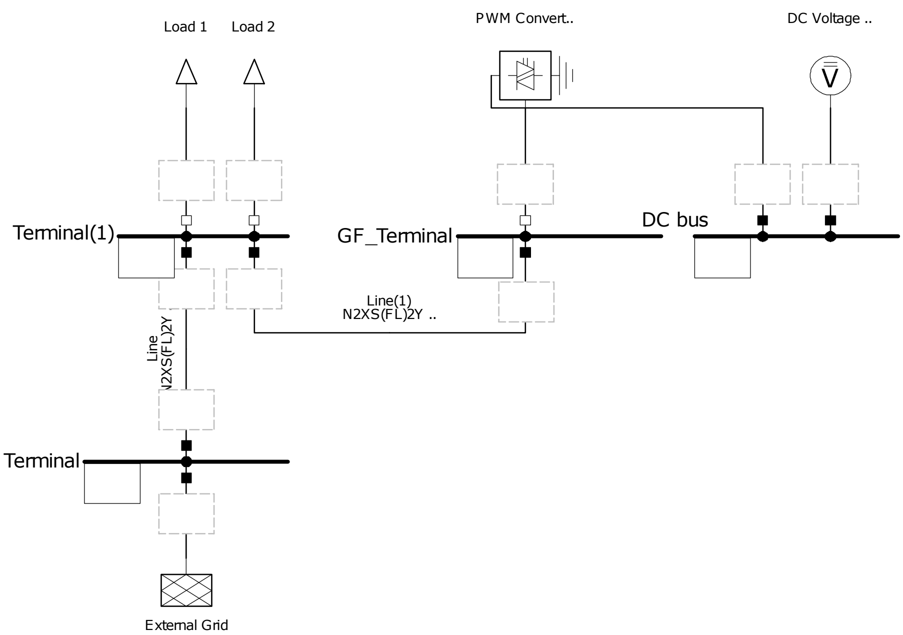

Figure A.1: System layout of the initial model in the project with VSG.

One concern with GF converter based on droop control is the rate of change of frequency (RoCoF) in the electrical power system. The VSG model emulates the behaviour of a SG and it is implemented virtual inertia via swing equations. Therefore VSG should have advantages in terms of RoCoF. To analyse the difference between the VSG based and droop control based GF converter, the system parameters are designed as same as the introduced case study in section 4.1. Briefly, the external grid is implemented a vertical droop curve. The simulation is initiated with no-load and 1 $[MW]$ load is switched in at 10 $[s]$. To make an ideal comparison in terms of RoCoF, the primary response of the VSG is implemented the same droop curve GF converter has. Also, the secondary response of the VSG is deactivated by setting the k_i to 0. The inertial time constant of the virtual inertia is set as 1 $[s]$.

The simulations regarding VSG model is performed for both RMS and EMT. Performing RMS and EMT simulation was one of the objective during initial phase of the project. However, the project was moved another direction after switching to droop control based GF converter. Some designs which performed after the switching to droop control based GF converter, are complete GF converter with a RES, DC link, and capacitor, a BESS system and two adaptive droop control.

Fig. A.2 displays the frequency response of the power system after the load switching for both VSG based and droop curve based GF converter. It can be seen that VSG models have lower RoCoF. It can be concluded that the virtual inertia in VSG has a contribution to system inertia. Even though the EMT and RMS models are identical, step sizes are different and 0.001 and 0.01 $[s]$, respectively. In the results EMT analysis results in lower RoCoF than RMS analysis. Also EMT analysis consists ripples after the switching. However, it should be re-evaluated that how realistic ripples in the EMT frequency curve. Frequency of a system mostly likely calculate based on a time window and the figure consists ripples which have the length of the step size of the simulation. The solver of the software might have some affect on the analysis of the frequency.

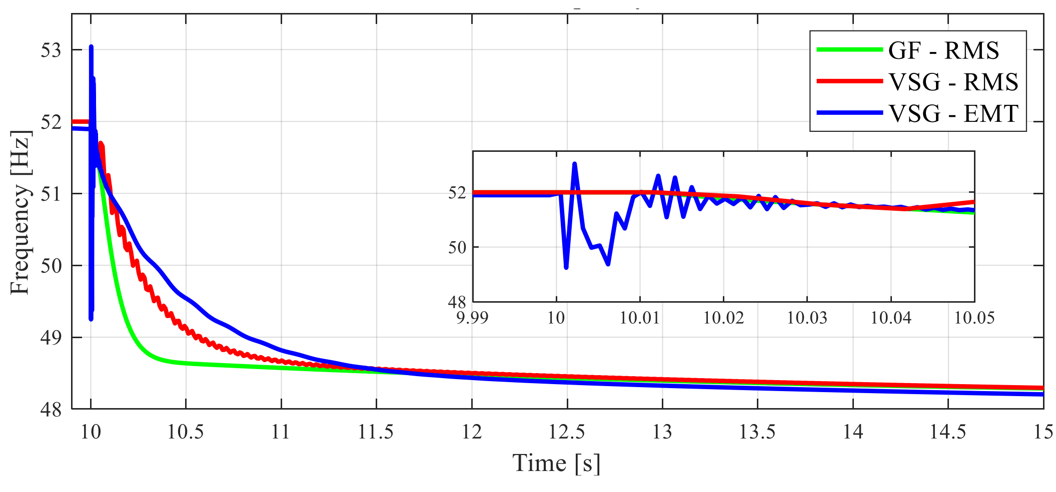

Figure A.2: Comparison of the system frequency with droop control based and VSG based GF converter.

From the power curves, displayed in A.3, droop based GF converter has the smoothest curve, whereas VSG model consist ripples for both RMS and EMT analysis. GF converter does not provide direct control on active power flow and adapts its speed based on the electrical power output. On the other hand, VSG control follows the grid frequency and controls the output power via virtual inertia block. The reason behind the ripples can be the power control loop of the VSG model and GF converter provides a smooth increase in the power output as it does not try to regulate it. However every method provide the same amount of power to the gird after a 5 [s] of time window.

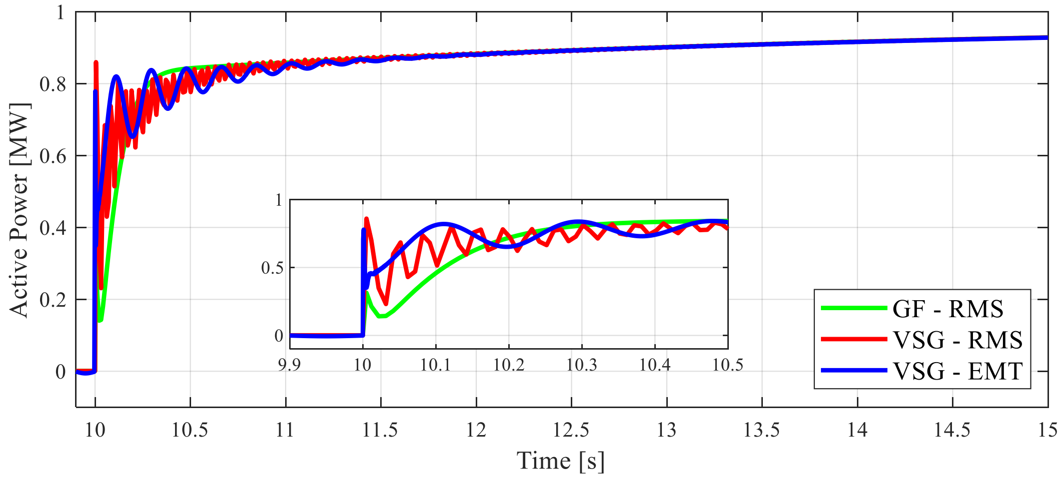

Figure A.3: Comparison of the active power output of GF converter with droop control and VSG.

VSG control differs from droop based GF control in terms of its active power loop, or in other words the way it finds out the frequency set point for GF converter. For voltage set point, VSG and droop based GF converter have the same droop implementation. From the following reactive and voltage figures, Fig. A.5 and Fig. A.4, the response of the converters are almost identical in steady state. However VSG control consists ripples as it had in the previous frequency and voltage figures. The reason in the ripples in VSG model might be that the ripples in the power loop can be reflected to the voltage control via internal converter controller which is cascaded voltage and current controller.

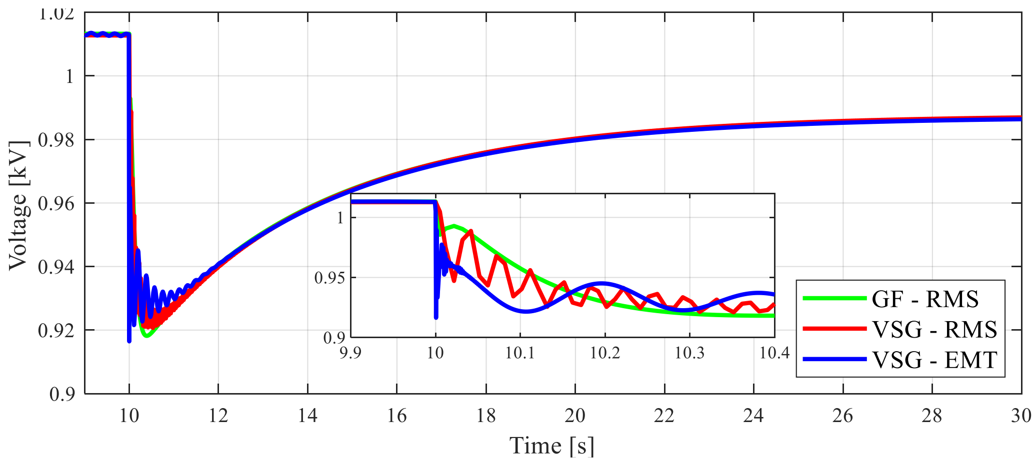

Figure A.4: Comparison of the AC bus voltage with droop control based and VSG based GF converter.

As it is mentioned above, the VSG based GF converter model is built during the initial phase of the project. The authors decided to add the results regarding the VSG model and perform a comparison towards to end of the project where there was a limited time for extra work.The results are useful for the understanding of the contribution of the virtual

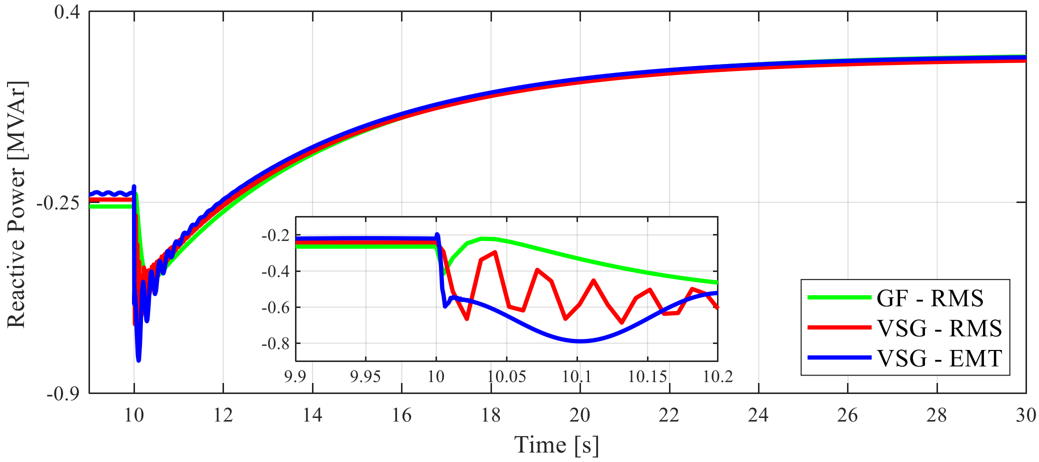

Figure A.5: Comparison of the reactive power output of GF converter with droop control and VSG.

inertia implementation in the VSG to system frequency change. However, authors did not have the time for a deep analysis on the reason of the ripples displayed in the figures. The previously mentioned reasons regrading to the ripples are the most potential reasons.

Logical Controls B

The logical controls presented in the previous chapters will be explain in detail in this chapter. Prior to explaing the logical controls, the common functions PowerFactory function will be explained.

Parameter	Definition
f_grid	electrical frequency in $[pu]$

Table B.1: Power system parameters.

B.1 Functions

This section includes the commonly used PowerFactory functions for his study. The explanations are based on PowerFactory user manual [14].

select_const(boolean expression, x, y): If the expression is TRUE, the functions outputs x. If the expression is FALSE, the functions outputs y.

B.2 Logical Controls

The section presents the design of the logical controls and the definitions of the variables in it.

B.2.1 Logical Controls in Adaptive Droop Control Shifting Method

Activation Above 50+ΔF_{active} $[Hz]$:
select_const(f_grid>1+Delta_f_activate,1,0)

$P_{min\_with\_\Delta P\_set}$ **Constrain:**
select_const(Pel>P_min_with_DeltaP_set, 1,0)

Activation Below 50-ΔF_{active} $[Hz]$:
select_const(f_grid<1-Delta_f_activate,1,0)

$P_{max\_with\_\Delta P\_set}$ **Constrain:**
select_const(Pel<P_max_with_DeltaP_set, 1,0)

$P_{min\_with\_\Delta P\_set}$ **Constrain or** $P_{max\_with\_\Delta P\_set}$ **Constrain or Resetting Zone:**
select_const(Pel<P_min_with_DeltaP_set.or.Pel>P_max_with_DeltaP_set.or.

select_const(f_grid<(1+Delta_f_deactivate).and. f_grid>(1-Delta_f_deactivate), 1,0), 1,0)

B.2.2 Logical Controls in Adaptive Droop Control Variable Slope Method

Activation Above 50+ΔF_{active} $[Hz]$ or Below 50-ΔF_{active} $[Hz]$:
select_const(f_grid>1+Delta_f_activate.or.f_grid<1-Delta_f_activate,1,0)

$P_{min\_with\_\Delta F}$ **and** $P_{max\_with\_\Delta F}$ **Constrain:**
select_const(Pel>P_min_with_DeltaF.and.Pel<P_max_with_DeltaF,1,0)

$P_{min\_with\_\Delta F}$ **Constrain or** $P_{max\_with\_\Delta F}$ **Constrain or Resetting Zone:**
select_const(Pel<P_min_with_DeltaF.or.Pel>P_max_with_DeltaF.or.
select_const(f_grid<(1+Delta_f_deactivate).and. f_grid>(1-Delta_f_deactivate), 1,0), 1,0)

Results C

C.1 Extra Figures for Shifting Method Case Study

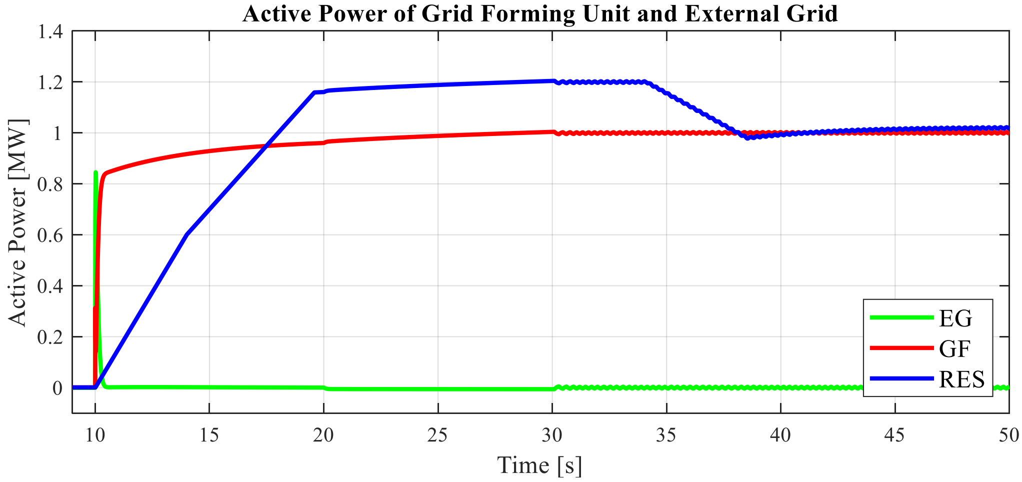

Figure C.1: Active power outputs of EG, GF converter and RES during GF converter response with ideal shifting method case.

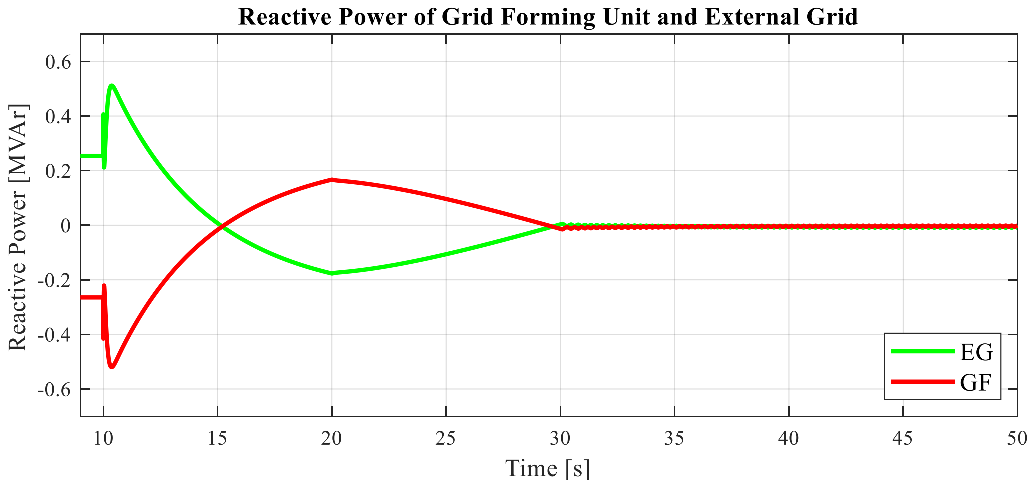

Figure C.2: Reactive power outputs of EG, GF converter and RES during GF converter response with ideal shifting method case.

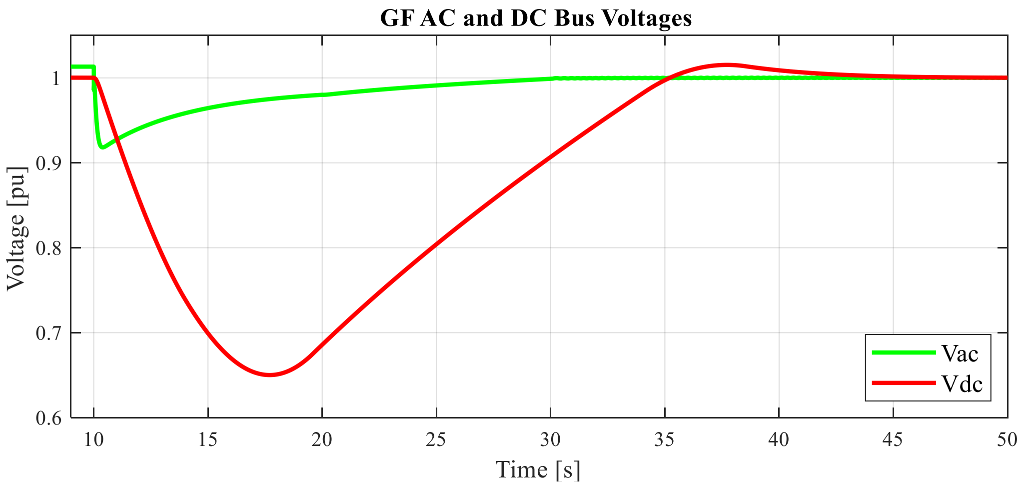

Figure C.3: AC and DC bus voltages during GF converter response with ideal shifting method case.

C.2 Extra Figures for Variable Slope Method Case Study

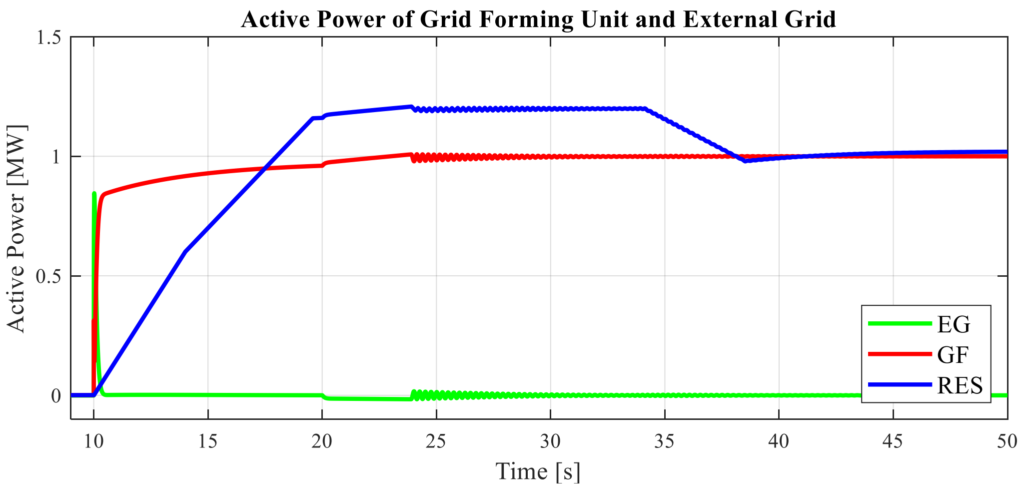

Figure C.4: Active power outputs of EG, GF converter and RES during GF converter response with ideal variable slope method case.

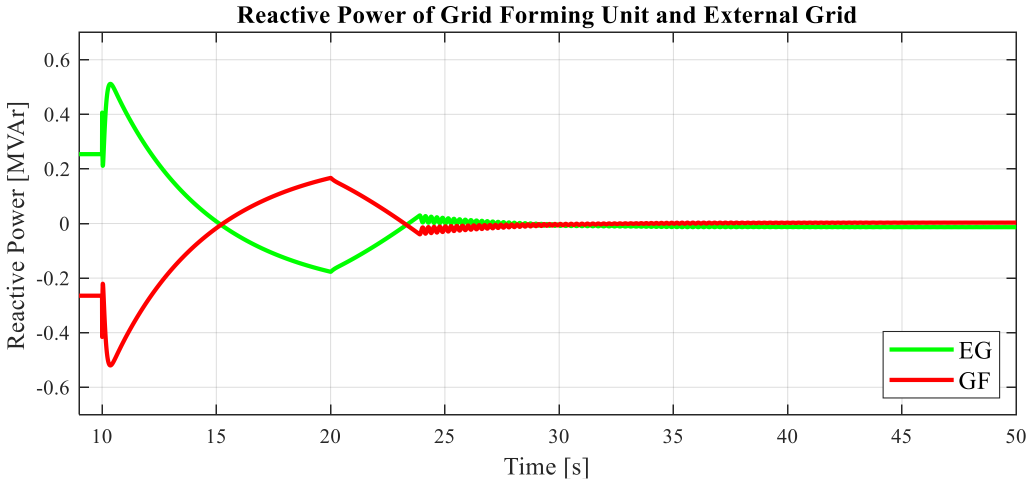

Figure C.5: Reactive power outputs of EG, GF converter and RES during GF converter response with ideal variable slope method case.

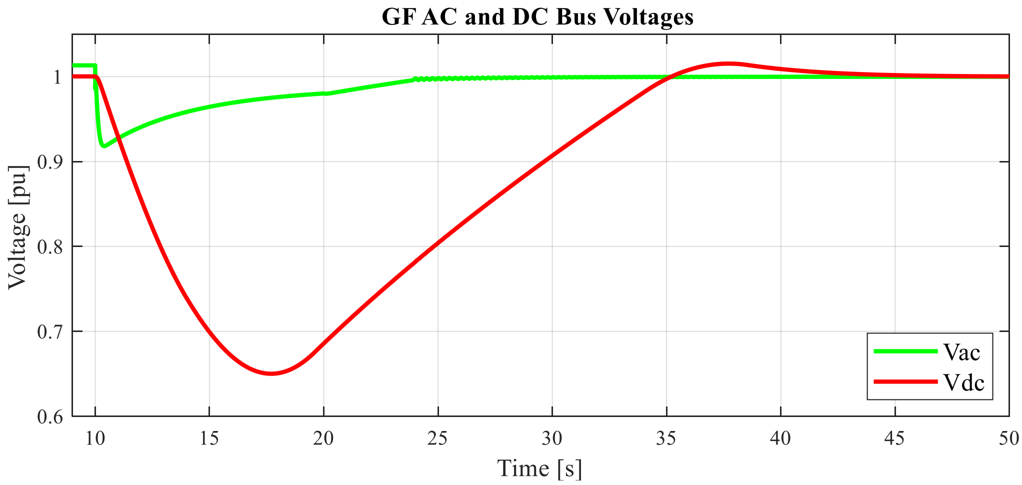

Figure C.6: AC and DC bus voltages during GF converter response with ideal variable slope method case.

C.3 GF Converter Response with Realistic Constraints Case with Adaptive Droop Control Variable Slope Method

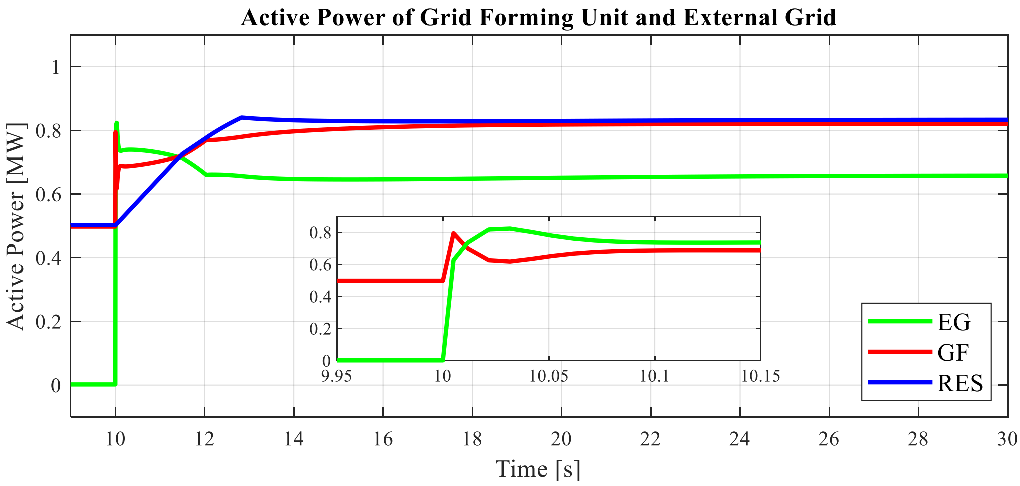

Figure C.7: Active power outputs of EG, GF converter and RES during Realistic Constraints case with variable slope method.Active power outputs of EG, GF converter and RES during GF Converter Response with Realistic Constraints case.

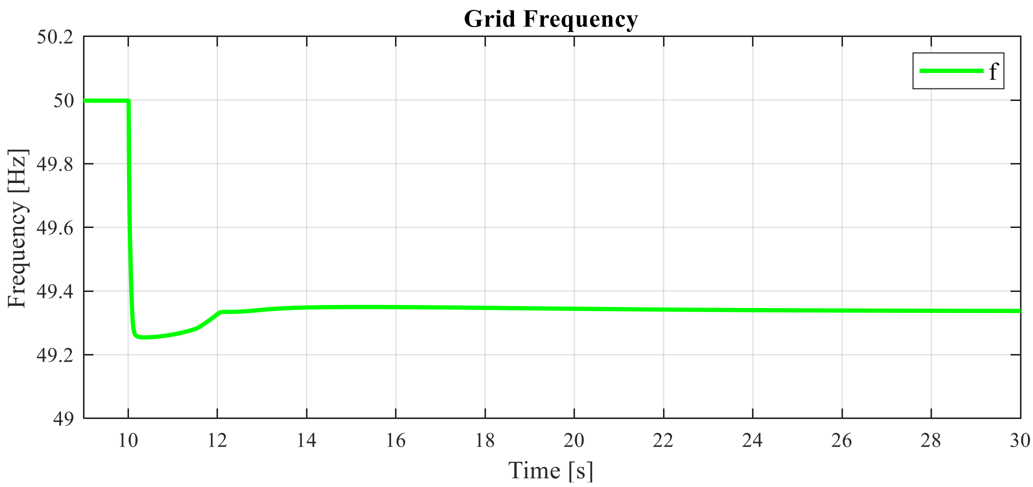

Figure C.8: Grid frequency during GF Converter Response with Realistic Constraints case with variable slope method.

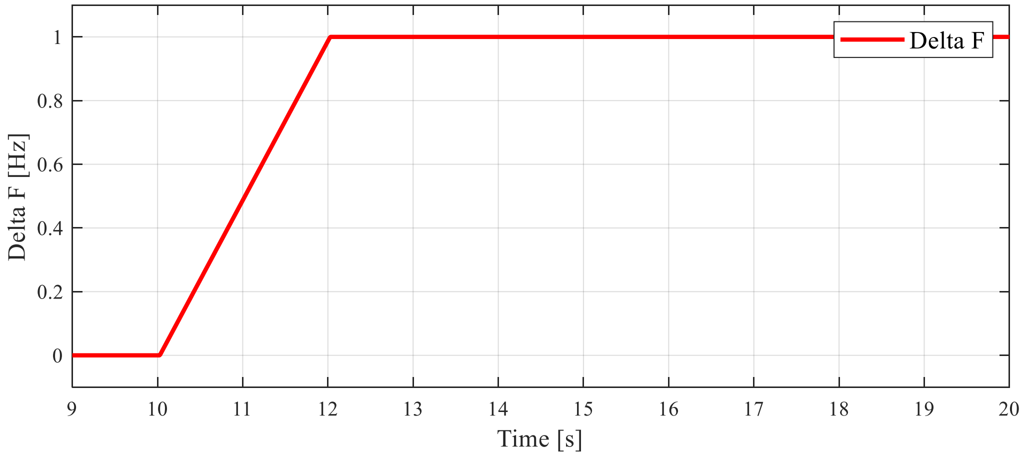

Figure C.9: Deviation from 48 $[Hz]$ for maximum operation point during GF Converter Response with Realistic Constraints case with variable slope method.

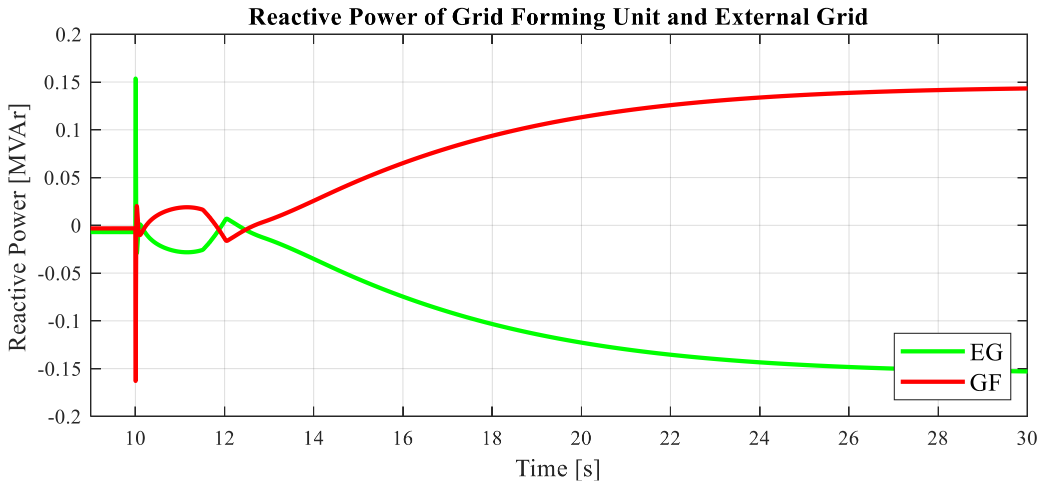

Figure C.10: Reactive power outputs of EG, GF converter and RES during GF Converter Response with Realistic Constraints case with variable slope method.

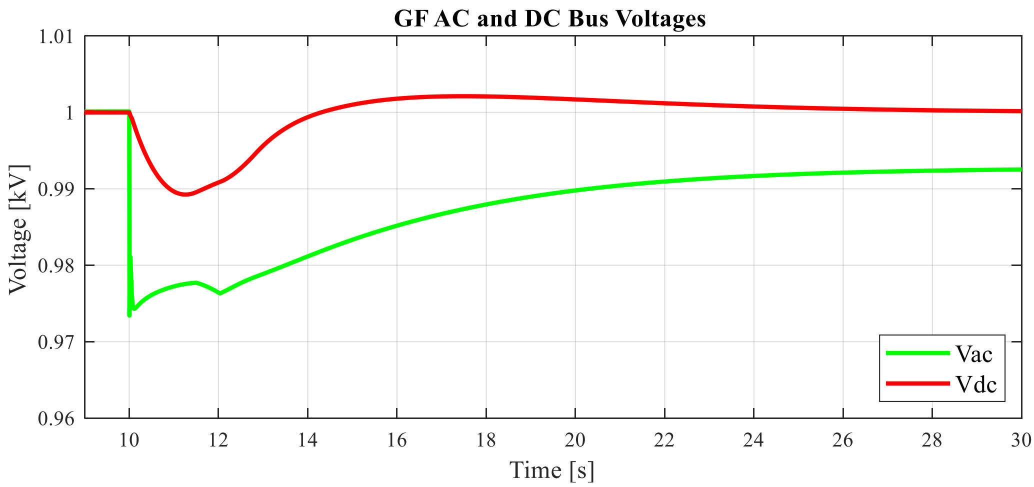

Figure C.11: AC and DC bus voltages during GF Converter Response with Realistic Constraints case with variable slope method.

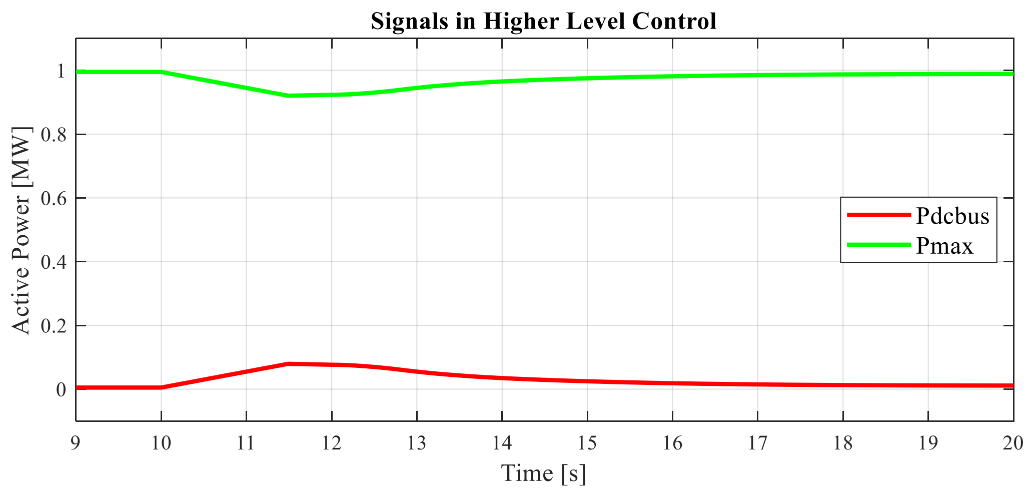

Figure C.12: Maximum operation point signal for GF converter, P_{max}, and power reference for capacitor charging, P_{dc_bus}, during GF Converter Response with Realistic Constraints case with variable slope method.

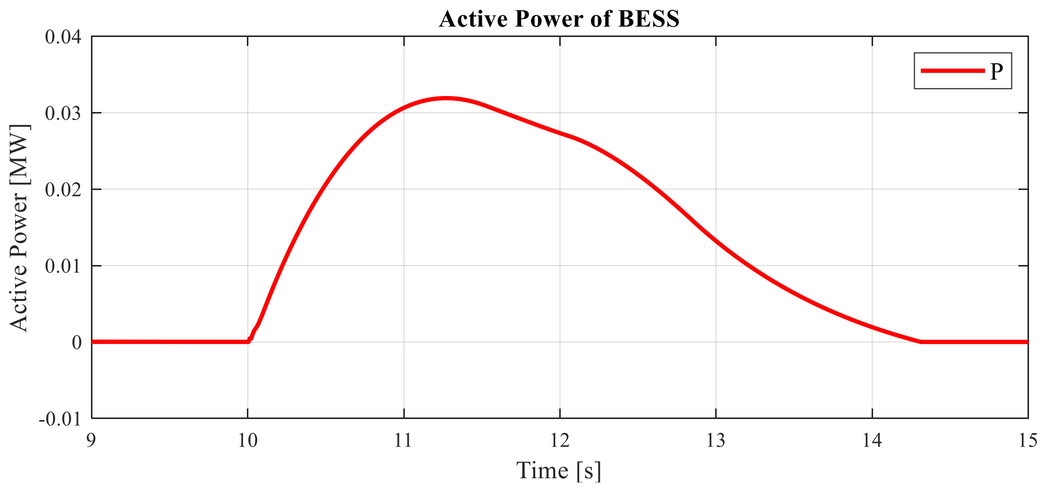

Figure C.13: Power output of BESS during GF Converter Response with Realistic Constraints case with variable slope method.

Screenshots D

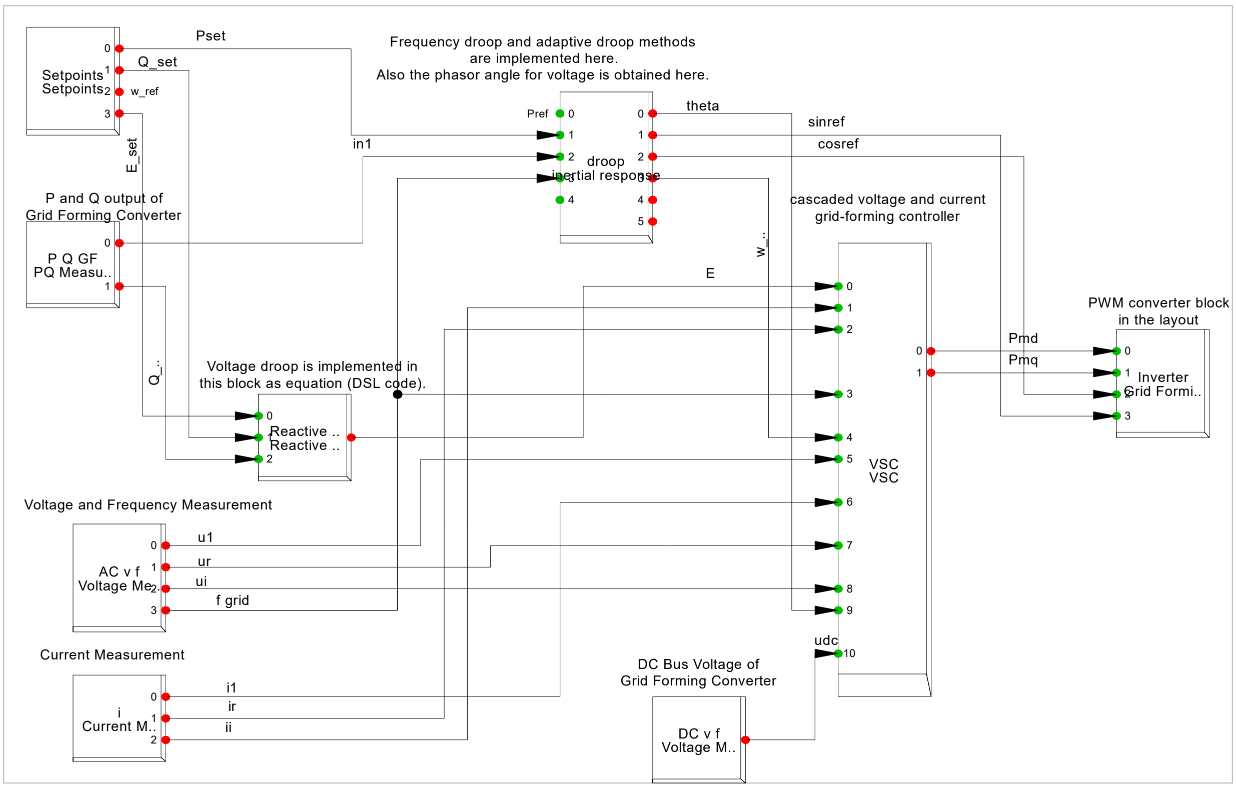

Figure D.1: GF converter

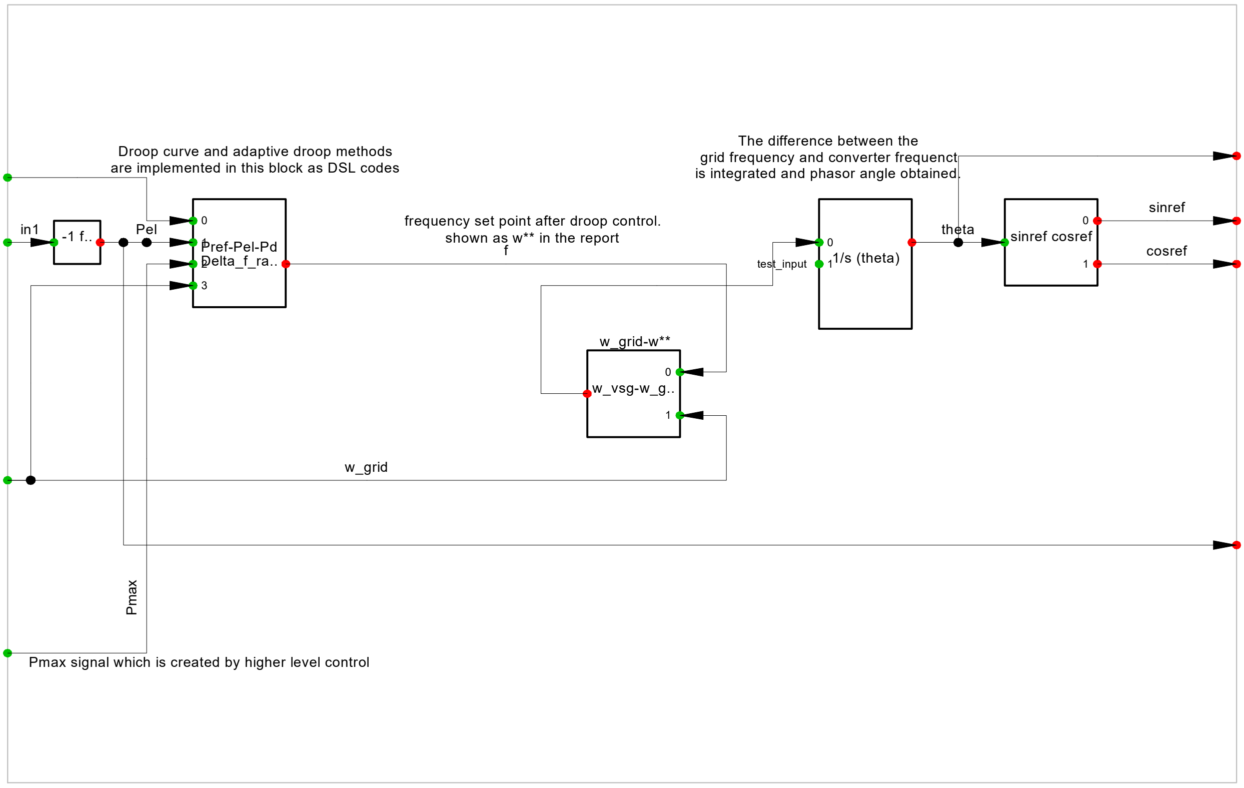

Figure D.2: Frequency droop control and calculation of phasor angle

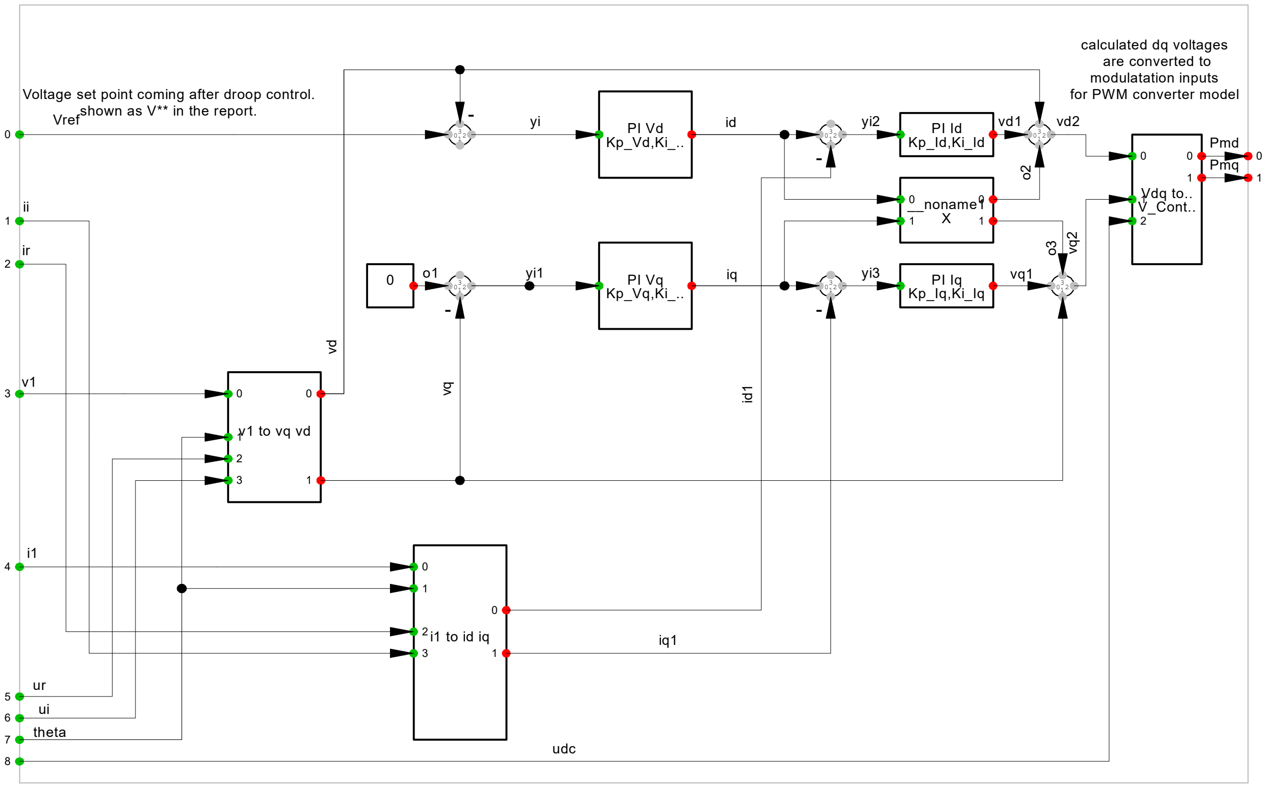

Figure D.3: Gf covnerter internal control

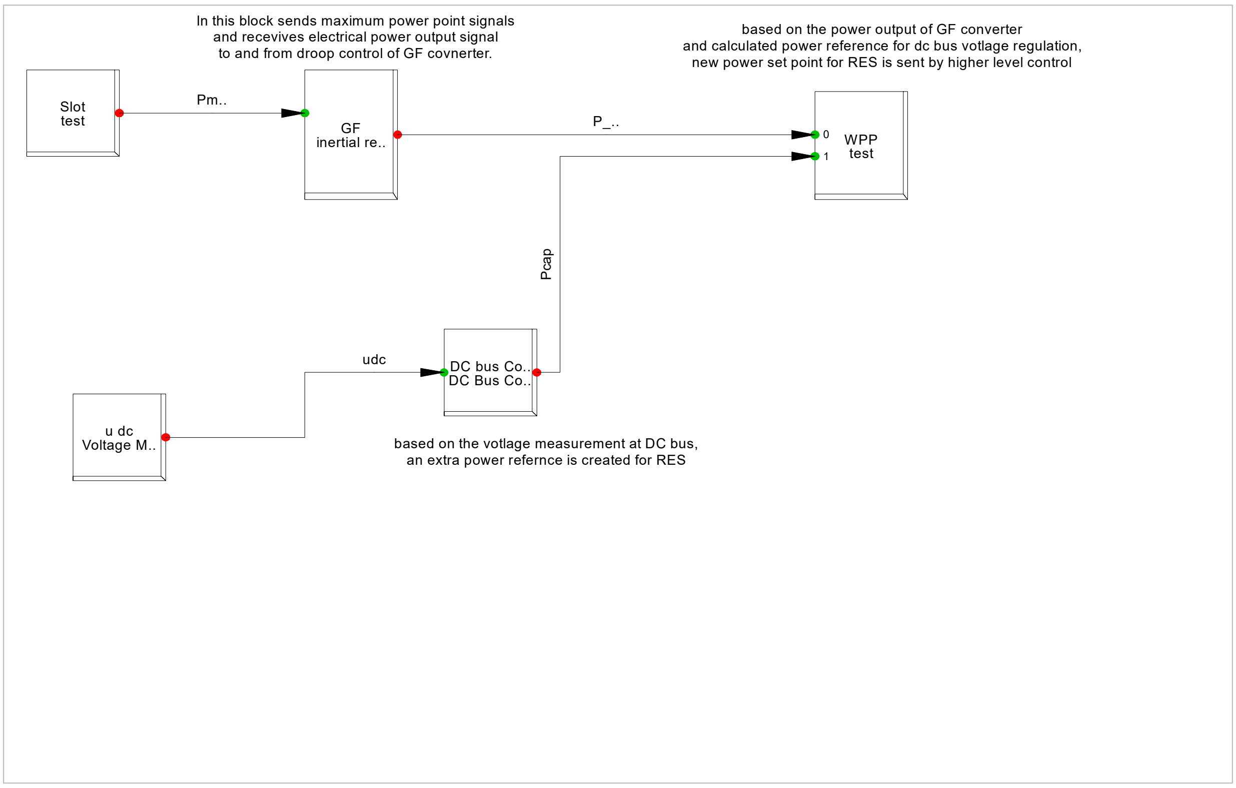

Figure D.4: higher level control

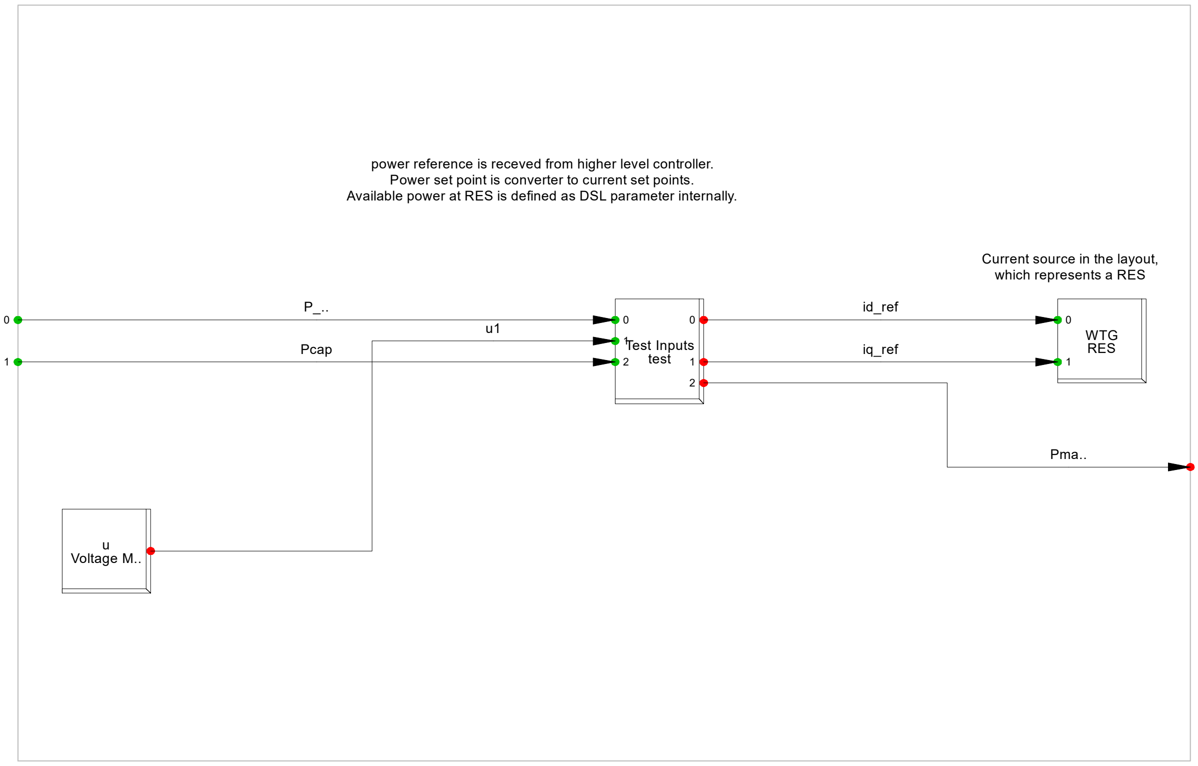

Figure D.5: RES control

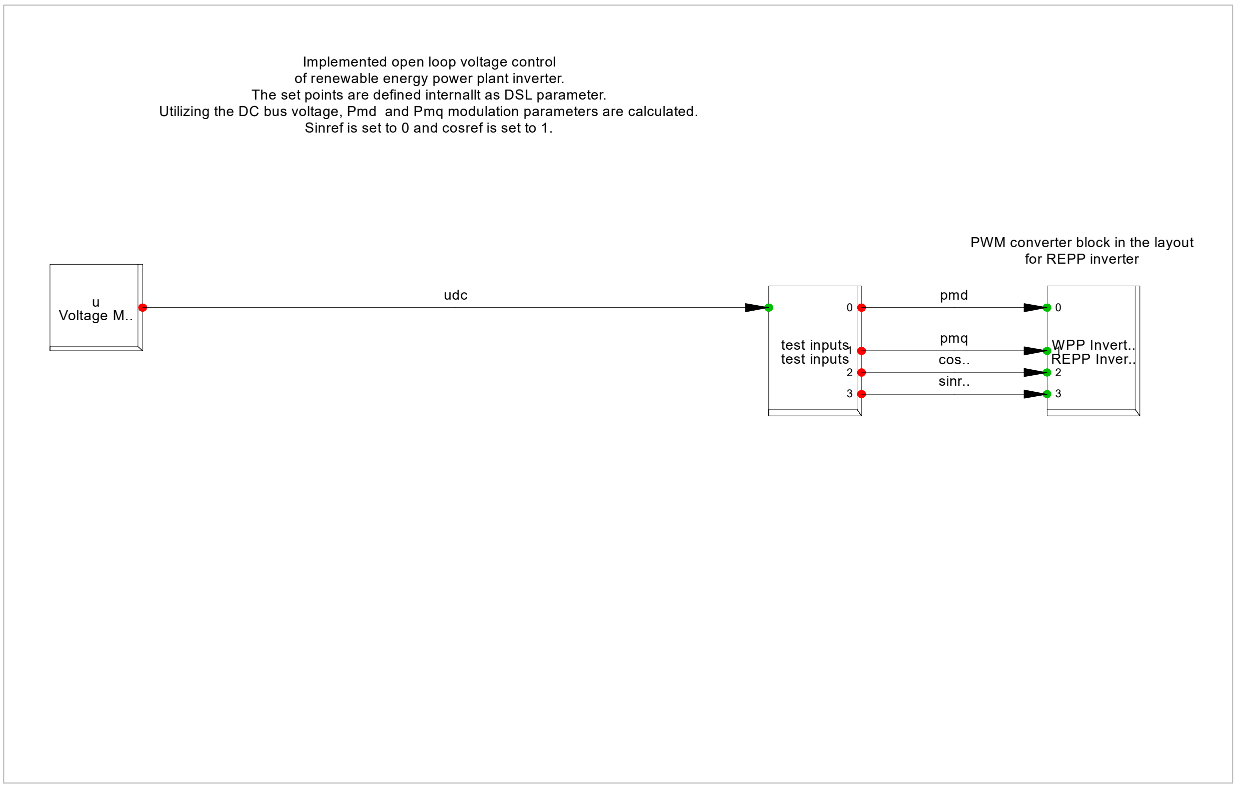

Figure D.6: Renewable energy power plant inverter control